Technical Report 444

A Radar Interferometer Study of Venus at 3.8 cm

A. E. E. Rogers
T. Hagfors
R. A. Brockelman
R. P. Ingalls
J. I. Levine
G. H. Pettengill
F. S. Weinstein

14 February 1968

Prepared under Electronic Systems Division Contract AF 19(628)-5167 by

Lincoln Laboratory
MASSACHUSETTS INSTITUTE OF TECHNOLOGY
Lexington, Massachusetts

The work reported in this document was performed at Lincoln Laboratory, a center for research operated by Massachusetts Institute of Technology, with the support of the U.S. Air Force under Contract AF 19(628)-5167.

MASSACHUSETTS INSTITUTE OF TECHNOLOGY

LINCOLN LABORATORY

A RADAR INTERFEROMETER STUDY OF VENUS AT 3.8 cm

A. E. E. ROGERS *R. P. INGALLS*
T. HAGFORS *J. I. LEVINE*
R. A. BROCKELMAN *G. H. PETTENGILL*
F. S. WEINSTEIN

Group 31

TECHNICAL REPORT 444

14 FEBRUARY 1968

LEXINGTON MASSACHUSETTS

ABSTRACT

The 120-foot antenna of the Haystack Microwave Facility and the 60-foot antenna of the Westford Communications Terminal, both operated by M.I.T. Lincoln Laboratory, were coupled to form a planetary radar interferometer operating at X-band and were used to observe Venus at a wavelength of 3.8 cm during the 1967 inferior conjunction. The antennas are separated by approximately 4000 feet along a line 22° east of north. At maximum projection in the direction of the planet, this baseline gives a fringe spacing of 5 seconds of arc, or a maximum of about 10 fringes across the planetary disk at inferior conjunction.

By transmitting a CW signal from the 120-foot antenna and frequency analyzing the received echo, it was possible to resolve the planetary surface scattering into strips parallel to the apparent axis of rotation. Crosscorrelation of the complex frequency components obtained at the two sites yielded corresponding spatial Fourier components which resolved the scattering along the strips. With 1-Hz frequency resolution and a maximum of 10 fringes along the rotation axis, the planetary hemisphere visible to the radar during inferior conjunction was mapped with approximately 100 resolution intervals along a direction perpendicular to the apparent rotation axis, with 10 resolution intervals in the orthogonal direction.

For a limited region on the planet, surrounding the center of the visible disk, higher resolution was obtained by transmitting pulses of 500-μsec effective length. The pulse resolution enabled the planet to be resolved in echo delay, leaving only a twofold hemispheric ambiguity to be resolved by the interferometer. In addition, in the range-gated observations the effects of significant interferometer sidelobes (arising from the limited range of projected baselines available) were avoided.

Maps obtained from the observations show Venus to be smoother on the average than the moon at 3.8 cm, although some regions of the planet exhibit strong local radar-scattering enhancement. The positions of these regions agree well with those previously reported if the rotation period of Venus is assumed to be earth-synchronous at 243.16 days retrograde.

Accepted for the Air Force
Franklin C. Hudson
Chief, Lincoln Laboratory Office

CONTENTS

LIST OF SYMBOLS

$\vec{r}_1$	baseline vector from Haystack to Westford
$\vec{r}_2$	Westford antenna offset
$\hat{r}_3$	unit vector toward subradar point
D	baseline length
d	offset length
A_p	azimuth of planet
E_p	elevation of planet
A_W	azimuth of baseline
E_W	elevation of baseline
c_e	velocity of propagation along baseline
τ_d	differential delay between antennas
ω	frequency in radians per second
c	velocity of propagation in free space
L_p	hour angle of planet
δ_p	declination of planet
L_B	hour angle of baseline
δ_B	declination of baseline
RA_p	right ascension of planet
r_p	radius of planet
$\vec{\Omega}$	apparent rotation vector of planet
$\vec{\Omega}_p$	intrinsic rotation vector of planet
RA_a	right ascension of rotation axis
δ_a	declination of rotation axis
Lat_H	latitude of Haystack
A	angle between RA_p and RA_a plus 90°
Θ	90° minus δ_a; angle of incidence
P	sidereal rotation angle
Lat_R	latitude of subradar point
$Long_R$	longitude of subradar point
D	angle between celestial north and direction of apparent rotation
X_o	distance from observer to center of planet
x_T	transmitted signal
x_i	incident wave
α, β	attenuation constants

x_R	received signal
$s(Y, Z)$	complex scattering function
$S(Y, Z)$	power scattering function
V_r	radial velocity of subradar point
τ	delay
G	antenna gain
λ	center wavelength of radar system
F	center-to-limb Doppler shift
ℓ	projected baseline
τ_e	code element length
τ_r	total code length
$A_c(\ell_Z)$	complex fringe amplitude for projected baseline ℓ_Z
$S(\Theta)$	mean planet scattering law
$a_{c, n}$	area of range-Doppler cell
T_S	system temperature corresponding to noise
T_H	Haystack antenna temperature equivalent to received signal
T_W	Westford antenna temperature equivalent to received signal
$S_\delta(Y, Z)$	deviation from mean planet
P_H	Haystack power
P_W	Westford power
P_{HW}	cross power

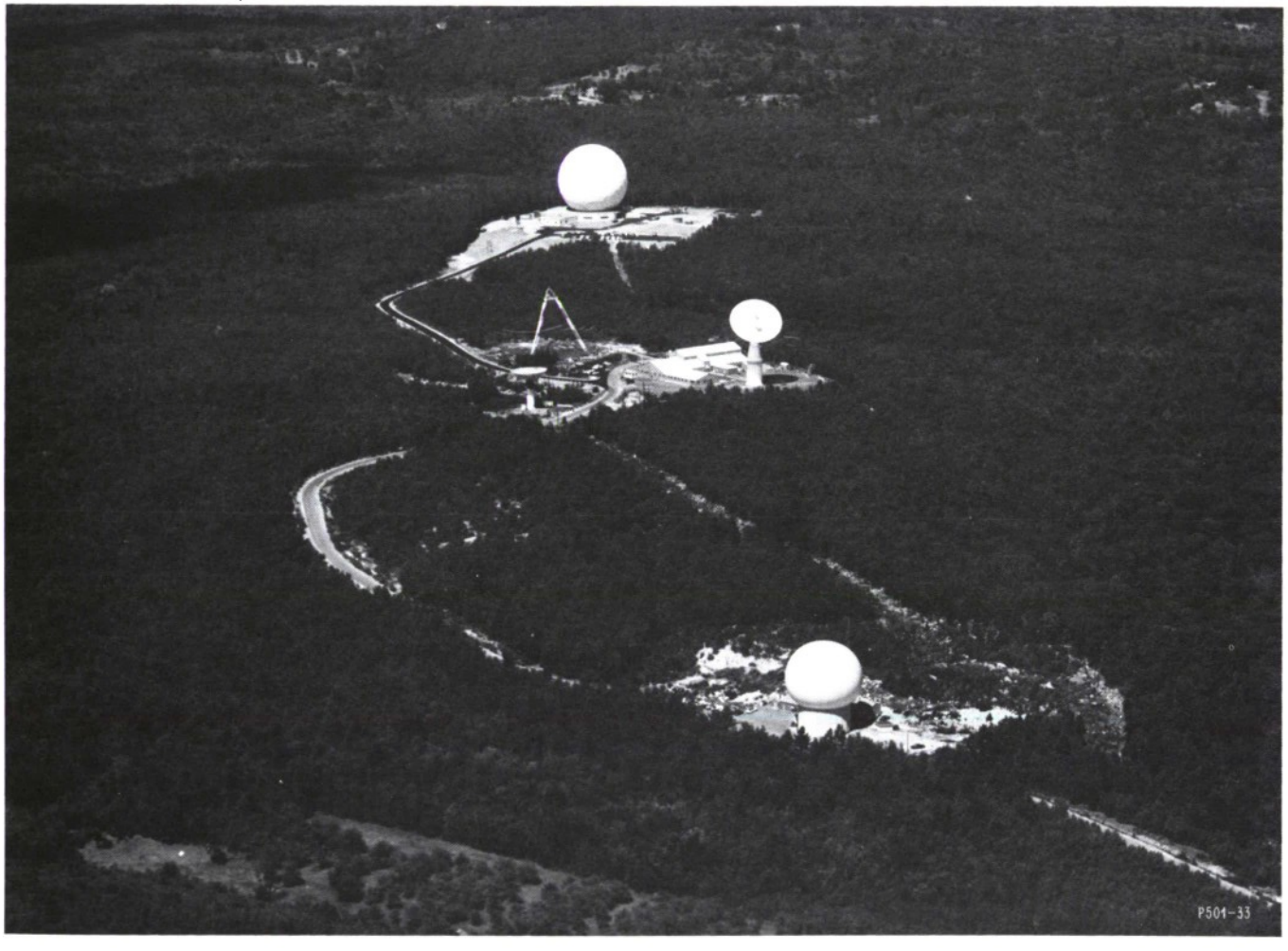

Millstone Hill complex.

A RADAR INTERFEROMETER STUDY OF VENUS AT 3.8 cm

I. INTRODUCTION

The planet Venus is surrounded by an optically opaque atmosphere such that neither the nature of its surface nor its period of rotation can be determined with eertainty from telescopic observation. However, its atmosphere is reasonably transparent at radio wavelengths, and much information has been gained from earth-based radar observations. For example, radar observations made during both the 1962 and 1964 inferior eonjunetions at the Jet Propulsion Laboratory (JPL)[1] have shown anomalous peaks in the speetrum of the reeeived echo which appear to be caused by regions of loeally enhaneed radar baekseatter on the planetary surfaee. The locations of these regions, as well as the surface rotation, were determined through a least-squares fitting procedure. From these observations, a sidereal rotation period of 250 (+4, −7) days retrograde and a north polar direction of 255° (+10°, −4°) in right ascension and 68° (±4°) in declination were obtained.

Measurements in which echo delay, as well as frequency information, was used were reported from the Arecibo Ionospheric Observatory (AlO)[2] for the 1964 inferior conjunction of Venus. These data, which are intrinsically more powerful as a means of determining pole position, yielded a rotational period of 245.1 (±2) days retrograde at 270.3° (±1°) right ascension and 66.7° (±1°) declination.

Measurements involving both a simple CW echo analysis, as well as a more complex combination of delay and frequency data, can benefit from the inclusion of additional information concerning the spatial distribution of the received echo. Since the disk diameter of Venus, even at inferior conjunction, does not exeeed roughly one minute of arc, this information to be useful must have a resolution of better than a few tens of seconds of arc. With this in mind, therefore, Lincoln Laboratory in late summer of 1967 undertook an observing program in which the existing 120-foot-diameter Haystack planetary radar system and the Westford 60-foot-diameter antenna were interconnected at a frequency of 7840 MHz as a phase-coherent radar interferometer. Measurements using both simple CW transmissions, as well as more complex time-eodcd signals, were made.

In this report, the theory of radar interferometry is first developed, followed by sections dealing with surface-mapping techniques and descriptions of the actual equipment and data-reduction procedures employed. Only a modest amount of interpretation of the results has been attempted, sinee it is anticipated that several journal articlcs will treat this aspeet of the research in greater detail.

II. THEORY OF RADAR INTERFEROMETRY

A. Interferometer Geometry

The interferometer geometry is shown in Fig. 1. The coordinate system used is centered at Haystack. $\vec{r}_1$ is a fixed vector from the intersection of the azimuth and elevation axes of Haystack, to the intersection of the azimuth axis and a horizontal plane through the elevation axis of Westford; $\vec{r}_2$ is a vector in that plane representing the offset of the elevation axis of the Westford antenna; and $\hat{r}_3$ is a unit vector‡ toward the apparent position of the subradar point on the planet being observed (parallax between the sites can be neglected). These vectors can be expressed as

$$\vec{r}_1 = D \sin E_W \hat{i}_{ZE} + D \cos E_W \sin A_W \hat{i}_{EA} + D \cos E_W \cos A_W \hat{i}_{NO} \tag{1}$$

$$\vec{r}_2 = d \sin A_p \hat{i}_{EA} + d \cos A_p \hat{i}_{NO} \quad \text{(differences in zenith neglected)} \tag{2}$$

$$\hat{r}_3 = \sin E_p \hat{i}_{ZE} + \cos E_p \sin A_p \hat{i}_{EA} + \cos E_p \cos A_p \hat{i}_{NO} \tag{3}$$

where D ($=|\vec{r}_1|$) is the distance between Haystack and Westford, d ($=|\vec{r}_2|$) is the elevation axis offset of Westford, A_p and E_p are the apparent azimuth and elevation of the planet, and A_W and E_W are the azimuth and elevation of Westford as seen from Haystack. The portion of the differential delay which is azimuth and elevation dependent is given by

$$\tau_d = \frac{1}{c_e}(\vec{r}_1 + \vec{r}_2) \cdot \hat{r}_3 = \frac{D}{c_e}[\sin E_W \sin E_p + \cos E_W \cos E_p \times \cos(A_p - A_W)] + \frac{d}{c_e} \cos E_p \tag{4}$$

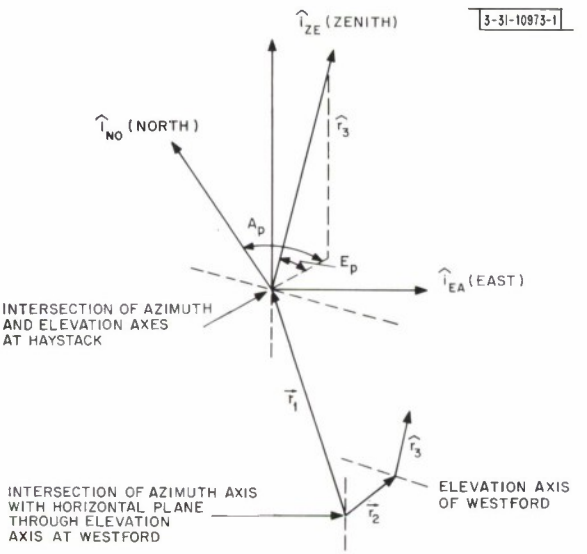

Fig. 1. Interferometer geometry.

‡ Throughout this report, the symbol (^) is used for o unit vector.

where c_e is the velocity of propagation along the baseline. Results of a baseline survey gave the following values for the baseline parameters:

$$D = 4066.16 \text{ feet}$$
$$A_W = S21°53'47" W \pm 6"$$
$$E_W = -1°22'53" \pm 4"$$
$$d = 12.5 \text{ inches.}$$

τ_d is a funetion of time as a result of the motion of the planet and gives rise to a differential Doppler effect or fringe rate of $(\omega/2\pi)\,[d\tau_d(t)/dt]$. The change of τ_d with position in the sky produces an interferometer fringe pattern for which it is more convenient to use celestial coordinates wherein

$$\tau_d \approx \frac{D}{c}\,[\sin\delta_B \sin\delta_p + \cos\delta_B \cos\delta_p \cos(L_p - L_B)] \tag{5}$$

where L_B and δ_B are the hour angle and deelination of the baseline. The expression is only approximate, as refraetion ean only be taken into aeeount to first order (plane parallel atmosphere) in this coordinate system. However, the expression is quite preeise enough to eompute the fringe spacing. Expressing $\vec{r}_1$ in eelestial coordinates ($|\vec{r}_2|$ is mueh smaller than $|\vec{r}_1|$ and is neglected), the projections of $\vec{r}_1$ in a plane normal to the direction of the planet are

$$e\,\frac{d\tau_d}{d\delta} = (\vec{r}_1)_N = D\,[\cos\delta_p \sin\delta_B - \cos\delta_B \sin\delta_p \cos(L_p - L_B)] \tag{6}$$

$$\frac{c}{\cos\delta_p}\,\frac{d\tau_d}{dL} = (\vec{r}_1)_W = D \cos\delta_B \sin(L_S - L_B) \quad . \tag{7}$$

The fringe spaeing in radians is the reeiprocal of the projeeted baseline component in wavelengths. Figure 2 shows a plot of the projeeted baseline in wavelengths for Venus on the day of the 1967 inferior conjunetion.

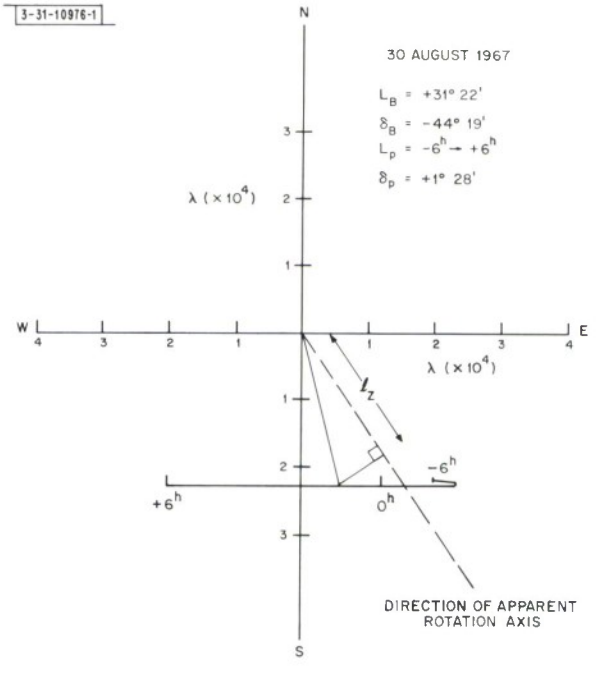

Fig. 2. Projected baseline (ℓ) for Venus.

B. Earth-Venus Geometry

Since, in this discussion, we are primarily interested in the mapping of the planetary surface, the orbital and rotation parameters will be assumed known. Any inconsistencies which might be attributed to errors in these parameters will be discussed in Sec. VI-C. The orbit of Venus will be described by its geocentric right ascension RA_p, declination δ_p, and distance.

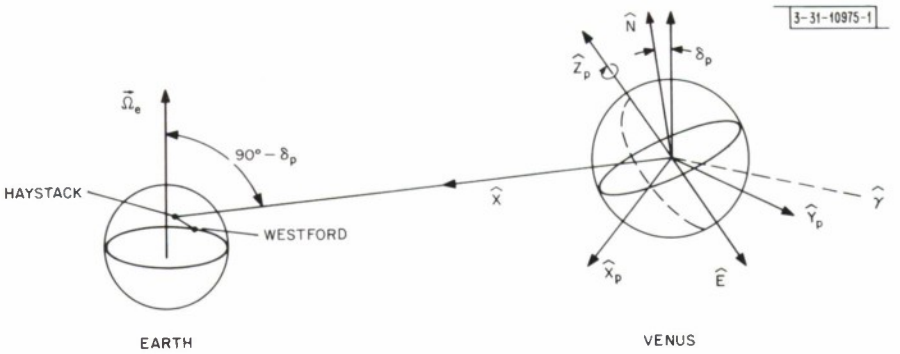

Fig. 3. Earth-Venus geometry.

It will also be assumed that Venus is a sphere of radius r_p which rotates with an angular velocity Ω_p relative to the local star system. The direction of Ω_p is given by its right ascension RA_a and declination δ_a. Figure 3 shows the Earth-Venus geometry. Three Venus-centered coordinate systems are used in the complete description of the radar-mapping process. The first is a system (X, Y, Z) where $\hat{X}$ is directed toward the transmitter, and $\hat{Z}$ is in the direction of the projection of the apparent rotation axis $\vec{\Omega}$ on a plane normal to $\hat{X}$. In this system, the subradar point is $(r_p, 0, 0)$. The second coordinate system (X, E, N) is the first rotated so that $\hat{N}$ is in the direction of increasing declination. The third coordinate system (X_p, Y_p, Z_p) is fixed to the planet so that $\hat{Z}_p$ is the pole or the direction of $\vec{\Omega}_p$, and $\hat{X}_p$ goes through the circle of zero longitude, $-40°$ being defined as the longitude of the subradar point on 20 June 1964 at 0^h UT (Ref. 1). Thus,

$$X_p = r_p \cos(\text{Lat}) \cos(\text{Long})$$

$$Y_p = r_p \cos(\text{Lat}) \sin(\text{Long})$$

$$Z_p = r_p \sin(\text{Lat}) \tag{8}$$

where Lat and Long are the latitude and longitude of a point on the surface of Venus. Conversion from (X, E, N) to (X_p, Y_p, Z_p) requires four rotations. The first rotation about $\hat{E}$ by the angle δ_p makes $\hat{N}'$ parallel to the earth's axis

$$X' = X \cos\delta_p + N \sin\delta_p$$

$$E' = E$$

$$N' = N \cos\delta_p - X \sin\delta_p \quad . \tag{9}$$

The second rotation about $\hat{N}'$ by the angle A makes $\hat{E}''$ in the opposite direction to the right ascension of the rotation axis, so that

$$A = RA_p - RA_a + 90° \tag{10}$$

as illustrated in Fig. 4. Thus,

$$\begin{aligned} X'' &= X' \cos A - E' \sin A \\ E'' &= E' \cos A + X' \sin A \\ N'' &= N' \quad . \end{aligned} \tag{11}$$

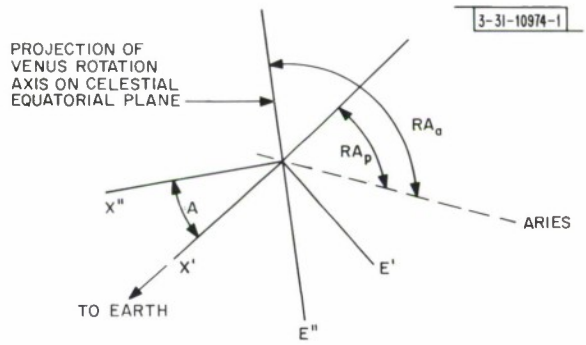

Fig. 4. View of Eorth-Venus geometry from celestial pole.

The third rotation about $\hat{X}''$ by Θ makes $\hat{N}'''$ parallel to $\hat{Z}_p$, where

$$\Theta = 90° - \delta_a \tag{12}$$

so that

$$\begin{aligned} X''' &= X'' \\ E''' &= E'' \cos\Theta + N'' \sin\Theta \\ Z_p = N''' &= N'' \cos\Theta - E'' \sin\Theta \quad . \end{aligned} \tag{13}$$

From Eqs. (9), (11), and (13),

$$\begin{aligned} X''' &= X \cos A \cos\delta_p - E \sin A + N \sin\delta_p \cos A \\ E''' &= X(\sin A \cos\delta_p \cos\Theta - \sin\Theta \sin\delta_p) + E(\cos A \cos\Theta) \\ &\quad + N(\sin\Theta \cos\delta_p + \cos\Theta \sin A \sin\delta_p) \\ Z_p &= X(-\cos\Theta \sin\delta_p - \sin\Theta \sin A \cos\delta_p) - E(\cos A \sin\Theta) \\ &\quad + N(\cos\Theta \cos\delta_p - \sin\Theta \sin\delta_p \sin A) \quad . \end{aligned} \tag{14}$$

The final rotation about $\hat{Z}_p$ by angle P makes $\hat{X}_p$ go through the definition of zero longitude,[1]

$$P = P_o + \Omega_p t \tag{15}$$

where P_o is the angle between $\hat{X}_p$ and the direction $(RA_a + 90°)$ when t = 0. Thus,

$$X_p = X''' \cos P - E''' \sin P$$

$$Y_p = E''' \cos P + X''' \sin P \quad . \tag{16}$$

Since the subradar point is given by

$$X_p = r_p$$

$$E = 0$$

$$N = 0$$

the latitude of the subradar point is

$$Lat_R = \sin^{-1}(-\cos\Theta \sin\delta_p - \sin\Theta \sin A \cos\delta_p) \tag{17}$$

from Eq. (14) by setting E = N = 0. Similarly, the longitude of the subradar point is

$$Long_R = P + \tan^{-1}\left(\frac{\sin A \cos\delta_p \cos\Theta - \sin\Theta \sin\delta_p}{\cos A \cos\delta_p}\right) \tag{18}$$

from Eqs. (14) and (16).

The transformation from (X, Y, Z), in which Z is the apparent rotation axis, to (X, E, N) requires one rotation by the angle D which is computed from the components of center-to-limb Doppler. The apparent rotation consists of the projection of the planet's rotation on the plane normal to the direction $\hat{X}$ plus the rotation due to the change in position of the planet,

$$\Omega_N = \Omega_p(\sin\delta_a \cos\delta_p - \sin\delta_p \cos\delta_a \sin A) - \frac{dRA_p}{dt} + \frac{r_e \Omega_e \cos(Lat_H) \cos L_p}{X_o} \tag{19}$$

and

$$\Omega_W = \Omega_p \cos\delta_a \cos A + \frac{d\delta_p}{dt} \tag{20}$$

where Lat_H is the latitude of Haystack, r_e is the radius of the earth, Ω_e is the rotation of the earth, and X_o is the distance to Venus. The last term is a correction for the earth's rotation which has to be included if the right ascension and declination of the planet are computed for the geocenter. From Eqs. (19) and (20),

$$D = \tan^{-1}(\Omega_W/\Omega_N) \quad . \tag{21}$$

The values of X_o, RA_p, and δ_p can be obtained from ephemeris tables. The following rotation constants[2] were assumed for Venus:

$$\delta_a = 66.7°$$

$$RA_a = 270.3°$$

$$\Omega_p = 1 \text{ rotation per } 243.16 \text{ days} - \text{retrograde.}$$

Values of the latitude and longitude of the subradar point were checked with computations by I.I. Shapiro.[3]

C. Relation of Received Signal to Planet's Surface

Using the coordinate system (X, Y, Z) defined in Sec. B above, the wave incident on the surface of the planet is related to the transmitted signal $x_T(t)$ by

$$x_i(\omega, Y, Z) = \alpha x_T(\omega) \exp\{-\frac{i\omega}{c} [X_o(t) - X(t)]\} \tag{22}$$

where

$$x_T(\omega) = \int x_T(t) e^{-i\omega t} dt \tag{23}$$

$X_o(t)$ is the distance to the center of Venus, and α is an attenuation constant. The plane wave assumed in Eq. (22) will be justified in Eq. (40b). If it is now assumed that each element of unit surface area on the planet inclined at an angle Θ to the incident beam returns a signal

$$x_R(\omega, Y, Z) = x_i(\omega, Y, Z)\, s(Y, Z) \tag{24}$$

then the integrated return will be

$$x_R(\omega) = \alpha \iint x_T(\omega)\, s(Y, Z) \exp\{-\frac{2i\omega}{c} [X_o(t) - X(t)]\} \frac{dY\,dZ}{\cos\Theta} \tag{25a}$$

where

$$\cos\Theta = \frac{X}{r_p} = \frac{(1 - Y^2 - Z^2)^{1/2}}{r_p} \quad . \tag{25b}$$

Expanding $X_o(t)$ and $X(t)$ into a constant and time-changing component due to rotation Ω and radial velocity V_r,

$$X_o(t) - X(t) = X_o(t_o) - X(t_o) + V_r t + Y\Omega t \tag{26}$$

so that Eq. (25) becomes

$$x_R(\omega) = \alpha \iint x_T(\omega')\, s(Y, Z)\, e^{-i\omega\tau(Y, Z)} \frac{dY\,dZ}{\cos\Theta} \tag{27}$$

where τ is the delay to the element at (X, Y, Z)

$$\tau = \frac{2 [X_o(t_o) - X(t_o)]}{c} \tag{28}$$

and ω' is the Doppler-shifted frequency

$$\omega' = \omega - \frac{\omega}{c} (2Y\Omega + 2V_r) \quad .$$

If the planet's orbit is known, it is possible to refer the signal to the center of the planet by continuously shifting one of the local oscillators by the amount

$$\frac{\omega}{c} 2V_r(t)$$

so that

$$x(\omega) = x_R(\omega) \exp[\frac{i\omega}{c} 2X_o(t)] = \alpha \iint x_T(\omega'')\, s(Y, Z)\, e^{-i\omega\tau(Y, Z)} \frac{dY\,dZ}{\cos\Theta} \tag{29}$$

where $\omega'' = \omega - (2\omega Y\Omega/c)$. The simplest signal to transmit is a sine wave (to within the frequency stability of the standard), in which case

$$|x_T(\omega)|^2 = \mu_o(\omega - \omega_o) \quad . \tag{30}$$

For a single antenna whose antenna beam is much larger than the planet, the receiver spectral power is

$$|x(\omega)|^2 = \alpha^2 \iiiint x_T(\omega'')\, x_T^*(\omega''\dagger)\, s(Y, Z)\, s^*(Y\dagger, Z\dagger) \times e^{-i\omega\tau(Y, Z)}\, e^{+i\omega\tau(Y\dagger, Z\dagger)}\, \frac{dY\,dZ\,dY\dagger\,dZ\dagger}{\cos^2\Theta}$$

$$= \alpha^2 \int S\left[\frac{c(\omega_o - \omega)}{2\Omega\omega},\ Z\right] \frac{dZ}{\cos\Theta} \tag{31}$$

where the power-scattering function S(Y, Z) is a real function

$$S(Y, Z) = \iint s(Y, Z)\, s^*(Y - y, Z - z)\, e^{-i\omega\tau(Y, Z)}\, e^{i\omega\tau(Y-y, Z-z)}\, dydz \quad . \tag{32}$$

The function within the integral is a delta function in y and z so that the power at frequency ω originates from a line

$$Y = \frac{(\omega_o - \omega)\, c}{2\Omega\omega} \tag{33}$$

parallel to the apparent rotation axis. α is the two-way attenuation which is related to the antenna gain G by

$$\alpha^2 = \frac{G^2\lambda^2}{64\pi^3 X_o^4}$$

provided S is defined as unity for a perfect isotropic scatterer. For simplicity, it is convenient to change the scale of the coordinates so that

$$X_n = X/r_p$$

$$Y_n = Y/r_p$$

$$Z_n = Z/r_p \tag{34}$$

and to introduce the center-to-limb Doppler shift F so that

$$|x(\omega)|^2 = r_p^2\alpha^2 \int S\left(-\frac{F\Delta\omega}{2\pi},\ Z_n\right) \frac{dZ_n}{\cos\Theta} \tag{35}$$

where

$$\Delta\omega = \omega - \omega_o \quad .$$

If the spectral analysis of the received signal is performed with a frequency resolution function $f(\omega)$, which for Fourier analysis of a sample of length T is

$$\left\{\frac{\sin\left[(\omega - \omega_c)\,\frac{T}{2}\right]}{(\omega - \omega_c)\,\frac{T}{2}}\right\}^2 \tag{36}$$

then the output of each "frequency channel c" is

$$|x_c|^2 = \int |x(\omega)|^2 f_c(\omega) \frac{d\omega}{2\pi} \tag{37}$$

since

$$x_c = \int_o^T x(t)\, e^{-i\omega t}\, dt \quad .$$

The signal y(t) received by the second antenna from an element on the planet is shifted in phase because of the different distances of the element from the two stations. From Fig. 5,

$$y(\omega) = \beta\alpha \iint x_T(\omega'')\, s(Y, Z)\, e^{-i\omega\tau(Y, Z)}\, e^{-i\omega\tau_d} \times e^{2\pi i Z_n \ell_Z}\, e^{2\pi i Y_n \ell_Y} \frac{dY\, dZ}{\cos\Theta} \tag{38}$$

where τ_d is the delay differential to the subradar point, given by Eq. (4).

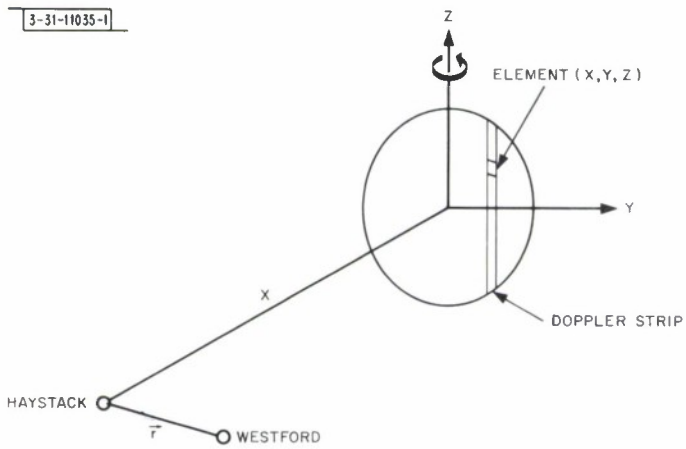

Fig. 5. Relative distance between two antennas and point on planet.

ℓ_Y and ℓ_Z are baseline projections in the $\hat{Y}$ and $\hat{Z}$ directions in units of wavelengths per planetary radius. Thus,

$$\ell_Y = \frac{(\vec{r})_Y\, \omega r_p}{2\pi c X_o}$$

$$\ell_Z = \frac{(\vec{r})_Z\, \omega r_p}{2\pi c X_o} \tag{39}$$

where the Y and Z components of the baseline can be obtained from the N and W components given in Eqs. (6) and (7).

$$(\vec{r})_Z = (\vec{r})_N \cos D + (\vec{r})_W \sin D$$

$$(\vec{r})_Y = -(\vec{r})_W \cos D + (\vec{r})_N \sin D \quad . \tag{40a}$$

The phase differences expressed in Eq. (34) assume the received signal components to be plane waves, but are in error at most by only

$$\frac{D^2\omega}{2X_o c 2\pi} \sim 10^{-6} \text{ radian} \quad (\omega/2\pi = 7840\,\text{MHz, and } X_o = 0.3 \text{ astronomical unit}) \tag{40b}$$

as a result of the wavefront curvature.

From Eqs. (30) and (38), the cross-spectral power of received signals is

$$y(\omega)\, x^*(\omega) = \beta\alpha^2 \iiiint x_T(\omega')\, x_T^*(\omega' \dagger)\, s(Y, Z)\, s^*(Y\dagger, Z\dagger)$$

$$\times e^{-i\omega\tau(Y,\,Z)}\, e^{i\omega\tau(Y\dagger,\,Z\dagger)}\, e^{-i\omega\tau_d}\, e^{2\pi i Z_n \ell_Z}\, e^{2\pi i Y_n \ell_Y}\, \frac{dY dZ dY\dagger dZ\dagger}{\cos^2\Theta}$$

$$= r_p^2 \beta\alpha^2 \int S(-\Delta\omega F, Z_n)\, e^{-i\omega\tau_d}\, e^{2\pi i Z_n \ell_Z}\, e^{-2\pi i \Delta\omega F \ell_Y}\, \frac{dZ_n}{\cos\Theta} \tag{41}$$

for a CW transmission. If $y(t)$ is rotated by $\exp[i\omega\tau_d]$, then the lines of constant phase become stationary on the planet. Further rotation by $\exp[2\pi i \Delta\omega F \ell_Y]$ makes the line of zero phase perpendicular to the Doppler axis. If the frequency resolution $\delta\omega$ used is sufficiently small that

$$\delta\omega F 2\pi \ell_Y << 1 \tag{42}$$

then the power and cross-power outputs for each channel are

$$|x_c|^2 = r_p^2 \alpha^2 \int S_c(Z_n)\, \frac{dZ_n}{\cos\Theta} \tag{43}$$

and

$$x_c y_c^* = r_p^2 \alpha^2 \beta \int S_c(Z_n)\, e^{2\pi i Z_n \ell_Z}\, \frac{dZ_n}{\cos\Theta} \tag{44}$$

where S_c is the scattering function integrated over the Doppler strip.

If the transmitted signal is phase-reversal coded by multiplication with a code $c(t)$ which has an element length τ_e and repeats every τ_r seconds, then

$$x_T(\omega) = \mu_o(\omega - \omega_o) \otimes c^*(\omega) \quad . \tag{45}$$

The decoding of the received signal is achieved by multiplication with the transmitted code delayed by different amounts. There are τ_r/τ_e delay channels formed which can then be spectrum analyzed in the same fashion as the CW signal previously described.

The code used in the coding process is controlled by a drifting clock (see Sec. IV-D) so that, if $c(\omega)$ is the frequency domain description of the coding signal, $c(\omega'')\exp[-i\omega\tau_n]$ is the frequency domain description for the n^{th} delay of decoding signal. After decoding, the frequency domain description of the signal for the n^{th} delay is

$$x_{T_n}(\omega) = \alpha \iint [\mu_o(\omega'' - \omega_o) \otimes c^*(\omega'')] \otimes c^*(\omega'')\, s(Y, Z)$$

$$\times e^{i\omega\tau_n}\, e^{-i\omega\tau(Y,\,Z)}\, \frac{dY dZ}{\cos\Theta} \tag{46}$$

$$= \alpha \int s(-\Delta\omega F, Z_n)\, R_c[\tau_n - \tau(-\Delta\omega F, Z_n)]\, \frac{dZ_n}{\cos\Theta} \tag{47}$$

where $R_c(\tau)$ is the autocorrelation function of the code.

This expression assumes the planet's Doppler spread is less than the code repetition rate, as it neglects the frequency foldover effects that are produced when this is not the case. Thus, the output of the n^{th} delay channel and c^{th} frequency channel is

$$|x_{c,n}|^2 = r_p^2 \alpha^2 (S^U_{c,n} + S^L_{c,n}) \tag{48}$$

and the output of the "cross channel" is

$$x_{c,n} y^*_{c,n} = r_p^2 \alpha^2 \beta \left(S^U_{c,n}\, e^{2\pi i |Z_n| \ell_Z} + S^L_{c,n}\, e^{-2\pi i |Z_n| \ell_Z} \right) \tag{49}$$

where $S_{c,n}$ is the scattering function integrated over the frequency (resolution along Y_n) and delay (resolution along X_n) resolutions. Since the delay resolution is ambiguous in the sign of Z_n, the superscripts U and L signify the upper and lower hemisphere points. If the frequency channel number is measured from the zero frequency or frequency of the return from the subradar point, and the delay channel number is measured from the delay that just grazes the subradar point,

$$\left.\begin{matrix} S^U_{x,n} \\ S^L_{x,n} \end{matrix}\right\} \cong \iint_{Y_n 1 \pm Z_n 1}^{Y_n 2 \pm Z_n 2} \frac{S(Y_n, Z_n)\, dY_n dZ_n}{\cos \Theta} \tag{50}$$

where

$$Y_n 1 = (c - \tfrac{1}{2}) \frac{\delta\omega}{2\pi} F$$

$$Y_n 2 = (c + \tfrac{1}{2}) \frac{\delta\omega}{2\pi} F \tag{51}$$

and

$$X_n 1 = 1 - \frac{(n-1)\, \delta\tau 2c}{r_p}$$

$$X_n 2 = 1 - \frac{n \delta\tau 2c}{r_p} \tag{52}$$

$$Z_n 1 = \sqrt{1 - [(X_n 1)^2 + (Y_n 1)^2]}$$

$$Z_n 2 = \sqrt{1 - [(X_n 2)^2 + (Y_n 2)^2]} \quad . \tag{53}$$

III. METHODS OF MAPPING SURFACE OF PLANET

A. One-Dimensional Interferometry to Reconstruct Received Power Distribution Along a "Doppler Strip"

It was shown in Sec. II that, when a CW signal is transmitted, the echo received in a given frequency channel, after correction for the Doppler shift to the subradar point (Doppler tracking), arises from a strip on the face of the planet toward the radar. While the power in a given frequency channel for a single antenna represents an integration along the entire Doppler strip, the crosscorrelation power between the two antennas of the interferometer yields a Fourier component of the distribution along the strip. After we correct for the planet's motion relative to the interferometer, the cross power is given by Eq. (44) which can be rewritten

$$A_c(\ell_Z) = \int S(c, Z_n)\, e^{2\pi i Z_n \ell_Z} \frac{dZ_n}{\cos\Theta} \quad . \tag{54}$$

$A_c(\ell_Z)$ is the complex fringe amplitude $(x_c y_c^*)$ for projected baseline ℓ_Z, omitting the attenuation constants. Equation (54) can be inverted by one-dimensional Fourier theory

$$\frac{S(c, Z_n)}{\cos\Theta} = \int A_c(\ell_Z)\, e^{-2\pi i Z_n \ell_Z} \frac{d\ell_Z}{2\pi} \tag{55}$$

where the limits of integration would have to be infinite for a perfect inversion. If the maximum projected baseline is $\ell_{Z\,max}$, then the resolution pattern is

$$\int_{-\ell_{Z\,max}}^{\ell_{Z\,max}} e^{-2\pi i Z_n \ell_Z} \frac{d\ell_Z}{2\pi} = \frac{\sin 2\pi Z_n \ell_{Z\,max}}{2\pi Z_n \ell_{Z\,max}} \tag{56}$$

or a half-power width of

$$\Delta Z_n \cong \frac{1}{2\ell_{Z\,max}} \tag{57}$$

in practice, it is difficult to cover a wide range of ℓ_Z without a fortuitous baseline orientation to make full use of changes with hour angle that result from a combination of those changes ℓ_N and ℓ_W illustrated in Fig. 2. (ℓ_Z is the projection onto the dashed line in Fig. 2.) However, since S is real,

$$A_c^*(\ell_Z) = A_c(-\ell_Z) \tag{58}$$

so that only the magnitude of the projected baseline is important; also, it can be assumed the reflected power is limited to the planet surface so that

$$S(c, Z_n) = 0 \tag{59}$$

for values of $|Z_n| \geq Z_{n\,max}$, where

$$Z_{n\,max} = \sqrt{1 - Y_n^2(c)} \quad . \tag{60}$$

This restriction of $S(c, Z_n)$ allows $A_c(\ell_Z)$ to be reconstructed from sampled values. From the sampling theorem, $A_c(\ell_Z)$ need only be sampled at intervals of

$$\Delta\ell_Z = \frac{1}{2Z_{n\,max}} \quad . \tag{61a}$$

If only the Fourier components of the spatial distribution corresponding to baseline projections between $\ell_{Z\,min}$ and $\ell_{Z\,max}$ are measured, then the equivalent resolution pattern for a uniformly weighted transform is

$$\frac{\cos[\pi Z_n(\ell_{Z\,min} + \ell_{Z\,max})]\, \sin[\pi Z_n(\ell_{Z\,max} - \ell_{Z\,min})]}{\pi Z_n(\ell_{Z\,max} - \ell_{Z\,min})} \quad . \tag{61b}$$

B. Resolution of "Range-Doppler Ambiguity" with Two-Element Interferometer

When the transmitted signal is coded so that single-antenna measurements resolve the planet into range-Doppler cells, there is a twofold ambiguity, that is, two points on the planet

have the same range and Doppler shift. However, the cross-power range-Doppler cells are the vector sum of contributions from the ambiguous points as shown in Eqs. (48) and (49).

$$P(c,n) = S^{U}_{c,n} + S^{L}_{c,n} \tag{62}$$

and

$$A(c,n) = S^{U}_{c,n}\, e^{i\varphi(c,n,\ell_Z)} + S^{L}_{c,n}\, e^{-i\varphi(c,n,\ell_Z)} \tag{63}$$

where $P(c,n)$ is the single-antenna power, and $A(c,n)$ is the cross power for the c^{th} frequency channel and n^{th} delay. The interferometer phase for the upper or northern-range Doppler cell is $\varphi(c,n,\ell_Z)$. Equation (63) assumes that range-Doppler cell is much smaller than the fringe spacing. The range-Doppler mapping geometry is illustrated in Fig. 6(a-b). Equations (62) and (63) can be solved for S^U and S^L provided φ is not a multiple of 2π. However, if measurements are made over some change of baseline projection ℓ_Z, a least-squares fit to the data can be performed, thereby eliminating the case of φ being a multiple of 2π. The least-squares solution to Eq. (63) is

$$\left.\begin{matrix} S^{U}_{c,n} \\ S^{L}_{c,n} \end{matrix}\right\} = \frac{\left[\sum_{\ell_Z} \mathrm{Re}\, A(c,n) \cos\varphi(c,n,\ell_Z) \sum_{\ell_Z} \sin^2\varphi(c,n,\ell_Z) \pm \sum_{\ell_Z} \mathrm{Im}\, A(c,n) \sin\varphi(c,n,\ell_Z) \sum_{\ell_Z} \cos^2\varphi(c,n,\ell_Z)\right]}{\sum_{\ell_Z} \sin^2\varphi(c,n,\ell_Z) \sum_{\ell_Z} \cos^2\varphi(c,n,\ell_Z)} \tag{64}$$

which provides the best estimate of the ratio $S^{U}_{c,n}/S^{L}_{c,n}$, while the single-antenna measurements are used to estimate the sum of S^U and S^L.

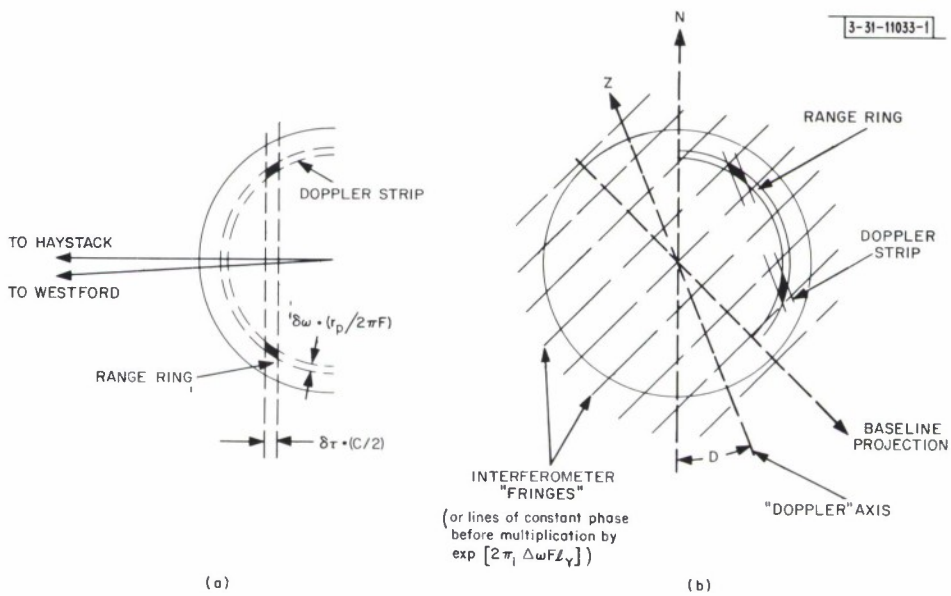

Fig. 6. (a) Twa regians with same range and Dappler shift; (b) their lacations in interferameter fringe pattern.

C. Signal-to-Noise Ratio Analysis

It is convenient to convert received power into temperature and to assign a system temperature T_S to the receiver and sky background noise. From Eq. (48),

$$P_{c,n} = \alpha^2 P_T r_p^2 (S^U_{c,n} + S^L_{c,n}) \tag{65}$$

where P_T is transmitted power. If the planet were uniformly rough, then it could be described by a scattering function which is only a function of the angle of incidence Θ, in which case

$$P_{c,n} = \alpha^2 P_T r_p^2 \frac{S(\Theta)}{\cos\Theta} a_{c,n} \tag{66}$$

where a is the area of the range-Doppler cells in the Y_n, Z_n plane. Converting to temperature,

$$T_H(c, n) = \frac{G^2 \lambda^2 P_T r_p^2 S(\Theta)\, a_{c,n}}{64\pi^3 X_o^4 K \cos\Theta} \tag{67}$$

where K is Boltzmann's constant. The fractional cross section relative to a perfect isotropic reflector is

$$\frac{\int \frac{S(\Theta)}{\cos\Theta}\, dY_n dZ_n}{\pi} \quad . \tag{68}$$

The Westford antenna temperature is

$$T_W = \frac{T_H G_W}{G_H} \tag{69}$$

and effective system temperature for the cross power is

$$T_S = \sqrt{T_{S_H} T_{S_W}} \quad . \tag{70}$$

From the theory of a Gaussian process, the rms deviation in the measured temperature is

$$\Delta T_{H_{rms}} = \frac{\left(T_{S_H} + T_H\right)}{\sqrt{\Delta f T}} \tag{71}$$

where Δf is the frequency resolution, and T is the integration time. The "noise threshold" of the cross power is

$$|\Delta T_{WH}|_{rms} = \frac{\sqrt{\left(T_{S_H} + T_H\right)\left(T_{S_W} + T_W\right)}}{\sqrt{\Delta f T}} \tag{72}$$

and the rms deviation of the measured phase is

$$\Delta\epsilon_{rms} = \frac{\sqrt{\left(T_{S_H} + T_H\right)\left(T_{S_W} + T_W\right)}}{\sqrt{2}\,|T_{WH}|\,\sqrt{\Delta f T}} \quad . \tag{73}$$

IV. DESIGN AND CONSTRUCTION

A. Radio Frequency and Local Oscillator Systems

The radio frequency (RF) portions of the interferometer are shown in Fig. 7. The transmitter is coupled to the right-handed circular polarization port of Haystack, while both receivers

are coupled to the orthogonal polarization (left-handed) ports. A system temperature of about 60°K was achieved at Haystack using a maser, and about 150°K at Westford using a parametric amplifier.

The local oscillator (LO) system is the critical part of the interferometer, since phase coherence and stability depend on the LO's relative phase noise and stability. The first and most critical LOs are klystron oscillators (at 7710 MHz) which are phase locked to reference signals derived from a station standard. Figure 8 shows a block diagram of the LO phase-lock system in which the klystron is servo controlled to the 64^{th} harmonic of 120 + 30 MHz.

B. Intersite Coupling

In order to maintain constant phase difference between the klystrons at the stations, it was necessary to compensate for changes in the electrical length of the cables carrying the reference signals between the two stations. The transmission line servo system shown in Fig. 9 maintains constant electrical length by reflecting some of the 120-MHz reference so that a phase comparison with the transmitted signal can be performed and used to provide an error signal. In order to identify the reflected signal, a 100-kHz phase-reversal modulation is applied to the reflected signal. Figure 10(a) shows the mechanical line "stretchers" used to correct the line length. Figures 10(b), (c), and (d) show the Westford receiver and parametric amplifier.

C. Data Interface to CDC 3300 Data-Processing Computer

The final intermediate frequency (IF) of both the Haystack and Westford receiver channels was 2 MHz. The CDC 3300 Direct Data Interface converted the signals into a form suitable for digital processing in the CDC 3300 data-processing computer.

The IF signals were first band limited to reduce the dynamic range requirements of the signal processing. Then, each channel was frequency translated to a 0-Hz IF by two identical balanced mixers fed by quadrature reference signals at 2 MHz. The resulting pair of quadrature video signals represented orthogonal components of a complex signal. These video signals were then filtered by an identical pair of low-pass filters that produced the equivalent effect of a single bandpass filter at IF.

The filters used for the CW data were 5-pole low-pass filters with cutoff frequencies at 256 Hz, which defined the total processing bandwidth of 512 Hz (±256). The filters used for the coded-pulse data were rectangular 500-μsec pulse-matched filters.

In the coded-pulse case, the planetary Doppler frequency spread was used to limit the spectral width of the signal data processed. Noise data were unavoidably aliased by the subsequent sampling. The CW signals were deliberately offset in frequency by +100 Hz so that a symmetrical noise comparison bandpass was available and to avoid centering the signal on the troublesome zero-frequency point. (DC offsets in the analog system show up as false zero-frequency signals in the subsequent processing.)

Filtered signals were amplified and simultaneously sampled by a 4-input analog sample-and-hold multiplexer (these four signals are the two pairs of complex signals for Haystack and Westford receivers). The "held" signals were then sequentially encoded by an 8-bit A/D converter. Encoder output was placed in the proper format and transmitted directly to the lower 16K core memory of the CDC 3300 data-processing computer by the Direct Data Interface.

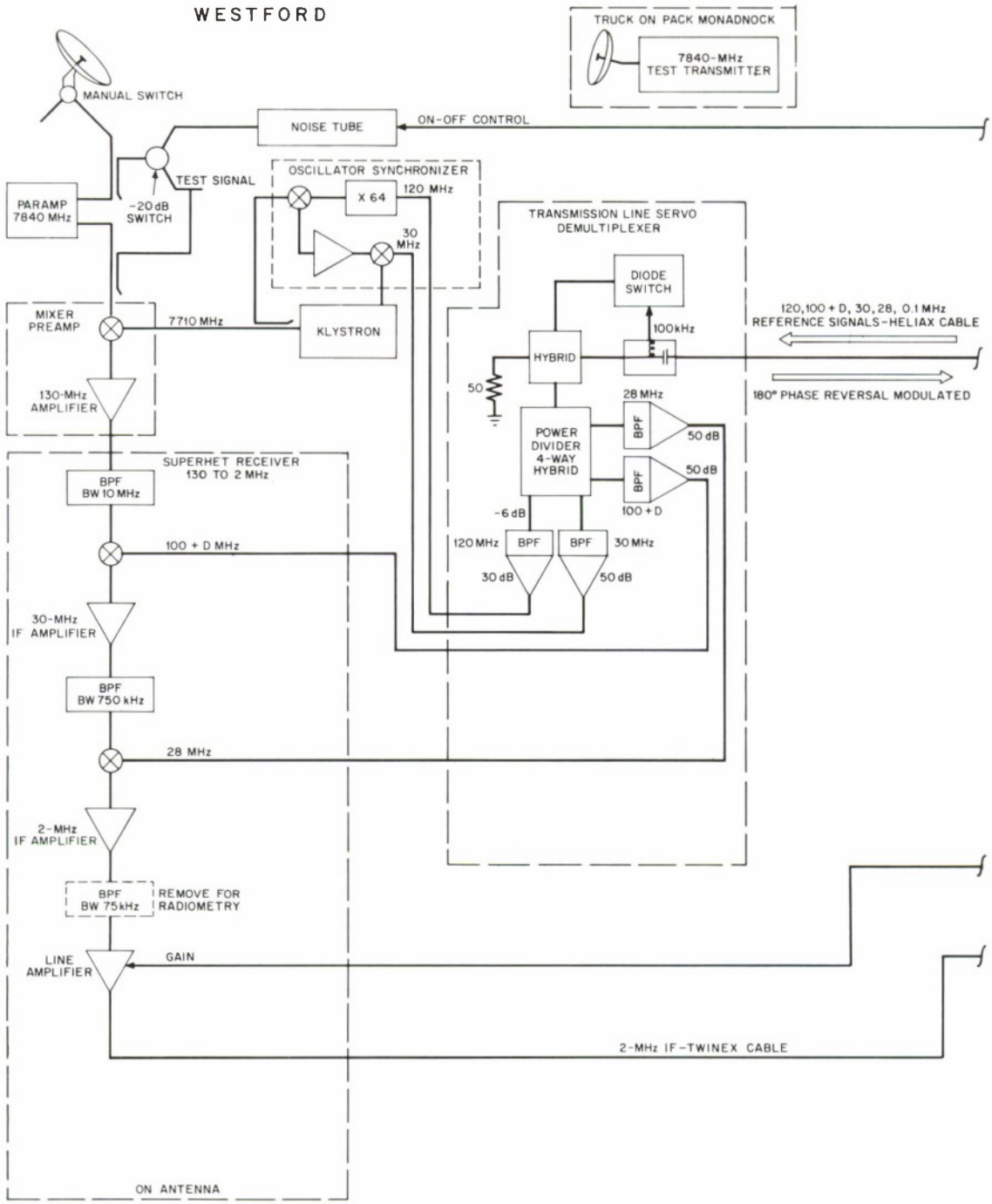

Fig. 7. RF black diagram.

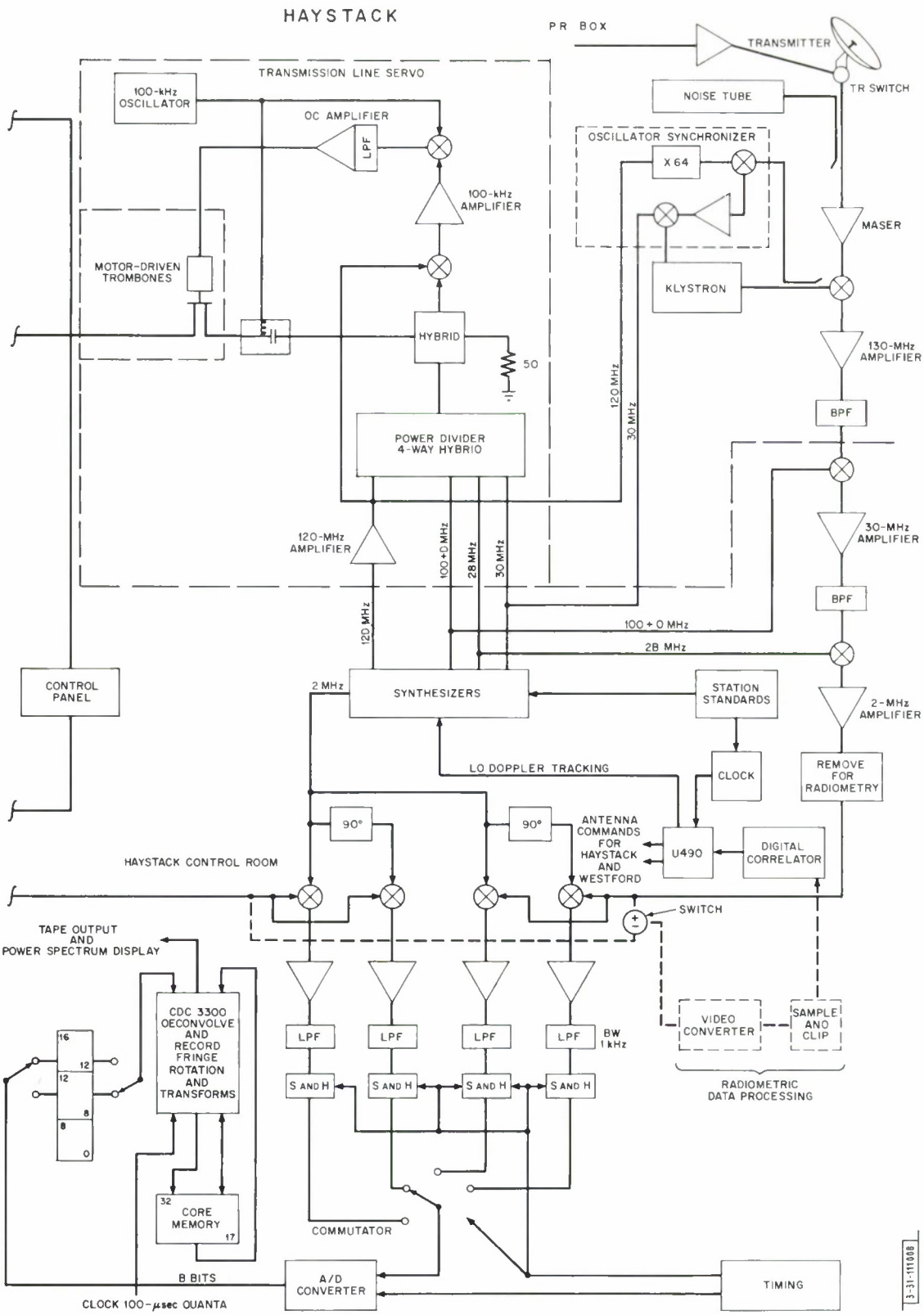

Fig. 7. Continued.

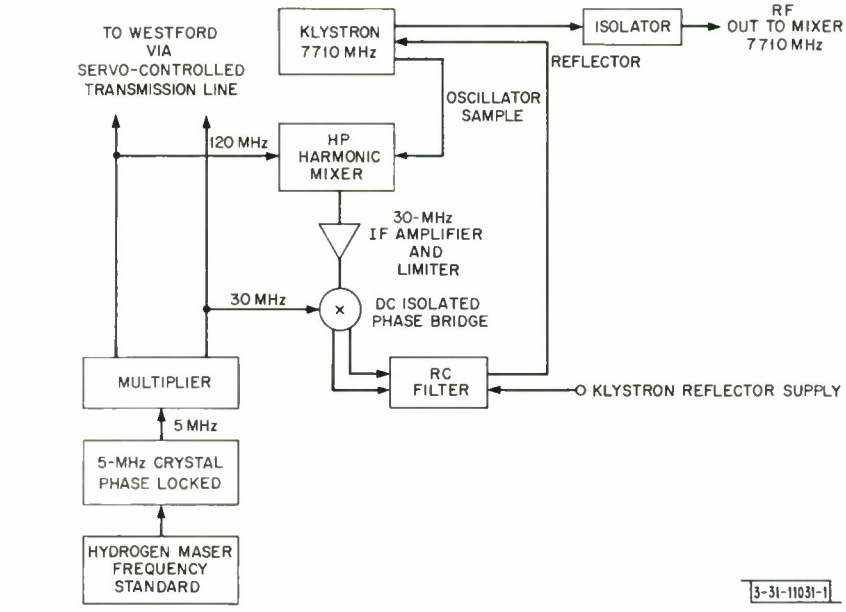

Fig. 8. LO phase-lack system.

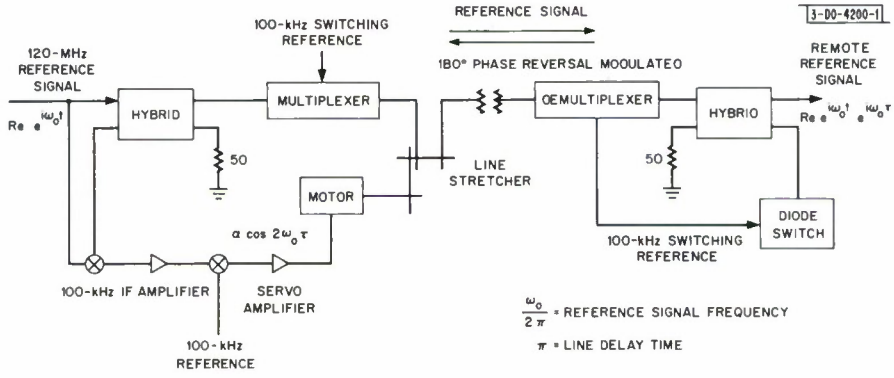

Fig. 9. Transmission line servo system.

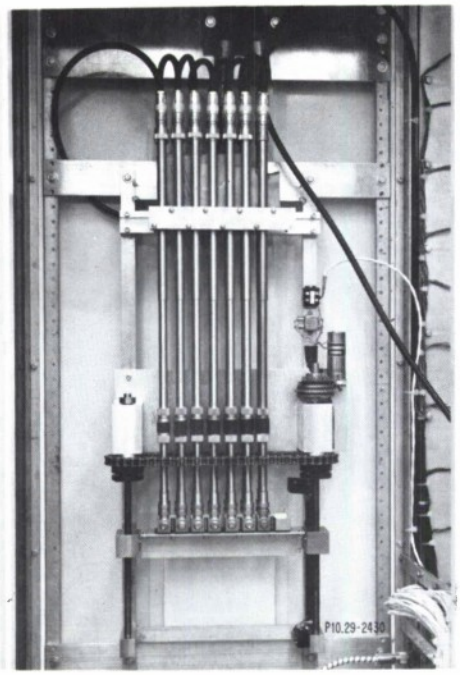

Fig. 10(o). Line stretchers.

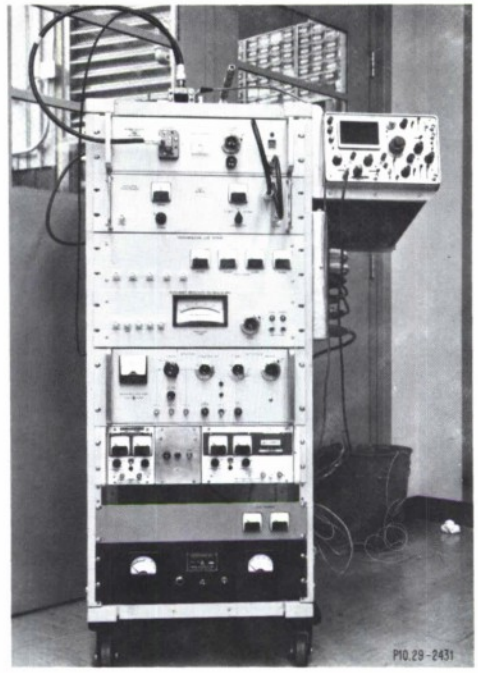

Fig. 10(b). Westford receiver at Haystock.

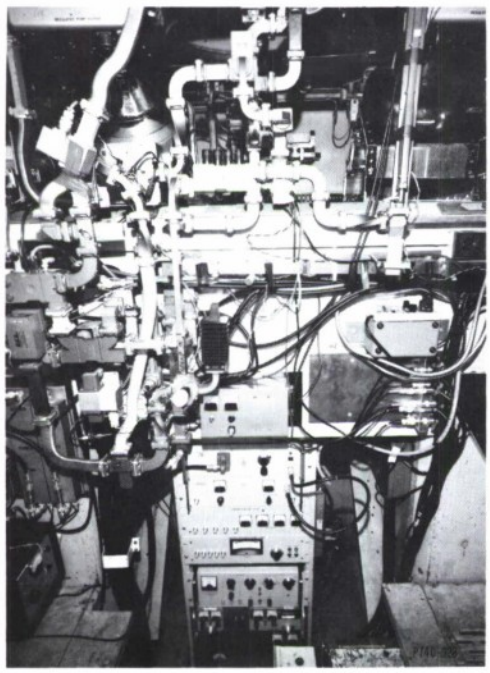

Fig. 10(c). Westford receiver at Westford.

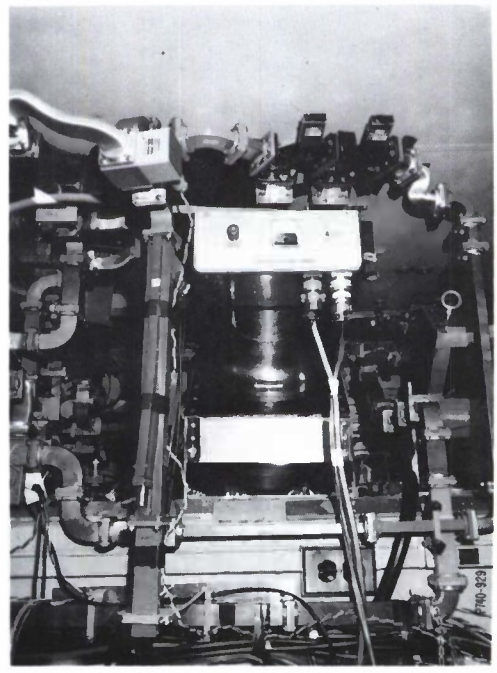

Fig. 10(d). Close-up view of Westford porometric omplifier.

The Interface is under timing control of the Radar Sequencer, which generates start and stop functions as well as supplying range rate offset sampling pulses. The Interface directly controls the location in core memory for each data word, and periodically communicates control and time information to the computer program by a standard computer communication channel, to synchronize the computer program cycling to the radar timing.

The CW data were sampled at a rate of 512 samples per second for each complex pair of samples, covering an unambiguous frequency range of 512 Hz. The coded-pulse data were sampled for 31 points at 500-μsec spacing for each code interval of 15.5 msec. Each range box then effectively covered an unambiguous frequency range of 64.5 Hz, which produces some frequency aliasing of the noise in the analog signal bandwidth being encoded.

D. Doppler and Range Rate Tracking

During the experiments, the radar receiver was continuously tuned to remove the Doppler frequency shift of the received signal arising from the motion of the planet's center with respect to the observer. The ranging experiments also required a clock signal that was offset in frequency to compensate for the range rate of the moving planet. Equipment used for tracking both the Doppler shift and range rate was under control of the Univac 490 pointing computer. The basic frequency control information was derived from the planetary ephemeris.

Doppler frequency was removed by offsetting the second receiver LO at 100 MHz by the amount of the predicted Doppler shift. This LO signal was generated using a digitally controlled frequency synthesizer (HP5100A). The frequency was incremented in 0.1-Hz steps by command of the U490 pointing computer at a rate of 20 commands per second. Since the typical rate of change of frequency was less than 2 Hz/sec, the Doppler shift was compensated with a precision of ±0.1 Hz and with an accuracy determined by the basic ephemeris and knowledge of time. Since the coherent data processing did not attempt an equivalent frequency resolution finer than 1 Hz, the frequency tuning system itself should not have produced significant spectral smearing or offset. Although the frequency of the synthesizer was stepped 20 times per second, phase discontinuities of the LO were produced only by 1-kHz control digit changes which occurred typically at 15-minute intervals.

The equipment used for generating the range rate offset clock signal took advantage of the fact that the fractional frequency offset required is the same as the ratio of Doppler frequency shift to carrier frequency. The carrier frequency was 7840 MHz and the basic clock was derived from the 1-MHz station standard frequency. The generated Doppler frequency offset present in the second LO signal conceptually was divided by 7840 and applied as a single-sideband modulation to the standard 1-MHz clock signal, preserving sign as well as magnitude. The actual hardware implementation was, in fact, more complex but did produce an offset clock signal that was used to sample the received signal for digital processing. In effect, a moving time base that tracked the planetary motion was used to produce a "stationary" target with respect to the computer data processing.

E. System Sequencer

The timing signals for the Hayford experiments are controlled by the Haystack Radar Sequencer. All experiments start on a selected minute. Transmission is then enabled for an interval equal to the round-trip signal flight time (received from the target ephemeris and quantized in 1-μsec increments).

After the flight time has elapsed, control lines are activated which signal the changeover from transmit to receive. The signal A/D converter and computer interface are enabled in preparation for the data-taking phase.

On the occurrence of a preset time pulse (about 30 sec later), sample commands are generated and transferred to the A/D control unit. The incoming return is sampled, the resulting 8-bit word is formatted, and the characters are transferred into the computer's storage bank. Samples are taken continuously until another flight-time interval has elapsed, at which time stop commands are generated, control is transferred to the computer program, and the system is readied for another run.

All timing during the receive interval is based on a Doppler-corrected 1-MHz clock which compensates for the time compression (expansion) of the target return. The sample pulse generators and interval counters thereby track the return in time. System timing functions are generated relative to the initial start with a precision of ±125 nsec and to an accuracy of 1 μsec.

F. System Tests

Assuming that both systems already operate as single-antenna planetary radars, the major tests are those concerned with testing the operation of the system as an interferometer. The first test consisted of running both receivers adjacent to each other (at Haystack), with the intersite coupling cables making a loop through the Millstone radar (approximately half way between Haystack and Westford). By feeding a test signal into both receivers, the relative phase stability of the interferometer receivers could be checked directly. Figure 11 shows the long-term phase stability, while Figs. 12(a) through (c) indicate short-term stability or phase noise of the system.

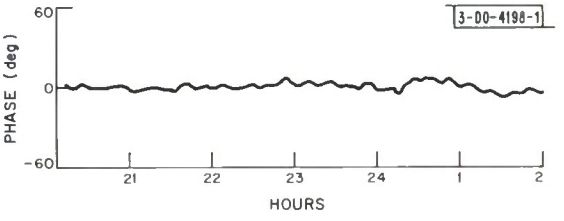

Fig. 11. Instrumental phase stability.

Further phase stability tests were made with the Westford receiver installed on the 60-foot antenna. These tests were first made with a test transmitter located on a pattern truck 50 km away. Large relative phase fluctuations were observed, as shown in Fig. 13; however, these fluctuations were shown to be largely due to refractive index fluctuations by repeating the test with a test transmitter at Haystack (Fig. 14).

V. DATA-REDUCTION TECHNIQUES

A. Atmospheric Fluctuations and Refraction

When computing the fringe pattern or the position of the lines of constant phase relative to the celestial sphere, it is necessary to take careful account of the refraction in the earth's atmosphere and ionosphere. If the earth's atmosphere and ionosphere were plane parallel and uniform along the plane, then the ray paths reaching two antennas at equal elevations are equal, so that the interferometer phase $\omega\tau_d$ could be computed from Eq. (5). In other words, in this case the baseline can be considered to be outside the atmosphere since the atmosphere does not affect the fringe pattern location. Because of the curvature of the earth and the nonuniformity of the atmosphere, a precise estimate of the location of the fringe pattern can only be made by integrating the electrical length along the ray path to each antenna. However, the effect of earth

Fig. 12(o). Phosor of Haystack (top trace) and relotive phase (lawer trace) with bright spot shawing zero-frequency affset.

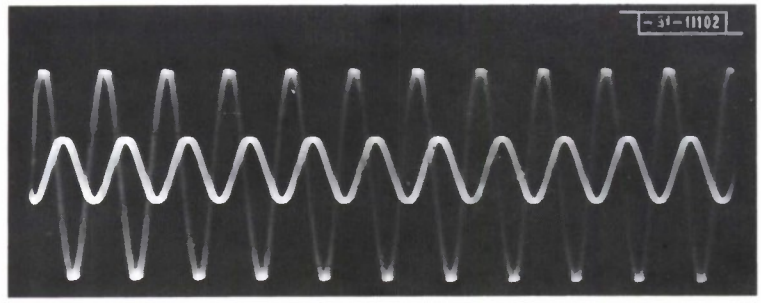

Fig. 12(b). Phose naise af Haystock and Westfard signals relative ta statian stondard (10-sec exposure of 2-MHz signals with the statian standard 1 MHz as scope sync).

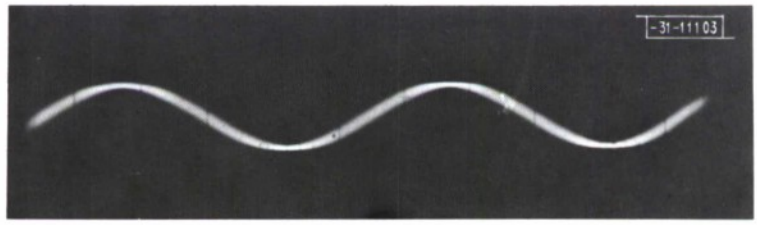

Fig. 12(c). Relotive phase naise (10-sec exposure of Hoystock 2-MHz IF with Westford IF as scope sync).

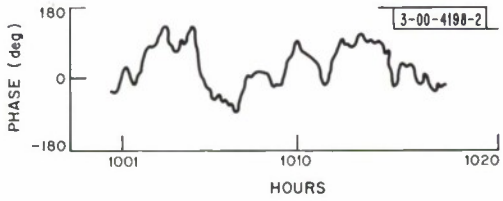

Fig. 13. Differential phose between Westfard ond Haystack measured using test signol trons-mitted from pottern truck 50 km owoy.

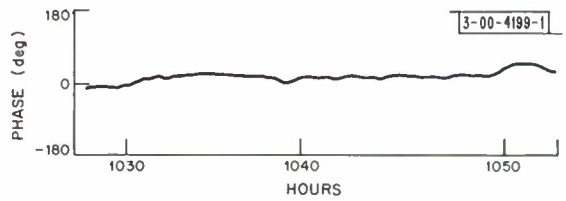

Fig. 14. Phase between Westford and Hoystack far one-woy tronsmission of test signol from Hoystock to Westford.

curvature can be taken into account, when the antennas are spaced only a few miles apart or less, by using Eq. (4). The apparent elevation E_p differs from the elevation without the atmosphere by the refractive bending ϵ. When E_W and d are zero, Eqs. (4) and (5) give the same result if ϵ is approximated by

$$\epsilon \approx (N \times 10^{-6}) \cot E_p \tag{74}$$

where N is the refractive index on the ground in N-units. More precise bending values, together with refractive index values, have been tabulated by Bean and Dutton.[4] At X-band, the ionospheric refractivity is only a few N-units (owing to a decrease proportional to frequency squared), while the major contributions to the tropospheric refraction are water vapor (~100 N-units for 90-percent relative humidity) and the dry atmosphere (~220 N-units at 25°C). Unfortunately, the contribution of the water vapor to the refraction is liable to be very nonuniform and can result in large relative path differences between the two antennas. The relative electrical path difference which produces a phase shift in the fringe pattern of $2\pi\Delta N\Delta D/\lambda$ radians is time varying and results in "bad seeing." For example, a cloud of 15 N-units, 3000 feet deep, will produce a phase shift of 2π radians over a time span of a few minutes as it drifts through the beam of one and then the other antenna. Clouds are not the only form of atmospheric irregularities – weather fronts and turbulence also produce bad seeing conditions. Figure 13 shows the interferometer phase fluctuations produced by relative path differences of a signal from a pattern track, while Fig. 15 shows the phase fluctuation of the subradar point on Venus as measured with the planetary radar interferometer. Since the subradar region on Venus is constrained by the range-Doppler gate, it is difficult to see how those fluctuations could arise from Venusian atmosphere rather than the earth's atmosphere.

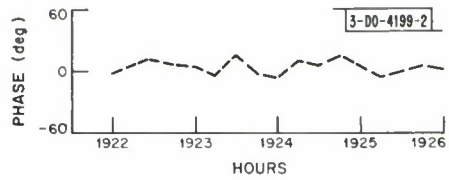

Fig. 15. Interferometer phase of region around subradar point.

B. Use of Subradar Point as Phase Calibrator

As a result of the refractive fluctuation discussed in Sec. A above, it was desirable to stabilize the fringe pattern relative to the planetary surface. This was done by referring all the measured phases to that of the first range box and zero Doppler on the cell which surrounds the subradar point. In the "coded" mode, the maximum error of the phase calibration due to the energy within the range-Doppler cell being nonuniformly distributed is just the phase difference between the subradar point and the edge of the cell. Thus, it is most desirable to make the first range-Doppler cell as small as possible by making the first range box just graze the leading edge of the planet. Figure 16 illustrates the calibration box and the fringe pattern on the planet. In the CW mode, the phase calibration was performed on the zero-Doppler strip. This technique could have resulted in a large error, as the phase of this strip could be far removed from that of the subradar point. However, because of the strong highlight at the subradar point or the sharpness of $S(\Theta)$ about $\Theta = 0$, the phase is essentially determined by the return from the subradar point.

C. Removal of "Mean Planet"

The planet's scattering law $S(Y_n, Z_n)$, which is defined as the power returned from unit area of the planet for an incident plane wave of unit power per unit cross section, can be decomposed

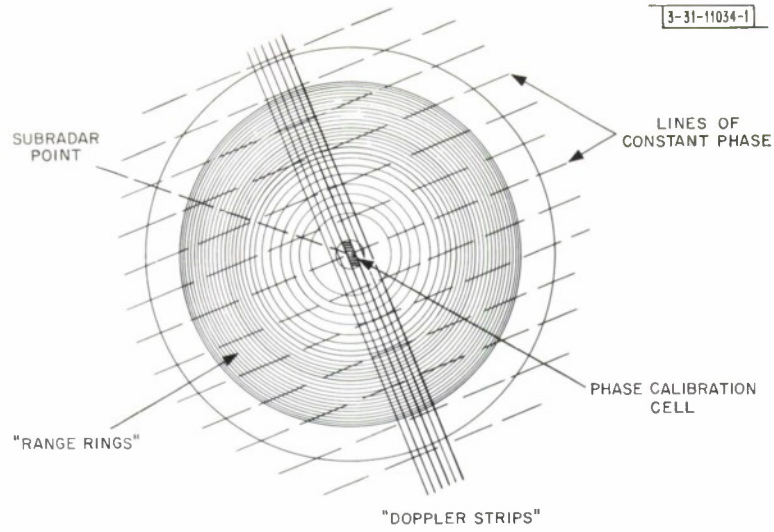

Fig. 16. Calibration cell.

into a "mean planet" scattering law $S(\Theta)$‡ and deviation from the mean planet $S_\delta(Y_n, Z_n)$. The $S(\Theta)$ is only a function of the angle of incidence Θ, while the deviation results from surface "features." From Eq.(50), the power in a particular delay-Doppler cell in the projected Y_n, Z_n plane is

$$\int \frac{S(\Theta)}{\cos\Theta}\, dY_n dZ_n + \int S_\delta(Y_n, Z_n)\, \frac{dY_n dZ_n}{\cos\Theta} \tag{75}$$

where the integration is carried over the area of the cell. In the CW mode, the power in each Doppler strip from the mean planet scattering law is

$$\int \frac{S(\Theta)}{\cos\Theta}\, dZ_n \tag{76}$$

if the Doppler strips are very thin, while the power in each range cell before frequency analysis is

$$\frac{S(\Theta)}{\cos\Theta} \times (\text{area of Doppler cell}) \tag{77}$$

or just $S(\Theta)$ since the area is proportional to $\cos\Theta$. Since

$$\cos\Theta = X_n = \frac{r_p - 2\tau c}{r_p} \tag{78}$$

Θ is determined by the delay.

The above decomposition into mean planet and features is especially useful when the mean planet dominates the signal returned. This is the case for Venus, which has a scattering function $S(\Theta)$ (for the polarized echo) which is highly peaked at $\Theta = 0$ and drops by more than 30 dB

‡ $S(\theta)$ includes effect of the planet's atmospheric attenuation.

at the limb or as $\Theta \to 90°$. The power in each range-Doppler cell at angle of incidence Θ is approximately

$$S(\Theta) \int \frac{dY_n dZ_n}{\cos\Theta} \tag{79a}$$

where

$$\int \frac{dY_n dZ_n}{\cos\Theta} = \int_{Y_{n_1}}^{Y_{n_2}} \arcsin \sqrt{\frac{1 - Y_n^2 - X_n^2}{1 - Y_n^2}}\, dY_n = \left[Y_n \arcsin \sqrt{\frac{1 - Y_n^2 - X_n^2}{1 - Y_n^2}} \right.$$

$$\left. - X_n \arcsin \frac{Y_n}{\sqrt{1 - X_n^2}} + \arcsin \frac{X_n Y_n}{\sqrt{1 - X_n^2}\sqrt{1 - Y_n^2}} \right]_{Y_{n_1}}^{Y_{n_2}} \tag{79b}$$

and

$$\cos\Theta = X_n = 1 - \frac{c\tau}{2r_p} \quad . \tag{79c}$$

If power in each cell after subtraction of the mean noise is divided by the mean scattering law, then the power in each cell will be proportional to

$$\left[1 + \frac{S_\delta(Y_n, Z_n)}{S(\Theta)}\right] \times \frac{\text{cell area}}{\cos\Theta} \tag{80}$$

or a planet with no features will appear uniformly bright. A similar scattering law compensation was performed on the CW data, where the power in each Doppler strip was divided by the integrated mean [Eq. (76)]. Also, the correlation function of the mean planet

$$\frac{\int S(\Theta) \cos 2\pi Z_n \ell_Z \frac{dZ_n}{\cos\Theta}}{\int S(\Theta) \frac{dZ_n}{\cos\Theta}} \tag{81}$$

was subtracted from the power so that only the features should appear in the transformation. This was done to eliminate the sidelobes of the mean planet that result from transformation [Eq. (55)].

D. Real-Time Computer Programs

The purpose of the real-time radar signal-processing program is to collect the sampled data of the received radar signal and to perform as much processing of these samples as the computer speed and rate of signal input will allow. Finally, the results of this processing must be saved (in this case digitally recorded) for any subsequent "off-line" analysis.

For the Hayford interferometer experiment, two real-time processing programs were written for the two basically different experiments that were attempted: the continuous wave, and the coded-pulse transmission, respectively. These programs were written for the CDC 3300 computer at the Haystack Microwave Facility. The CW and coded-pulse programs are described separately below.

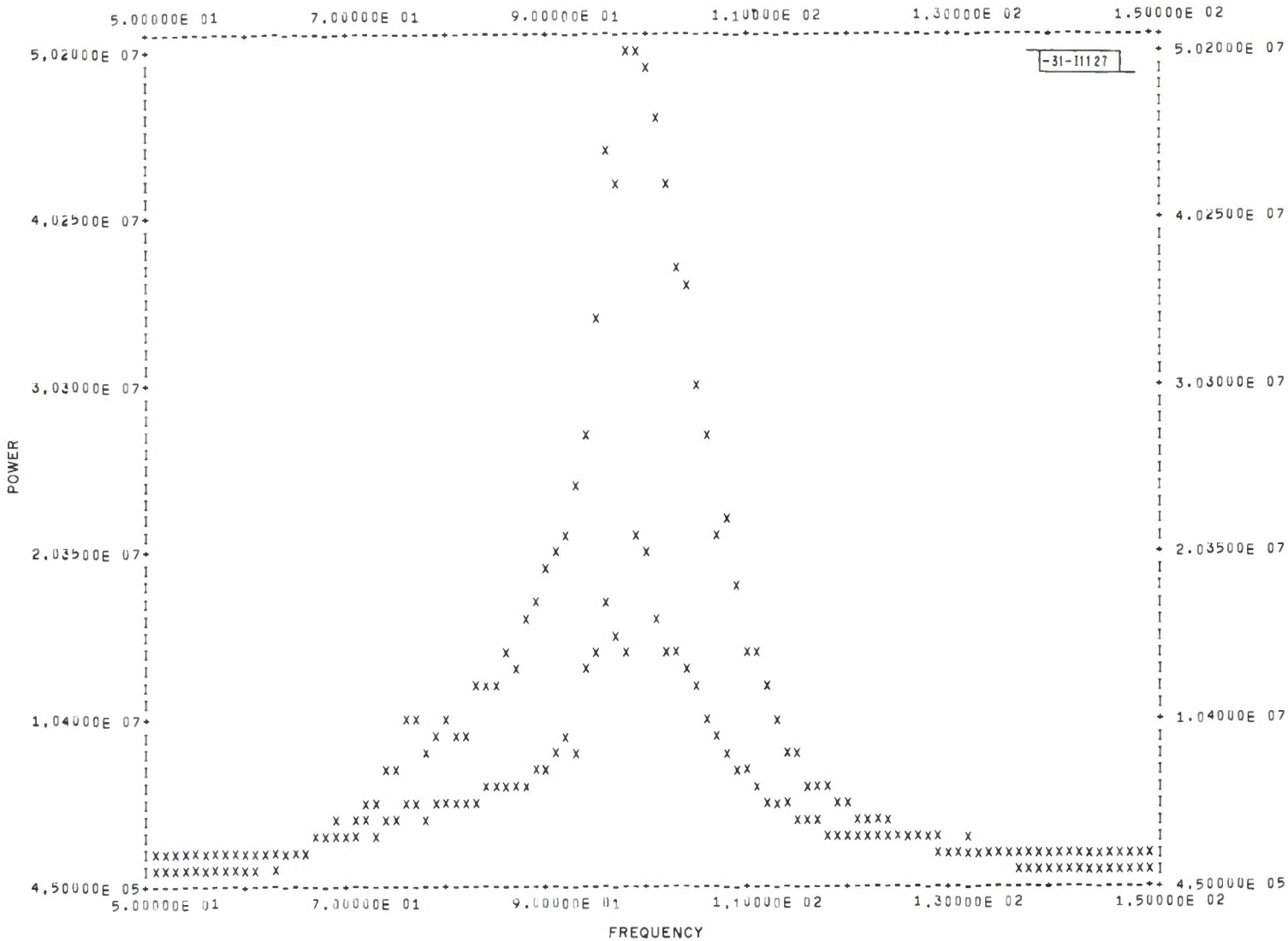

Fig. 17. Display of spectra from real-time CW program.

1. CW Program

Prior to a day's operation, the relative phase $\omega\tau_d$ and the rate of change of relative phase of the two received signals were computed from elements of the planetary ephemerides and the known interferometer geometry. Provisions for inputs relative to the expected atmospheric conditions expected were also provided for this calculation. These elements of phase rotation, in intervals of 1 minute, were stored on magnetic tape and used as an input to the real-time program. During the transmit portion of a run, the starting time of the receive period is input to the computer, the tape is searched, and the phase correction components are interpolated and stored in memory for every coherent interval (approximately 1 sec). Since 512 samples are taken within each coherent interval, the phase corrections for each sample are computed by interpolation in real time by means of the following recursion formulas:.

$$\cos\varphi_{K+1} = \cos\varphi_K \cos\Delta\varphi - \sin\varphi_K \sin\Delta\varphi \tag{82}$$

$$\sin\varphi_{K+1} = \sin\varphi_K \cos\Delta\varphi + \cos\varphi_K \sin\Delta\varphi \tag{83}$$

where φ_K is the phase rotation, and $\Delta\varphi$ is the phase rotation increment. This phase correction is then applied to the proper signal. Subsequent to the phase correction, the frequency spectra of the signals are computed by means of a fast Fourier transform routine[5] which produces complex spectra components for 512 1-Hz filters which are then recorded on magnetic tape. Sufficient time remains after this operation to produce incoherent sums of the two frequency spectra which are displayed at the end of each run as shown in Fig. 17.

2. Coded-Pulse Program

Since the modulation applied to the transmitted radar waveform is simply a phase-reversal type, the decoding process employed by the program consists of a pattern of additions and subtractions of the data samples identical to the pattern of phase shifts impressed on the transmission. The coding selected for this experiment was a 31-element shift register sequence with a baud length of 500 μsec. The decoding process yields 31 range sample components for each signal, with a sample interval equal to the baud length. At the start of each receive period, the time to 100 μsec is read into the computer from the station digital clock. This time is recorded on the output tape along with the decoded range samples, since it is necessary for computing the phase corrections in later analysis. Sufficient time remains after the decoding and recording to incoherently sum the power-vs-delay functions for each signal for display at the conclusion of the run as shown in Figs. 18(a) and (b).

Listings of the real-time programs appear in the Appendix.

E. Data-Averaging Programs

In the CW mode, the complex samples for each second are used to obtain the power and cross powers

$$P_H(\omega) = x_H(\omega)\, x_H^*(\omega) \tag{84}$$

$$P_W(\omega) = x_W(\omega)\, x_W^*(\omega) \tag{85}$$

$$P_{HW}(\omega) = x_H(\omega)\, x_W^*(\omega) \tag{86}$$

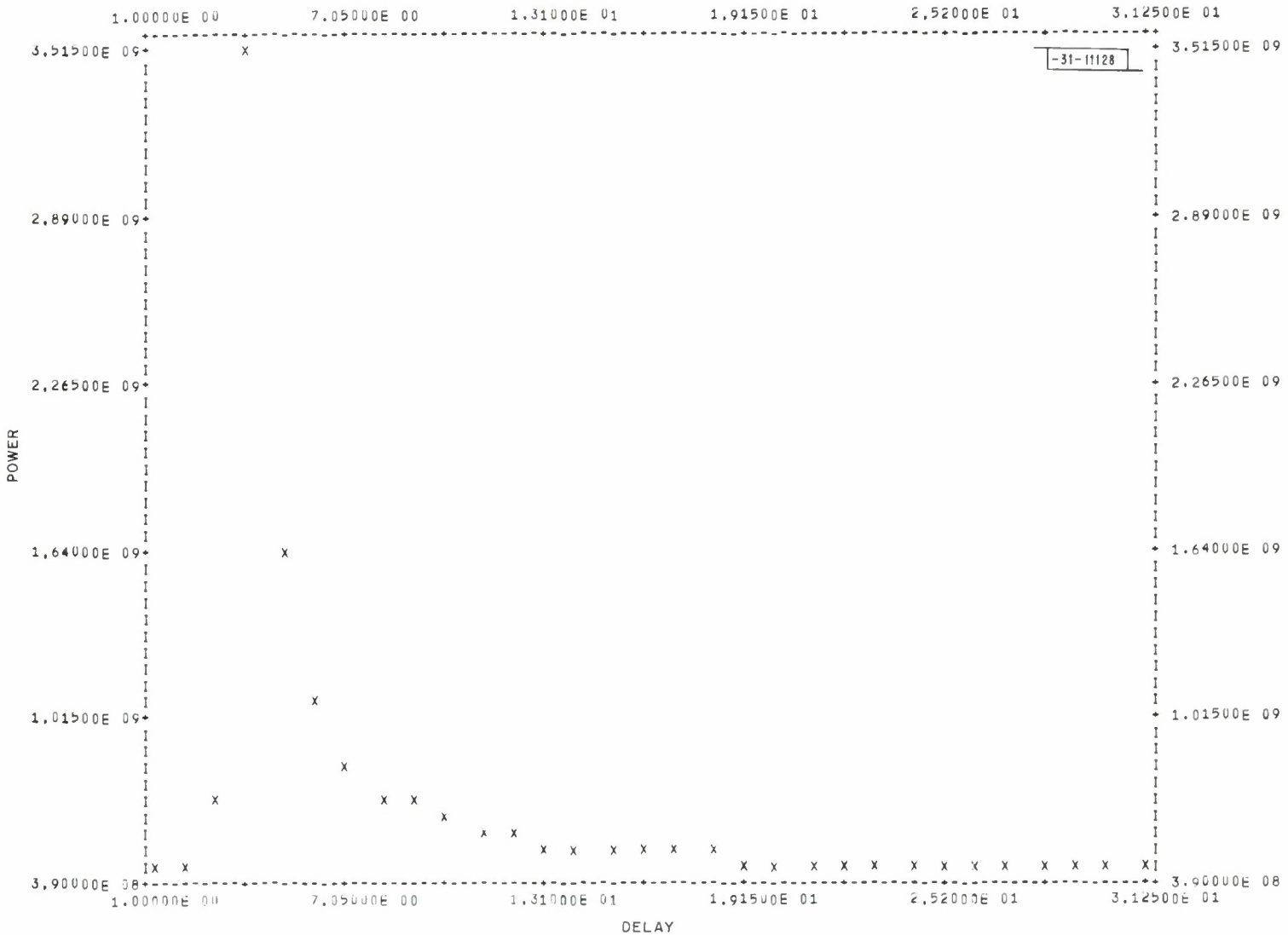

(a)

Fig. 18. Real-time display of power vs delay: (a) Haystack, (b) Westford.

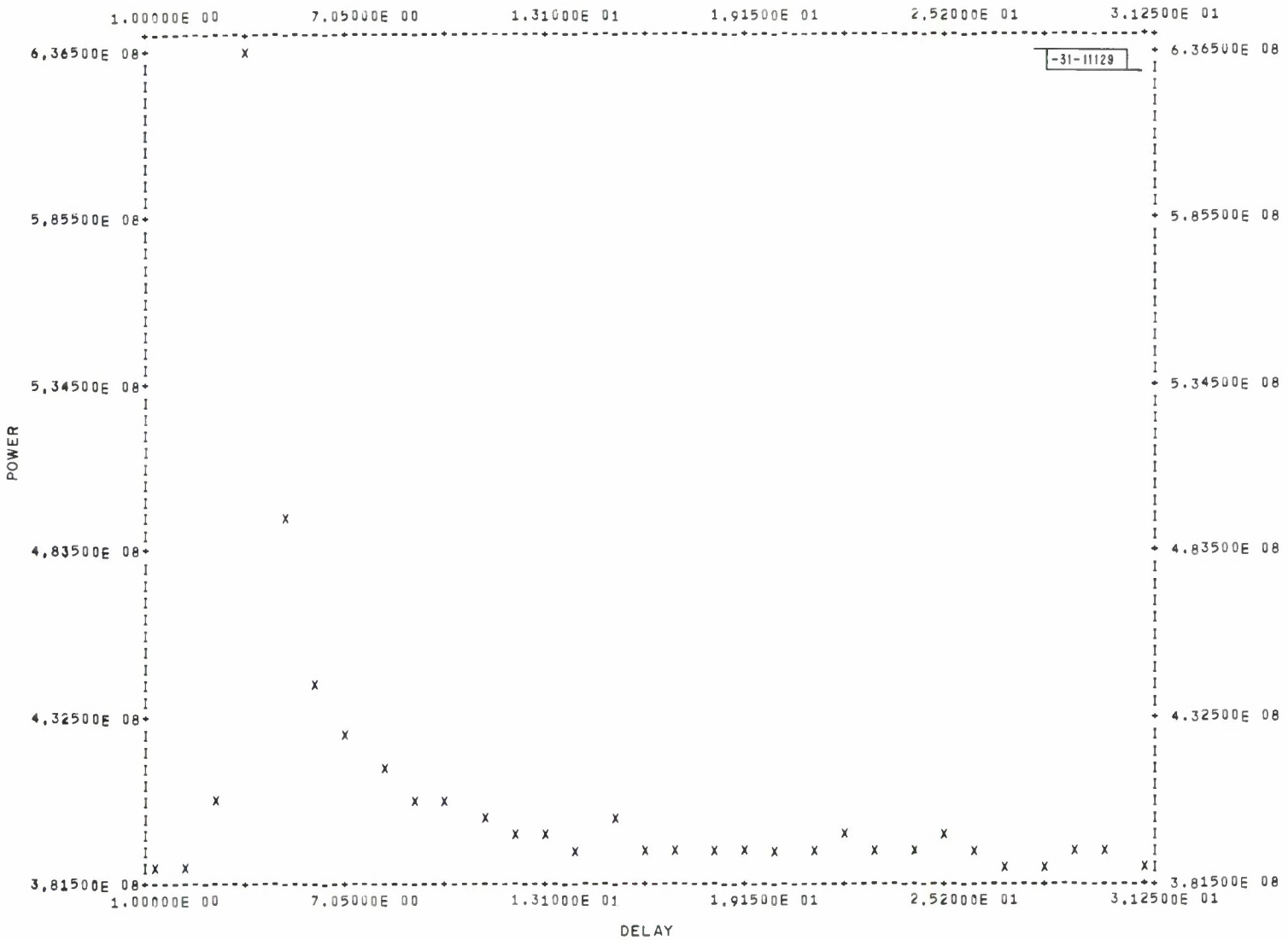

(b)

Fig. 18. Continued.

TABLE I

CW OBSERVATION DATES

Day No. (1967)	Range of Baseline (wavelengths per rodius along the apparent rotation oxis)	D (angle between apparent rototion axis ond celestial north) (deg)	F (center-to-limb Doppler) (Hz)	Lotitude of Subradar Point Lot_R (deg)	Longitude of Subrodar Point $Long_R$ (deg)	No. of Runs (~5 minutes each)
214	2.5 to 3.2	30	107	3.8	−80.5	15
222	2.4 to 3.7	32	88	5.5	−68.3	23
228	2.2 to 4.0	32	73	6.8	−60.5	18
229	2.3 to 3.9	31	70	7.0	−59.3	9
235	1.85 to 3.3	28	58	8.0	−53.0	13
241	1.95 to 3.75	25	52	8.7	−47.6	10
242	2.3 to 4.1	24	52	8.7	−46.8	20
249	2.7 to 3.8	17	59	8.7	−40.5	13
250	2.55 to 2.9	16	62	8.7	−39.6	10
256	2.45 to 3.45	13	75	8.0	−33.1	13

which are then summed for every 15 sec. The 15-sec averages of the cross powers are rotated by the phase of the zero-Doppler channel (the strip through the subradar point) to remove the atmospheric fluctuations as described in Sec. V-B. Further, the cross power is rotated by $\exp[2\pi i \Delta\omega F \ell_Y]$ to make the fringes perpendicular to the Doppler axis [see Eq. (41)], and the averages are taken for the whole run – a run being a complete round-trip transmit-receive sequence of about 5 minutes for the conjunction period.

The coded data are rotated and averaged in the same manner after the range boxes have been spectrum analyzed; 64 time samples are spectrum analyzed, yielding 1.008-Hz resolution.

F. Coordinate Transformation and Data Display

For each day's observations, the projected baseline changes in a manner similar to that illustrated in Fig. 2. In the CW mode, the cross power is transformed to give the distribution along a Doppler strip, at which point the data are in the (X, Y, Z) coordinate system which has subradar point at $(r_p, 0, 0)$ and Z-axis along Doppler axis. The data in each cell (1 Hz in Doppler and ~1/10 maximum fringe spacing) are transformed to a system (X_p, Y_p, Z_p) which is fixed to the planet's surface. Details of the transformation were presented in Sec. III.

The coded data are first transformed from the range-Doppler cells of the upper (northern) and lower (southern) hemispheres to a raster in (Y, Z) coordinates and then to (Y_p, Z_p) coordinates.

Details of the transformation were given in Sec. II. The coded data, which now exist as functions of X_n and Y_n, are also transformed into functions of planetary latitude and longitude by relations which again are the inverse of Eqs. (8) through (16). In addition, the ambiguity resolving function is applied to the data by multiplying each matrix point by $S^U_{c,n}$ or $S^L_{c,n}$ of Eq. (63) according to whether the value of Z_n is positive or negative. In this way, an 81×81 matrix of points is generated in a square planetographic grid, with the interval between each matrix point being equal to 1.25 planetary degrees. Spatial smoothing is obtained by actually computing the power every 5/12 of a degree and setting the matrix point equal to the average of nine of these values taken from a 3×3 array centered on the matrix point.

The data are now quantized to 45 discrete levels and transferred to an intensity plot by generating on a very accurate CRT display a raster, each point of which has a duration directly proportional to the value of the matrix point. This intensity plot is photographed by a special CRT camera.

VI. RESULTS OF VENUS MAPPING FOR 1967 CONJUNCTION

Venus was observed during the period 2 August through 13 September 1967 for several hours a few days a week. Most of the data were taken in the CW mode because of the larger baseline coverage needed to resolve the Doppler strips. However, during the period around conjunction (30 August), about half the observing time was spent in the coded mode.

A. Map from CW Transmissions

Because of limitations in the operating time and in the orientation of the Haystack-Westford baseline, it was not possible to obtain data over a wide range of projected baseline. Consequently, determination of the distribution of the power along a Doppler strip suffers rather seriously from sidelobe effects. Table 1 lists the days on which Venus was observed, as well as the range of the component of the projected baseline in the direction of the apparent rotation axis covered in each case. On many days, the baseline change is so small that the

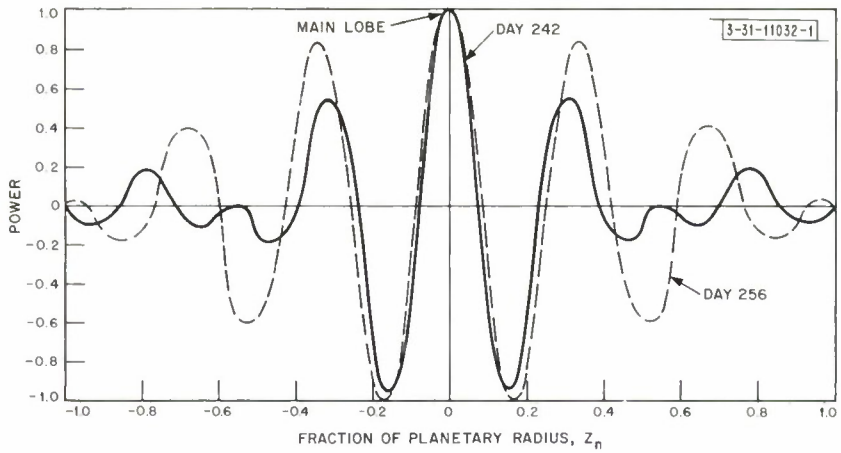

Fig. 19. Resolution patterns for doys 242 ond 256.

equivalent spatial resolution pattern differs little from a cosine function. The equivalent resolution patterns along a Doppler strip for days 242 and 256 are shown in Fig. 19. Due to the inability of the interferometer uniquely to resolve a planetary feature because of the large sidelobe effect, it is advantageous to use the change in the subradar point on the planet as well as the change in direction of the rotation axis as a means of distinguishing the mainlobe from the sidelobes. As the planet rotates, the angle between the Doppler axis and the planetary axis changes so that the locations of the interferometer sidelobes move with respect to the mainlobe as referred to the planetary surface. Thus, if a feature is inadvertently associated with the position of a sidelobe, it will appear to move from day to day, while correctly placed features remain fixed. However, rotation of the planet is sufficiently slow (~1° per day) that this effect will not be seen in one day's observations. Figure 20 shows a map of the features on Venus in the coordinate system defined by Carpenter.[1] The map represents the average of all the data for the entire observing period placed on a common coordinate system; the amount of data for the other side of the planet is insignificant, and consequently is not displayed. Figure 21 shows the same map, but indicates (by means of enclosures) those strong features which can be associated with the mainlobe of the resolution pattern. The test for these features was made by a search through the maps obtained for each individual day. The fact that some of the scattering centers do not appear to move during the observing period (days 214 to 256) lends confidence to the planetary rotation parameters assumed.

Fig. 20. CW map of Venus.

Figure 22 shows the lines of constant Doppler shift which pass through the enclosed features. The circles indicate the sidelobe positions for these features for different days on which observations were made. However, some days have been omitted for clarity. The dotted line indicates the position of the subradar point during the observation period.

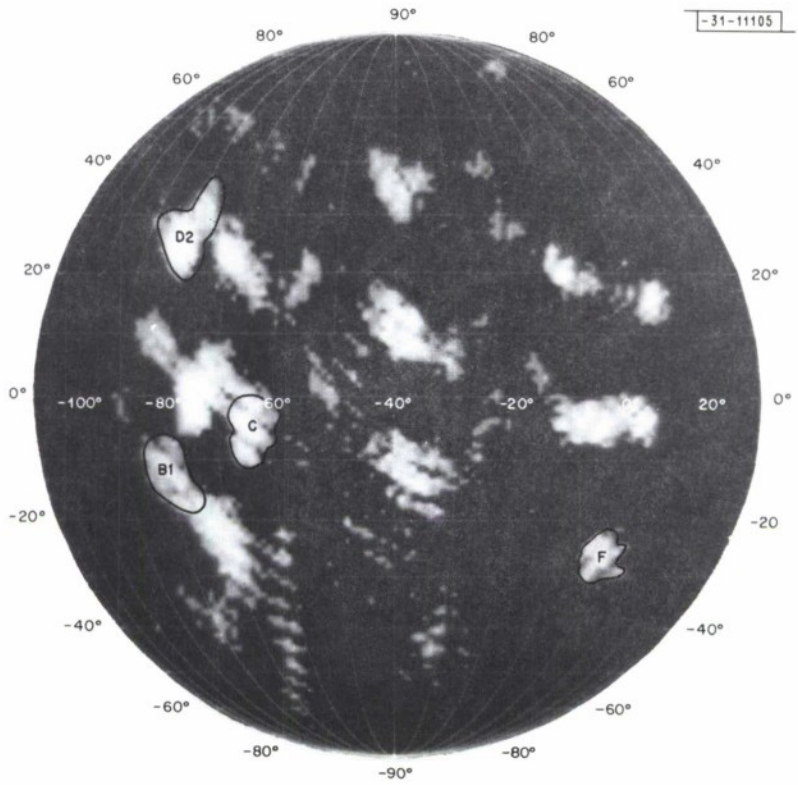

Fig. 21. CW map with features that remain statianary enclosed.

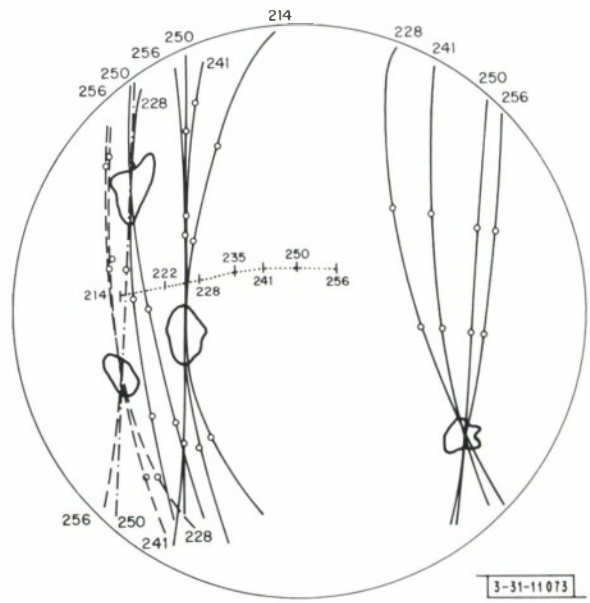

Fig. 22. Lines af canstant Dappler and sidelabe patterns for enclased features.

TABLE II

CODED OBSERVATION DATES

Day No. (1967)	F (center-to-limb Doppler) (Hz)	D (angle between apparent rotation axis ond planetary north) (deg)	Latitude of Subradar Point (deg)	Longitude of Subradar Point (deg)	No. of Runs (~5 minutes each)	Mean Angular Distance from Subradar Point for S/N Ratio	
						10 σ (deg)	3 σ (deg)
215	107	7.5	3.9	−78.4	3	20	29
228	74	10.4	6.6	−60.2	1	18	24
229	72	10.2	6.8	−59.1	2	20	29
235	59	9.0	7.8	−53.1	2	26	35.5
237	56	8.5	8.0	−51.2	2	26	35.5
241	53	4.8	8.3	−47.8	6	27	38
242	53	3.8	8.4	−46.9	4	26	38
243	53	2.8	8.4	−46.1	18	34	39
249	59	−3.1	8.2	−40.6	6	24	35.5
256	74	−6.4	7.5	−33.0	6	22	32

B. Maps from Coded Transmissions

Maps made from the results of the coded mode of operation do not suffer from the sidelobe effects seen in the CW data, but are not entirely free from ambiguities. First, the upper-lower hemisphere ambiguity is well resolved by the interferometer only when the signal-to-noise ratio is sufficient to produce small errors in the measured phase of the cross power. Second, the repetitive 31-element code is ambiguous in delay, since the planet is 81 code elements deep (40.5 msec). Also, there is a certain amount of frequency foldover, since the Doppler spread at the later delays was generally larger than the unambiguous frequency window of 64.5 Hz. The regions of frequency foldover have been eliminated from the maps. However, the regions which are aliased in delay cannot be removed and some features may, in fact, be associated with regions which lie 15.5 msec deeper into the planet. In general, however, the rapid falloff of power in the scattering law renders this possibility unlikely.

Figures 23(a) through (j) are intensity plots made from the power received at Haystack as a function of delay and Doppler. In these plots, the two ambiguous hemispheres are given equal weight. Thus, there is symmetry about the line $Z_n = 0$. Figures 24(a) through (j) are intensity plots with the cross powers $S_{c,n}^{U}$ and $S_{c,n}^{L}$ used to redistribute the power between the two hemispheres. Figure 23(k) shows the average of data from the whole experiment without hemispheric resolution, while Fig. 24(k) shows the corresponding average using the ambiguity resolution functions. Table II lists the number of runs for each day and the approximate distances from the subradar point for which the Haystack signal-to-noise ratio is both 10 and 3 times the standard deviation of the associated noise fluctuations (σ). In viewing the maps in which the cross power has been used, it should be noted that, owing to the smaller antenna size and higher system temperature at Westford, the weighting functions used to redistribute the Haystack power become very noisy for regions where the Haystack signal alone is less than about 10σ.

The basic spatial resolution is usually set by the delay-Doppler cell size, as given in Eq. (79b). Reference to Fig. 16 shows that these cells become larger near the Doppler equator. As an example, on Day 228, F = 74 so that at delay box 31 (about 49 planetary degrees from the subradar point) the width of the cell is 82 km and the length is about 99 km. In comparison with this, the cell bordering the Doppler equator is approximately 83 by 900 km.

C. Interpretation of Results

Mean Planetary Scattering Law:— A theoretical scattering law derived by Muhleman[6] was found to fit the data extremely well with the addition of 3-dB one-way attenuation for a vertical path through the Venusian atmosphere. The law used to fit to the CW data was

$$S(\Theta) = \frac{e^{-\beta \sec\Theta} \cos\Theta\alpha^3}{(\sin\Theta + \alpha\cos\Theta)^3} \tag{87}$$

where the exponential includes the effects of atmospheric attenuation. The best fit to the data was obtained using

$$\beta = 1.3 \pm 0.3$$

$$\alpha = 0.13 \pm 0.2 \quad .$$

From Muhleman's theory, the value of α yields an effective mean slope of about 7° at 3.8-cm wavelength.

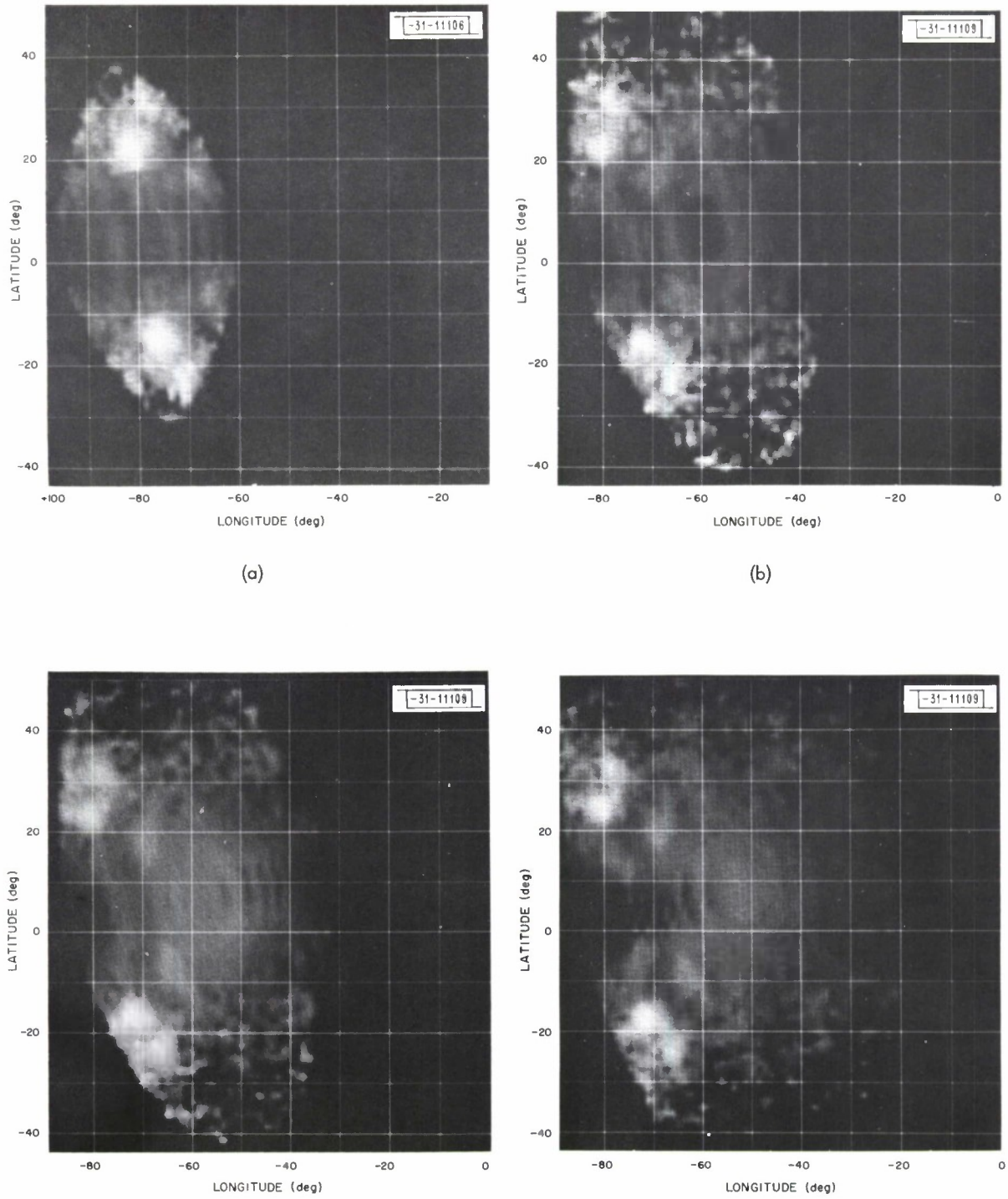

Fig. 23(a-k). Maps from Haystack caded data.

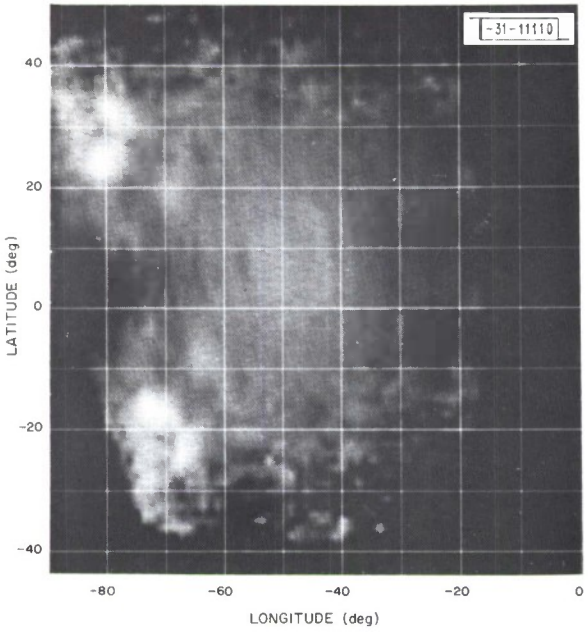

(e)

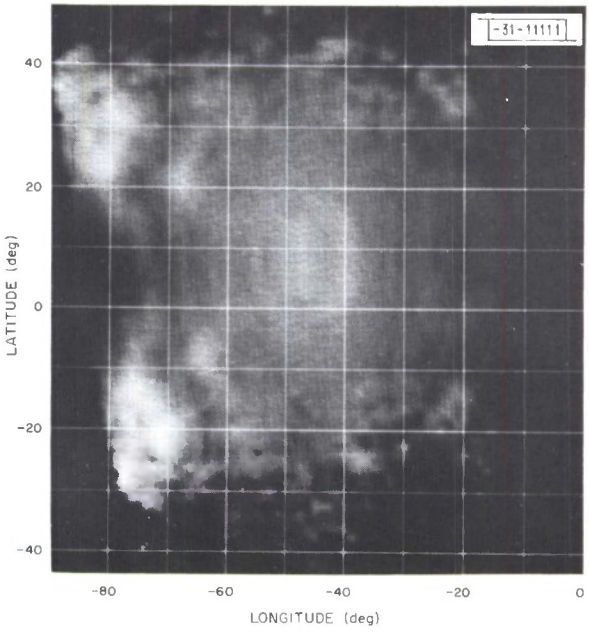

(f)

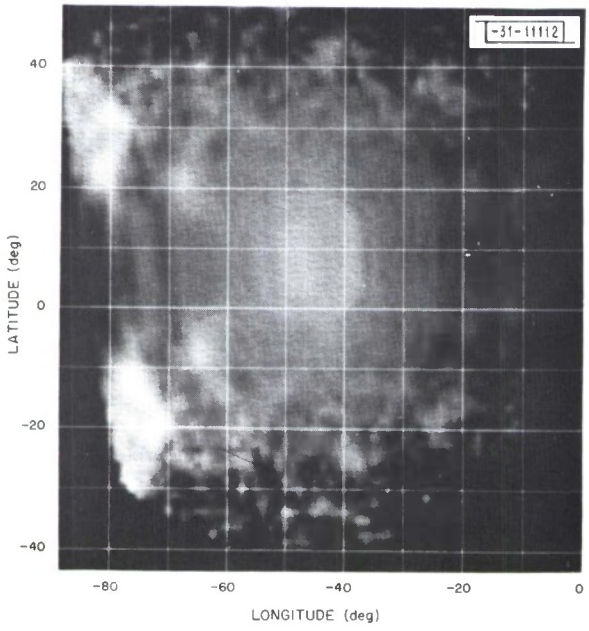

(g)

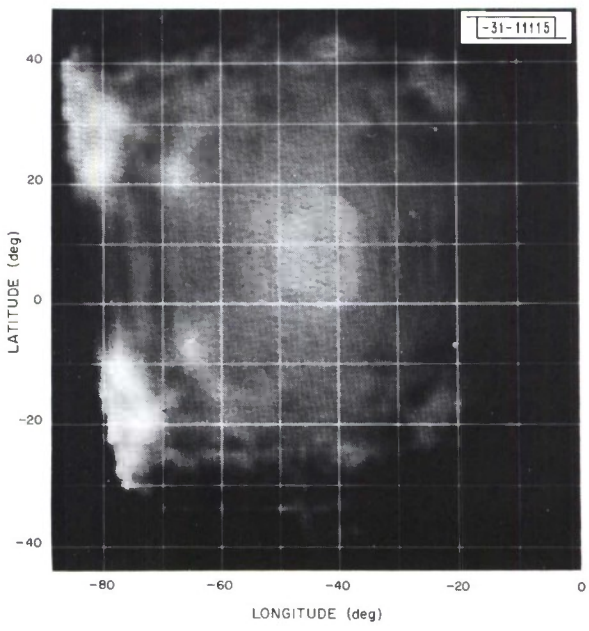

(h)

Fig. 23(a-k). Continued.

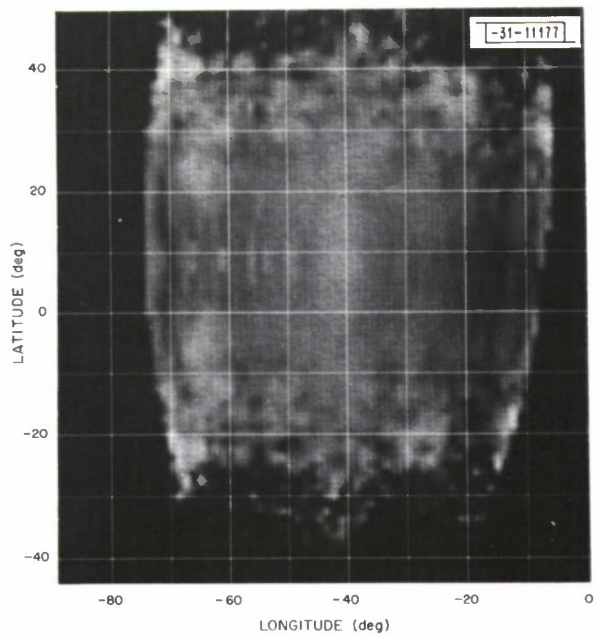

(i)

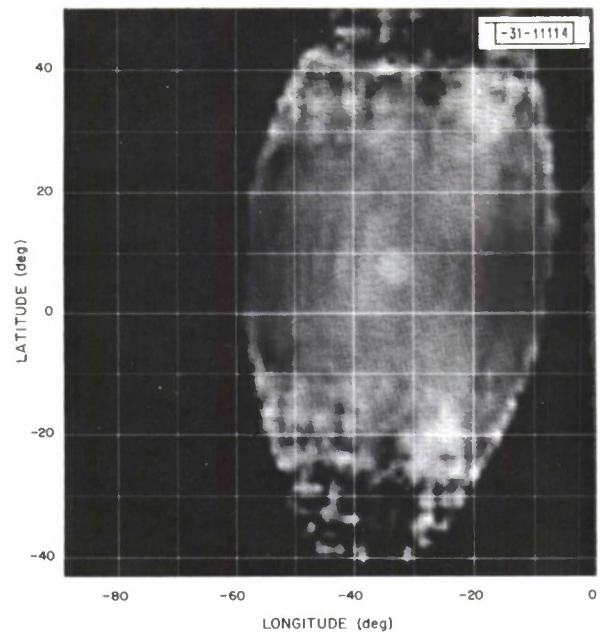

(j)

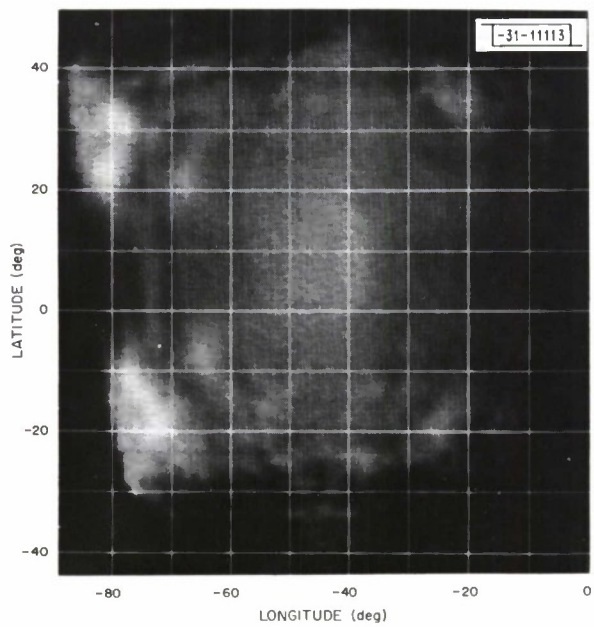

(k)

Fig. 23(a-k). Continued.

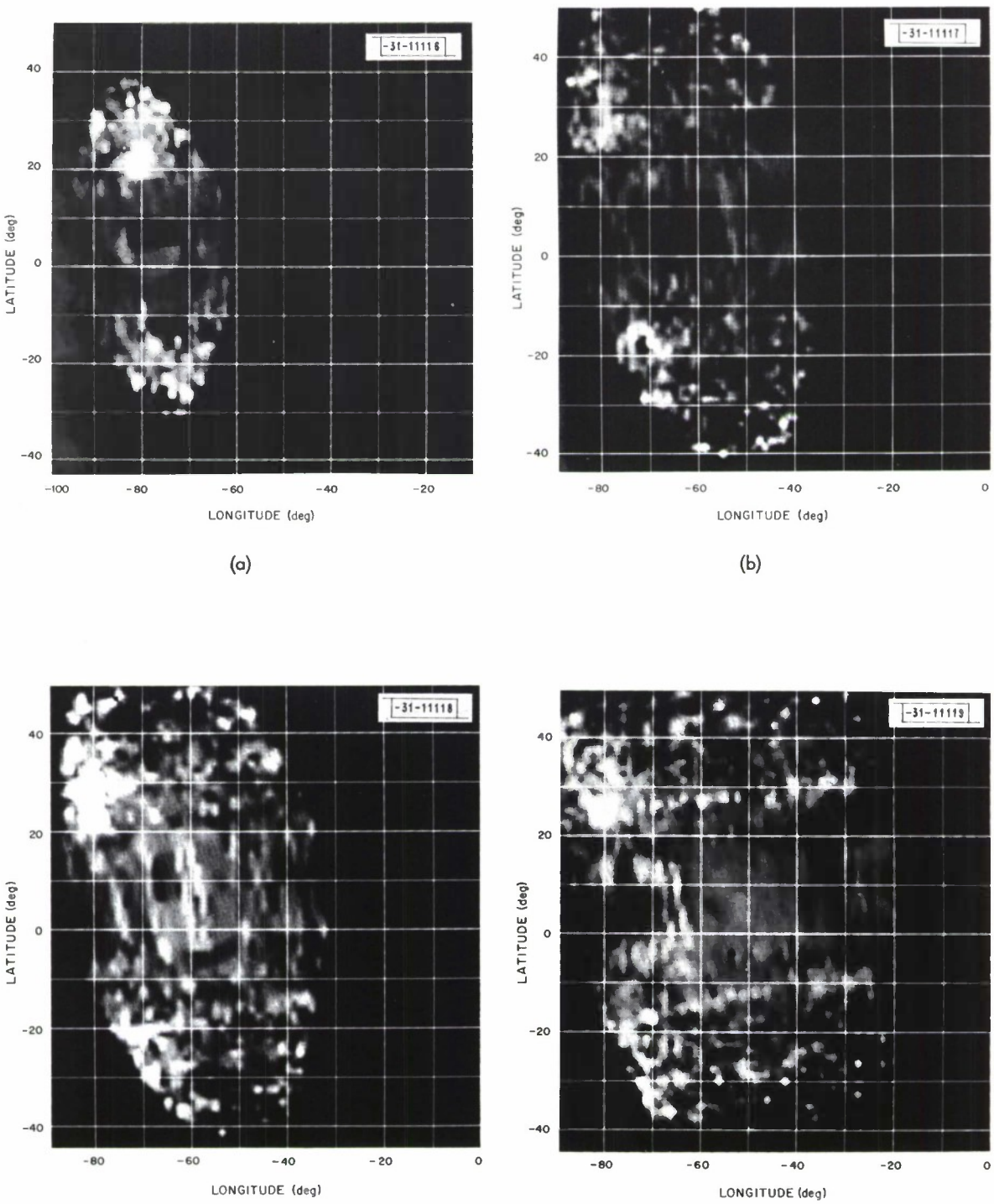

Fig. 24(a-k). Maps with coded interferometer data.

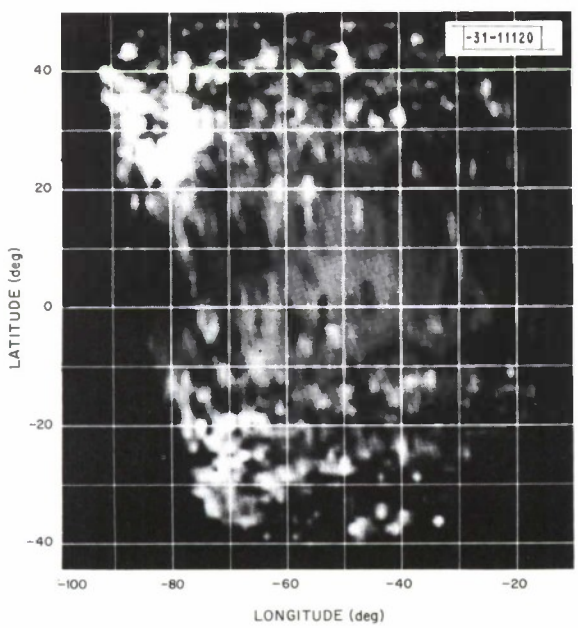

(e)

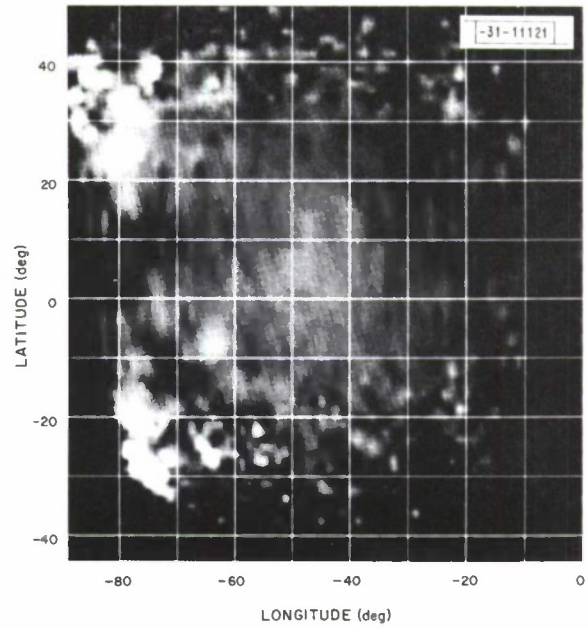

(f)

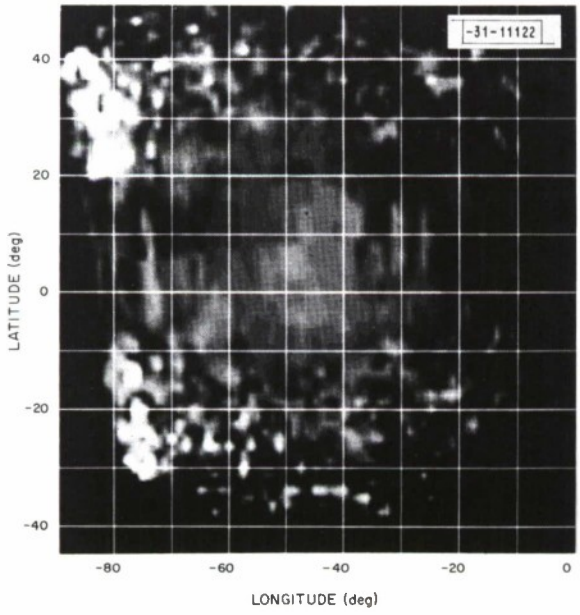

(g)

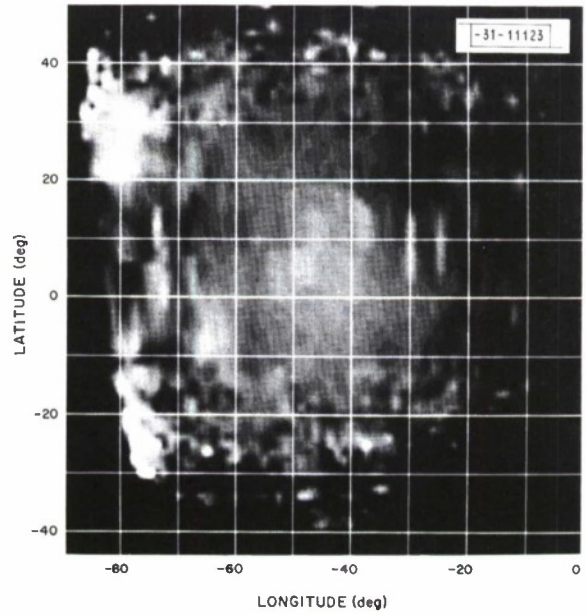

(h)

Fig. 24(a-k). Continued.

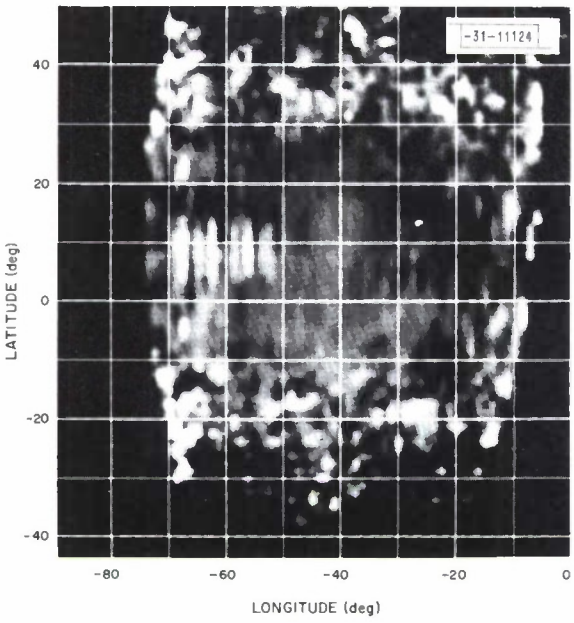

(i)

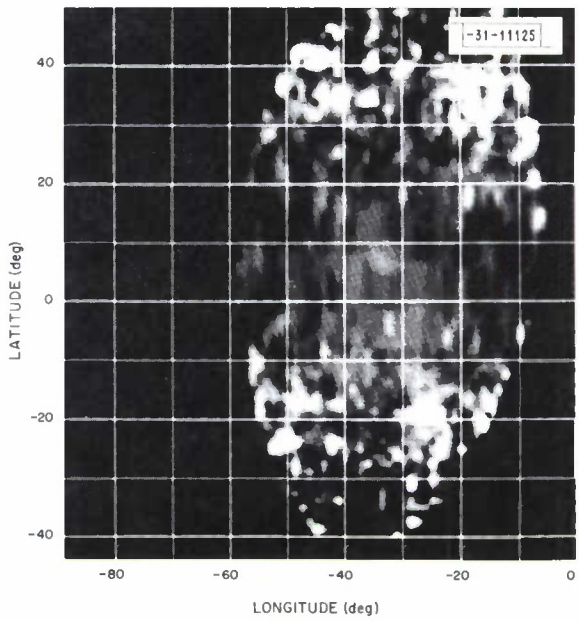

(j)

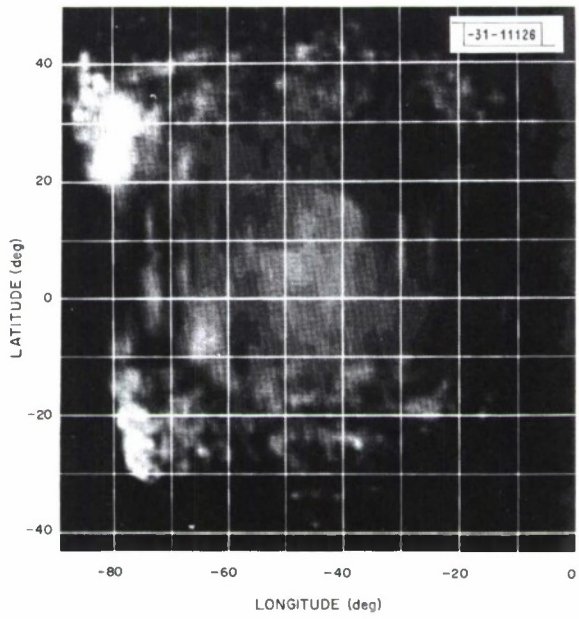

(k)

Fig. 24(a-k). Continued.

Surface Features:– From Figs. 20 through 24, a number of the planetary surface regions are seen to exhibit a local increase in the scattered power as compared with the average scattering behavior. Local reductions also exist, of course, but these are far less obvious in the data. The common characteristic of the enhancements is that they display relatively little dependence on angle of incidence, i.e., they contrast far more prominently with their mean-scattering surroundings when located far from the subradar point than when near it. From this behavior, it is deduced that they are unlikely to be composed primarily of relatively smooth, preferentially oriented inclined facets, but rather possess substantial roughness at the scale of the wavelength. Observation of their depolarized scattering properties would obviously be desirable to confirm this hypothesis, but such observations were not possible with the instrumentation available. Depolarized observations of these features have been made at longer wavelengths,[1,7-10] however, and these have in fact behaved in a way which is characteristic of diffuse scattering from a locally rough surface.

The question of the actual composition of the anomalously scattering features is unresolved. As discussed in the next section, it seems clear that these features are quite firmly attached to a rigid surface. But, whether they merely represent patches of locally rough horizontal surface or correspond to rough mountainous regions is impossible to tell from the present data. Long continued observation using extremely short observing pulsewidths might resolve the topography along the track of the subradar point to the order of several hundred meters. And if, as seems likely, there exists substantial atmospheric attenuation at centimeter observing wavelengths, it is possible that variations in the height of the subradar point could affect the observed radar cross section.

Location of Features and Rotation Period of Venus:– The system of planet-centered coordinates used in the reductions reported here is based on a sidereal rotational period of 243.16 days (retrograde), a north pole direction[2] of $RA_a = 270.3°$ and $\delta_a = 66.7°$, and an epoch[1] which defines the longitude of the subradar point as $-40°$ at 0^h UT, 20 June 1964. It is also required that the longitude of the subradar point increase in the positive sense with time, and that northerly latitudes be positive. These assumptions are based upon: (1) the growing suspicion that the sidereal rotational period of Venus is exactly equal to a resonance value in which Venus makes precisely four rotations, as seen by an earth-based observer, between successive inferior conjunctions; (2) the direction of the rotational pole of Venus, as determined from the delay-Doppler observations of Ref. 2; and (3) the epoch defined by Carpenter.[1] The last assumption is a convenience to facilitate comparison between the present results and those obtained earlier at JPL.

Based on this coordinate system, the features listed in Table III have been identified. The ordering is according to decreasing reliability: the first four features listed (I to IV) are considered to be quite reliably established; the last four features (A to D) are less firm. Also listed are the locations of matching features previously identified at the Jet Propulsion Laboratory during the 1964 inferior conjunction. From the agreement in position to about 2° in longitude, and from the fact that Venus is known to have made precisely eight rotations between 1964 and the present observations, the rotational period of assumption (1), above, can be verified as 243.16 ± 0.2 days, retrograde. The systematic agreement in position between five of the Haystack features and those identified earlier at JPL also requires that these features be firmly attached to the rigid surface of the planet and that they have a lifetime of at least three years. The failure

TABLE III

LOCATION OF RADAR FEATURES ON VENUS

Feature	Location from Our Observations		Probable JPL Identification	Location from JPL Observations	
	Latitude (deg)	Longitude (deg)		Latitude (deg)	Longitude (deg)
Haystock I	−26 ± 3	−1 ± 2	Goldstein[10] a	−29 ± 2	0 ± ?
			Corpenter[1] F	−26.7 ± 1.8	0 ± 0.7
Haystack II	+24 ± 2	−81 ± 2	Goldstein β	+23 ± 4	−78 ± 6
Hoystack III	+31 ± 2	−78 ± 2	None		
Haystack IV	−7 ± 3	−65 ± 3	Carpenter C	−6.8 ± 5.8	−68.9 ± 1.3
Haystack A	+23 ± 2	−68 ± 2	Carpenter D2	+22.7 ± 1.7	−70.0 ± 0.7
Haystack B	−12 ± 3	−81 ± 3	Carpenter B1	−11.9 ± 4.4	−75.8 ± 0.6
Haystack C	−13 ± 2	−36 ± 3	None		
Haystack D	+10 ± 4	−39 ± 4	Nane		

to observe other 1964 JPL features in some cases may be due to their lying outside the planetary region observed by us, and in others possibly by the confusion associated with JPL's use of a single parameter (Doppler frequency) to analyze the 1964 observations.

VII. CONCLUSION

Despite the fact that maps of the Venusian surface presently obtainable by radar are relatively crude, we feel that the techniques and basic applicability of planetary radar interferometry have been adequately demonstrated. Because of the opaque cloud cover, radar appears to be the only existing means of mapping the planet Venus. We hope that future interferometric studies can be made with a more complete projected baseline coverage, as well as with a greater system sensitivity. At the present time, the phase-stability limitations set by the earth's atmosphere have not been reached, and the corresponding limit to the resolution of the technique is still to be realized. Ultimately, of course, a limit will be reached, although operation at longer wavelengths or the use of an extraterrestrial phase calibrator may extend the available resolution even further.

ACKNOWLEDGMENTS

We are grateful to the entire staff of the Haystack Microwave Facility and the Westford Communications Terminal, particularly G.M. Hyde, H.V. Scharn, L. Melaney, P. Murray, R. Silva, E. McCurley, H. Camacho, and P. Goodie for their technical and engineering assistance; also, N. Brenner and B. Nanni for their assistance in the computer programming. We would also like to thank P.B. Sebring, M.L. Stone, B. Nichols, and H. Hoover for their enthusiasm in helping to organize the project.

REFERENCES

1. R.L. Carpenter, "Study of Venus by CW Radar – 1964 Results," Astron. J. 71, 142 (1966).
2. R.B. Dyce, G.H. Pettengill, and I.I. Shapiro, "Radar Determination of the Rotations of Venus and Mercury," Astron. J. 72, 351 (1967), DDC 658774.
3. I.I. Shapiro, private communication.
4. B.R. Bean and E.J. Dutton, "Radio Meteorology," Natl. Bur. Standards Monograph No. 92 (1966).
5. N.M. Brenner, "Three Fortran Programs that Perform the Cooley-Tukey Transform," Technical Note 1967-2, Lincoln Laboratory, M.I.T. (28 July 1967), DDC 657019.
6. D.O. Muhleman, "Radar Scattering from Venus and the Moon," Astron. J. 69, 34 (1964).
7. R.L. Carpenter, "Study of Venus by CW Radar," Astron. J. 69, 2 (1964).
8. G.S. Levy and D. Schuster, "Further Venus Radar Depolarization Results," Astron. J. 69, 29 (1964).
9. J.V. Evans, R.A. Brockelman, E.N. Dupont, L.B. Hanson, and W.A. Reid, "Radar Observations of Venus at 23 cm in 1965/1966," Astron. J. 71, 897 (1966), DDC 648056.
10. R.M. Goldstein, "Preliminary Venus Radar Results," J. Research Natl. Bur. Standards 69D, 1623 (1965).

APPENDIX

The computer program listings used in the reduetion of the Venus data are presented in this appendix.

Real-Time Programs:— Figure A-1 lists the eoded-pulse real-time program, and Fig. A-2 is the CW real-time program. Both these programs run on the CDC 3300 eomputer at Haystaek. Figure A-3 eonsists of the program used to generate an ephemeris tape for the real-time fringe rotation of the CW data.

Coded Post Real-Time Programs:— The post real-time phase ealibration program used to refer the phases of the eoded data to the subradar region is shown in Fig. A-4. Figure A-5 is the eoded-pulse averaging and weighting funetion generation program whieh averages the power for a complete day of observing and generates the hemispherie ambiguity resolution funetions. The programs used to transform the data to the planet's eoordinate system and display the data on a CRT are given in Fig. A-6.

CW Post Real-Time Programs:— Figure A-7 is the CW phase ealibration program whieh refers the phases to the subradar region. The CW averaging program (Fig. A-8) averages the data for runs with the same projeeted baseline and then takes the transform over different projeeted baselines. Figure A-9 lists the programs used to display the CW data in the planetary eoordinate system.

```
         ENTRY    MAIN,CINIT,RUN
         EXT      INPUT,INIT,ENDRUN
         EXT      CIT,CST,ABNORMAL
MAIN     UJP      **
LOC0     EQU      0
         SJ5      *+2                    SSWTCH 5 ON MAKE BOOTSTRAP TAPE
         UJP      START
         LDA      *-1
         STA      LOC0
         CON      6,0
         UJP      *-1
         SEL      8,0
         UJP      *-1
         ENA,S    0
         ENI      7,1
         STA      CST,1                  CLEAR CST
         IJD      *-1,1
         OUTW     0,0,77740B
         UJP      *-2
         EXS      2,0
         UJP      *-1
         EXS      2400B,0                CHECK FOR ERRORS
         HLT      *+1
         SEL      13,0
         UJP      *-1
         EINT     0
         HLT      77740B
START    RTJ      INPUT
RESTART  RTJ      INIT
         RTJ      RUN
         RTJ      ENDRUN
         UJP      RESTART
         EJECT
```

Fig. A-1. Hayford coded-pulse real-time processing program.

```
*
*       CINIT CLEARS ARRAYS AND SETS UP INTERRUPT LOCATIONS
*         ------------------------------
CINIT    UJP       **
         ENA,S     1
         STA       INT1-1              POWER FAILURE, TEMPORARY HALR
         ENI       ABNORMAL,1
         STA       1,1                 SET UP STOP IN ABNORMAL
         ENA,S     0
         STA       TIME1
         STA       TIME2
         STA       OUTBUF
         STA       NTAPES
         STA       ICNT
         STA       FCNT
         ENI       123,1
         STA       ICOH,1
         IJD       *-1,1
         ENI       8191,1
         LDA       BIAS
         STA       BUF0,1              CLEAR BUFFERS INITIALLY
         IJD       *-1,1
         ENI       4091,1
         STA       DATA,1
         IJD       *-1,1
         ENI       21,1
         LDA       CIT,1
         STA       CITSAVE,1           SAVE CIT TBL
         IJD       *-2,1
         UJP,I     CINIT               RETURN TO INIT
         EJECT
```

Fig. A-1. Continued.

```
*
*          RUN CONNECTS INTERFACE AND OUTPUT DEVICES
*          ----------------------------
RUN       UJP       **
          SJ1       *                        SSW 1 ON, WAIT FOR INTERFACE
          SSIM      17B
          CON       2000B,3
          UJP       *-1
          EXS       1,3                      TEST FOR READY
          UJP       *+2
          UJP       *-2
          SEL       5,3                      CLEAR CH3 INT.
          UJP       *-1
          IOCL      5                        CLEAR CHAN 0 AND 2
          CON       2,0                      CONNECT UNIT 2 TO CH 0
          UJP       *-1
          SEL       6,0                      SET 800 BPI UNIT 2
          UJP       *-1
          SEL       8,0                      REWIND UNIT 2
          UJP       *-1
          ENI       12,1
          ENA,S     MANUAL
          STA       CIT,1
          ENI       14,1
          ENA,S     CH0
          STA       CIT,1
          ENI       17,1
          ENA,S     CH3
          STA       CIT,1
          SEL       3,3                      ENABLE/START WRITE CORE
          UJP       *-1
          EXS       4,3                      TEST FOR WRITE CORE
          UJP       *+2
          UJP       *-2
          SEL       128,3                    READ TIME FUNCTION
          UJP       *-1
          INPW      3,TIME1,ICNT             READ IN START TIME
          UJP       *-2
          PAUS      10B
          UJP       *+1
          OUTW      0,ITITLE,ICNT
          UJP       *-2
          EXS       2,0
          UJP       *-1
          EINT      0
          UJP       *                        WAIT
          EJECT
```

Fig. A-1. Continued.

```
*
*         PROC IS THE MAIN PROCESSING ROUTINE
*          ----------------------------
PROC      ENA,S     0
          TAM       22B                 RESET CLOCK
          ENI       61,1
          ENI       122,2
A.1       LDAQ      DATA+3968,2         TRANSFER LAST CODE INTERVAL
          STAQ      DATA,2
          INI       -2,2
          IJD       A.1,1
          ENI       1983,1
          ENI       3966,2
A.2       LDAQ      BUF0,2              TRANSFER INPUT BUFFER TO DATA
          STAQ      DATA+124,2
          INI       -2,2
          IJD       A.2,1
          ENI       1983,1
          ENI       3966,2
          ENI       122,3
          REM       COMPUTE NEGATIVE SUM INCLUDING BIAS
A.3       LDAQ      BIAS                BIAS=00000177,00000177
          ADAQ      DATA+24,2
          ADAQ      DATA+28,2
          ADAQ      DATA+32,2
          ADAQ      DATA+44,2
          ADAQ      DATA+60,2
          ADAQ      DATA+68,2
          ADAQ      DATA+76,2
          ADAQ      DATA+80,2
          ADAQ      DATA+84,2
          ADAQ      DATA+88,2
          ADAQ      DATA+96,2
          ADAQ      DATA+100,2
          ADAQ      DATA+108,2
          ADAQ      DATA+120,2
          ADAQ      DATA+124,2
          STAQ      SAVEN
          LDAQ      DATA+4,2
          ADAQ      DATA+8,2
          ADAQ      DATA+12,2
          ADAQ      DATA+16,2
          ADAQ      DATA+20,2
          ADAQ      DATA+36,2
          ADAQ      DATA+40,2
          ADAQ      DATA+48,2
          ADAQ      DATA+52,2
          ADAQ      DATA+56,2
          ADAQ      DATA+64,2
          ADAQ      DATA+72,2
          ADAQ      DATA+92,2
          ADAQ      DATA+104,2
          ADAQ      DATA+112,2
          ADAQ      DATA+116,2
          SBA       SAVEN
```

Fig. A-1. Continued.

```
D.1     STA     DBLOCK0,2
        TOM     71B
D.2     MUA     DBLOCK0,2
        STA     ZAQ+1
        TMA     71B
        SBA     SAVEN+1
D.3     STA     DBLOCK0+1,2
D.4     MUA     DBLOCK0+1,2
        SHAQ    24
        ADAQ    ZAQ
        ADAQ    ICOH,3
        STAQ    ICOH,3
        TIA     3
        AZJ,NE  *+2
        ENI     124,3
        INI     -2,3
        INI     -2,2
        IJD     A.3,1
        LDA     OUTBUF
        AZJ,EQ  OUT0
        LDQ     OUTBUF
        LDA     ICNT
        STAQ    FIRST1
        OUTW,INT 0,FIRST1,DBLOCK1+3968
        UJP     *-2
        UJP     WAIT
OUT0    LDQ     OUTBUF
        LDA     ICNT
        STAQ    FIRST0
        OUTW,INT 0,FIRST0,DBLOCK0+3968
        UJP     *-2
WAIT    TMA     22B
        LDI     ICNT,1
        ISG     100,1
        STA     ITIME1,1
        EXS     4,3                     CORE WRITING
        UJP     *                        YES , THEN WAIT FOR EOB INTERRUPT
        REM     END OF RECEIVE PERIOD SENSED IN PROC -
        REM     FINNSH UP PHASE 1 AND START PHASE 2
ENDREC  IOCL    10B
        SEL     13,0                    END FILE TAPE 2
        UJP     *-1
        SEL     8,0                     REWIND TAPE 2
        UJP     *-1
        ENI     21,1
        LDA     CITSAVE,1
        STA     CIT,1                   RESTORE CIT TABLE
        IJD     *-2,1
        UJP,I   RUN                     RETURN TO MAIN PROGRAM
        EJECT
```

Fig. A-1. Continued.

```
*
*         CH3 INTERFACE INTERRUPT PROCESSOR
*          ----------------------------
CH3       UJP       **
          COPY      3                       COPY STATUS OF CH 3
          TAM       77B
          ANA,S     2100B
          AZJ,NE    FAULT
EOBTEST   TMA       77B
          ANA,S     60B
          AZJ,EQ    NOTEOB
          ASE       20B
          UJP       EOB1
          ENI       BUF0,2
          ENI       DBLOCK0,3               ADDRESSES FOR BUFFER 0
          ENA,S     0
          STA       OUTBUF
ADMOD     STI       A.2,2                   MODIFY A.2 FOR BUFFER
          STI       D.1,3                   MODIFY DBLOCK ADDRESSES
          STI       D.2,3
          INI       1,3
          STI       D.3,3
          STI       D.4,3
          ENA,S     1
          RAD       ICNT                      ICNT= NO. OF BUFFERS
          LDI       ICNT,2
          TMA       22B
          ISG       100,2
          STA       ITIME2,2
          SEL       10B,3
          UJP       *-1
EXIT3     ENI       PROC,1
          STI       INT1,1
NOTEOB    ENA,S     CH3
          ENI       CIT,1
          STA       17,1
          UJP,I     CH3                       RETURN
EOB1      ENI       BUF1,2
          ENI       DBLOCK1,3
          ENA,S     1
          STA       OUTBUF
          UJP       ADMOD
FAULT     ENA,S     1
          RAD       FCNT                    UP FCNT
          SEL       11B,3                     CLEAR FAULT INT
          UJP       *-1
          UJP       EOBTEST
          EJECT
```

Fig. A-1. Continued.

```
*
*         CH0  CHANNEL 0 (TAPE) INTERRUPT PROCESSOR
*         -----------------------------
CH0       UJP       *
          ENA,S     CH0
          ENI       CIT,1
          STA       14,1                RESTORE CIT+14
          COPY      0                   COPY STATUS, CH 0
          INCL      0001                CLEAR INT CH 0
          TAM       76B                 SAVE STATUS
          LDA       ICNT
          ASE       1200
          UJP       *+2
          UJP       EOT
          TMA       76B
          LPA       =02400              TEST FOR ERROR
          AZJ,NE    ERT
          UJP,I     CH0                 RETURN
EOT       SEL       13,0                END FILE TAPE 2
          UJP       *-1
          SEL       8,0                 REWIND TAPE 2
          UJP       *-1
          IOCL      1
          UJP       *+1
          CON       3,0
          UJP       *-1
          ENA,S     1
          STA       NTAPES
          UJP,I     CH0
ERT       ENA,S     1
          RAD       IERRTCNT            UP TAPE ERROR COUNT
          UJP,I     CH0
          REM       ERR INT ANS ROUTINE
ERR       UJP       **
          LDA       INT1+1
          LDQ       INT1
          HLT       *+1
          UJP,I     ERR
          REM       TEMPORARY HALT WITH LOCS 4 AND 5 IN Q AND A
MANUAL    UJP       **                  MANUAL INT ROUTINE
          SEL       4,3                 DISABLE WRITE CORE
          UJP       *-1
          UCS       0                   STOP
          SJ1       ENDREC              SENSE SWITCH 1 ON, GO TO END
          IOCL      10B                 OFF CLEAR INTERFACE,
          UJP       RESTART             RESTART
          EJECT
INT1      EQU       4
BUF0      EQU       8192
BUF1      EQU       12288
SAVEQ     OCT       0
SAVEN     BSS       2
BIAS      OCT       00000177
          OCT       00000177
```

Fig. A-1. Continued.

```
ZAQ       OCT       0
          OCT       0
DATA      BSS       4092
OUTBUF    BSS       1                    0 IF BUF0 JUST FULL, 1 FOR BUF1
          DATA
ICOH      BSS       124
FIRST0    BSS       2
DBLOCK0   BSS       3968
          COMMON
ITIME1    BSS       100
ITIME2    BSS       100
ITITLE    BSS       18
IRUN      BSS       1
TIME1     BSS       1
TIME2     BSS       1
ICNT      BSS       1
FCNT      BSS       1
IERRTCNT  BSS       1
NTAPES    BSS       1
CITSAVE   BSS       22
FIRST1    BSS       2
DBLOCK1   BSS       3968
          END       MAIN
;FORTRAN,L
      SUBROUTINE INPUT
      COMMON ITIME1(100),ITIME2(100)
      COMMON ITITLE(18),IRUN,ITIM1,ITIM2,ICNT,IFCNT,IER
      TYPE DOUBLE(2) ICOH
      COMMON/DATA/ICOH(62)
      IRUN=1
      READ(60,200) (ITITLE(I),I=1,18)
  200 FORMAT(18A4)
      RETURN
      END

      SUBROUTINE INIT
      COMMON ITIME1(100),ITIME2(100)
      COMMON ITITLE(18),IRUN,ITIM1,ITIM2,ICNT,IFCNT,IER
      TYPE DOUBLE(2) ICOH
      COMMON/DATA/ICOH(62)
      IER=0
      IRUN=IRUN+1
      CALL CINIT
      RETURN
      END
```

Fig. A-1. Continued.

```
      SUBROUTINE ENDRUN
      COMMON ITIME1(100),ITIME2(100)
      COMMON ITITLE(18),IRUN,ITIM1,ITIM2,ICNT,IFCNT,IER
      TYPE DOUBLE(2) ICOH
      COMMON/DATA/ICOH(62)
      DIMENSION HAY(31),WES(31),X(31)
C     CONVERT TO FLOATING POINT
      DO 1 I=1,31
      K=2*I
      HAY(I)=ICOH(K-1)
      WES(I)=ICOH(K)
    1 X(I)=I
      WRITE(61,200) (ITITLE(I),I=1,18)
  200 FORMAT(18A4)
      WRITE(61,2000) IRUN
 2000 FORMAT(9X,11H RUN NUMBER,I5)
      WRITE(61,7007) ICNT,IFCNT,IER
 7007 FORMAT(6X,17H NO. OF BUFFERS =,I8,16H NO. OF FAULTS =,I8,23H NO. O
     1F PARITY ERRORS =,I8)
      WRITE(61,100) (M,HAY(M),WES(M),M=1,31)
  100 FORMAT(1X,7HBOX NO.,4X,8HHAYSTACK,8X,8HWESTFORD,/,(3(1X,I5,F16.0,F
     116.0)))
      CALL SKETCH(X,HAY,31)
      CALL SKETCH(X,WES,31)
      WRITE(61,99) (ITIME1(I),ITIME2(I),I=30,40)
   99 FORMAT(2I8)
      RETURN
      END
```

Fig. A-1. Continued.

```
          EXT       FOURIER2
          EXT       INPUT,INIT,ENDRUN
          EXT       CIT,CST,ABNORMAL
MAIN      UJP       **
LOC0      EQU       0
          SJ5       *+2                 SWITCH 5 ON MAKE BOOTSTRAP TAPE
          UJP       START
          LDA       *-1
          STA       LOC0
          CON       6,0
          UJP       *-1
          SEL       8,0
          UJP       *-1
          ENA,S     0
          ENI       7,1
          STA       CST,1               CLEAR CST
          IJD       *-1,1
          OUTW      0,0,77740B

          UJP       *-2
          EXS       2,0
          UJP       *-1
          EXS       2400B,0             CHECK FOR ERRORS
          HLT       *+1
          SEL       13,0
          UJP       *-1
          EINT      0
          HLT       77740B
START     RTJ       INPUT
RESTART   RTJ       INIT
          RTJ       RUN
          RTJ       ENDRUN
          UJP       RESTART
```

Fig. A-2. Hayford CW real-time processing program.

```
        CINIT CLEARS ARRAYS AND SETS UP INTERRUPT LOCATIONS
          ---------------------------
CINIT   UJP       **
        ENA,S     1
        STA       INT1-1              POWER FAILURE HALT
        ENI       ABNORMAL,1
        STA       1,1                 SET UP STOP IN ABNORMAL
        ENI       6144,1
        LDA       BIAS
        STA       BUF0,1              CLEAR BUFFERS
        IJD       *-1,1
        ENA,S     0
        STA       ICNT
        STA       FCNT
        ENI       100,1
        STA       ITIME1,1
        STA       ITIME2,1
        IJD       *-2,1
        ENI       2047,1
        STA       DBLOCK,1
        STA       SPECTRA,1
        IJD       *-2,1
        STA       IERRTCNT
        LDA       COSTBL              LOAD INITIAL TRIG FUNCTIONS
        STA       COS0
        LDA       SINTBL
        STA       SIN0
        LDA       COSDTBL
        STA       COSD0
        LDA       SINDTBL
        STA       SIND0
        ENI       21,1
        LDA       CIT,1
        STA       CITSAVE,1           SAVE CIT TABLE
        IJD       *-2,1
        UJP,I     CINIT
```

Fig. A-2. Continued.

```
          RUN CONNECTS INTERFACE AND OUTPUT DEVICES
           ----------------------------
RUN       UJP       **
          DINT      0                       DISABLE INT SYSTEM
          SCIM      7767B                   CLEAR INTERRUPT MASK
          SSIM      17B
          CON       20008,3                 CONNECT CHAN 3
          UJP       *-1
          EXS       1,3                     TEST FOR READY
          UJP       *+2                     YES
          UJP       *-2
          SEL       5,3                     CLEAR CH3 INT
          UJP       *-1
          IOCL      5                       CLEAR CHAN 0 AND 2
          CON       2,2                     CONNECT UNIT 2 TO CHANNEL 2
          UJP       *-1
          SEL       6,2                     SET 800 BPI
          UJP       *-1
          ENI       16,1
          ENA,S     CH2                     SET UP CH2 INTERRUPT LOC.
          STA       CIT,1
          ENI       12,1
          ENA,S     MANUAL
          STA       CIT,1
          ENI       17,1
          ENA,S     CH3
          STA       CIT,1                   SET CH3 INT ADDRESS
          SEL       3,3                     ENABLE/START WRITE CORE
          UJP       *-1
          EINT      0                       ENABLE INTERRUPTS
          SJ2       REINIT
          EXS       4,3                     TEST FOR WRITE CORE
          UJP       *+2
          UJP       *-3
          OUTW      2,MOIS0,ITITLE+17

          UJP       *-2
          EXS       2,2
          UJP       *-1                     WAIT TILL FINISHED
          UJP       *                       WAIT FOR INTERRUPT
REINIT    SJ6       *+3
          SEL       8,2
          UJP       *-1
          IOCL      4
          SJ3       *+3
          CON       1,2
          UJP       *-1                      CONNECT UNIT 1
          UJP       RESTART
```

Fig. A-2. Continued.

```
          PROC IS THE MAIN PROCESSING ROUTINE
           ----------------------------
PROC      ENA,S     0
          TAM       22B                 RESET CLOCK
          LDI       ICNT,1
          ISG       610,1
          UJP       *+2
          UJP       TOOLONG
          ENI       2044,1
          ENI       511,2
A,1       LDAQ      BUF0,1
          SBA       BIAS
          STA       ITR,2
          SHAQ      24
          SBA       BIAS
          STA       ITI,2
          INI       -4,1
          IJD       A,1,2               THIS LOOP = 12 MS. APPROX
          RTJ       FOURIER2            HAYSTACK SPECTRUM  300 MS. APPROX
          ENI       2046,1
          ENI       511,2
          ENI       1022,3
A,2       LDA       ITR,2
          STA       DBLOCK,3
          MUA       ITR,2
          STA       ZR+1
          STQ       ZR
          LDA       ITI,2
          STA       DBLOCK+1,3
          MUA       ITI,2
          SHAQ      24                  Q=A
          ADAQ      ZR                  I**2+R**2
          SHAQ      -5
          ADAQ      SPECTRA,3
          STAQ      SPECTRA,3
A,3       LDAQ      BUF0,1
          SBA       BIAS
          TAM       70B
          SHAQ      24                  Q =A
          SBA       BIAS
          TAM       71B
          MUA       SIN0
          SHAQ      1
          STQ       TEMP1
          TMA       70B
          MUA       COS0
          SHAQ      25
          ADA       TEMP1               W*C*COS0+W*S*SIN0=WC
          STA       ITR,2
          TMA       70B                 W*C
          MUA       SIN0
          SHAQ      1
          STQ       TEMP2               W,C*SIN0
```

Fig. A-2. Continued.

```
        TMA     71B
        MUA     COS0
        SHAQ    25
        SBA     TEMP2                   W*S*COS0-W*C*SIN0=WS
        STA     ITI,2
        REM     END OF PHASE CORRECTION,BEGIN TRIG RECURSION
        LDA     COS0
        MUA     COSD0
        SHAQ    1
        STQ     TEMP3
        LCA     SIN0
        MUA     SIND0
        SHAQ    25
        ADA     TEMP3
        STA     COS0
        LDA     SIN0
        MUA     COSD0
        SHAQ    1
        STQ     TEMP4
        LDA     COS0
        MUA     SIND0
        SHAQ    25
        ADA     TEMP4
        STA     SIN0
        INI     -4,1
        INI     -2,3
        IJD     A,2,2
        RTJ     FOURIER2                WESTFORD SPECTRUM  277*369 MS
        ENI     1022,3
        ENI     511,2
A,4     LDA     ITR,2
        STA     DBLOCK+1024,3
        MUA     ITR,2
        STA     ZR+1
        STQ     ZR
        LDA     ITI,2
        STA     DBLOCK+1025,3           DBLOCK+2047 INITIALLY
        MUA     ITI,2
        SHAQ    24
        ADAQ    ZR
        SHAQ    -5
        ADAQ    SPECTRA+1024,3
        STAQ    SPECTRA+1024,3
        INI     -2,3
        IJD     A,4,2
        REM     PICK UP NEXT SECOND*S PHASE CORRECTIONS
        LDI     ICNT,1
        LDA     COSTBL,1
        STA     COS0
        LDA     SINTBL,1
        STA     SIN0
        LDA     COSDTBL,1
        STA     COSD0
        LDA     SINDTBL,1
```

Fig. A-2. Continued.

```
         STA       SINDO
         LDI       ICNT,1
         TMA       228
         ISG       100,1
         STA       ITIME1,1
RECORD   LDA       ICNT
         LDQ       SAVEQ
         STAQ      FIRST
         OUTW,INT  2,FIRST,DBLOCK*2048

         UJP       *-2
         ENA,S     0
         STA       SAVEQ
ENDTEST  EXS       4,3
         UJP       *                      YES,THEN WAIT
END      IOCL      10B                    CLEAR INTERFACE
         EXS       2,2
         UJP       *-1                    WAIT TILL FINISHED WRITING
         SEL       13,2                   ENDFILE UNIT 2
         UJP       *-1
         SJ6       *+3
         SEL       9,2                    REWIND AND UNLOAD IF SSW6 ON
         UJP       *-1
         EXS       2,2
         UJP       *-1
         IOCL      4                      CLEAR CH2
         CON       1,2                    CONNECT UNIT 1 TO CH2
         UJP       *-1
         ENI       21,1
         LDA       CITSAVE,1
         STA       CIT,1                  RESTORE CIT TABLE
         IJD       *-2,1
         DINT      0
         SCIM      10B
         SSIM      7B
         EINT      0
         UJP,I     RUN
```

Fig. A-2. Continued.

```
          CH3 INTERFACE INTERRUPT PROCESSOR
           ****************************
CH3       UJP       **
          COPY      3                    COPY STATUS OF CH 3
          TAM       77B
          ANA,S     2100B
          AZJ,NE    FAULT
EOBTEST   TMA       77B
          ANA,S     60B
          AZJ,EQ    NOTEOB
          ENI       BUF0,2
          ASE       20B
          ENI       BUF1,2
          STI       A,1,2                MODIFY A.1 FOR BUFFER
          STI       A,3,2                MODIFY A.1,A.3 FOR BUFFER
          ENA,S     1
          RAD       ICNT                   ICNT= NO. OF BUFFERS
          LDI       ICNT,2
          TMA       22B
          ISG       100,2
          STA       ITIME2,2
          SEL       10B,3
          UJP       *-1
EXIT3     ENI       PROC,1
          STI       INT1,1
NOTEOB    ENA,S     CH3
          ENI       CIT,1
          STA       17,1
          UJP,I     CH3                    RETURN
FAULT     ENA,S     1
          RAD       FCNT                 UP FCNT
          SEL       11B,3                  CLEAR FAULT INT
          UJP       *-1
          UJP       EOBTEST
```

Fig. A-2. Continued.

```
          CH2 TAPE CHANNEL INTERRUPT PROCESSOR
          ------------------------------
CH2       UJP       *
          ENA,S     CH2
          ENI       CIT,1
          STA       16,1                RESTORE CIT+16
          COPY      2
          INCL      0004                CLEAR INTERUPT CH2
          TAM       768
          LPA       =02400              TEST FOR ERROR
          AZJ,NE    ERT
          UJP,I     CH2                 RETURN
ERT       ENA,S     1
          RAD       IERRTCNT            UP TAPE ERROR COUNT
          UJP,I     CH2
MANUAL    UJP       **                  MANUAL INT ROUTINE
          SEL       4,3                 DISABLE WRITE CORE
          UJP       *-1
          UCS       0                   STOP
          SJ1       END                 SENSE SWITCH 1 ON, GO TO END
          IOCL      10B                 OFF CLEAR INTERFACE,
          UJP       RESTART             RESTART
TOOLONG   SBCD      0                   SET BCD FAULT LITE
          UJP       ENDTEST
INT1      EQU       4
BUF0      EQU       8192
BUF1      EQU       12288
BIAS      OCT       177
SAVEQ     BSS       1
COS0      BSS       1
SIN0      BSS       1
COSD0     BSS       1
SIND0     BSS       1
TEMP1     BSS       1
TEMP2     BSS       1
TEMP3     BSS       1
TEMP4     BSS       1
CITSAVE   BSS       25
ZH        BSS       2
          DATA
ITR       BSS       512
ITI       BSS       512
SPECTRA   BSS       2048
COSTBL    BSS       610
SINTBL    BSS       610
COSDTBL   BSS       610
SINDTBL   BSS       610
          COMMON
MOIS0     BSS       5
IRUN      BSS       1
ITITLE    BSS       18
IERRTCNT  BSS       1
ICNT      BSS       1
FCNT      BSS       1
FIRST     BSS       2
DBLOCK    BSS       2048
ITIME1    BSS       100
ITIME2    BSS       100
          END       MAIN
```

Fig. A-2. Continued.

```
      SUBROUTINE INPUT
      COMMON MOIS0,JOUR0,IHR0,FIMN0
      COMMON IRUN,ITITLE(18),IER,ICNT,IFCNT,IBLOCK(2050)
      COMMON ITIME1(100),ITIME2(100)
      TYPE DOUBLE(2) SPECTRA
      COMMON/DATA/ITR(512),ITI(512),SPECTRA(1024)
      COMMON/DATA/ICOSP0(610),ISINP0(610),ICOSD0(610),ISIND0(610)
      DIMENSION IDENT(72),IDATES(72)
      READ(60,200) (ITITLE(I),I=1,18)
  200 FORMAT(18A4)
C     SENSE SWITCH 3 ON, TEST ROTATION
      GO TO(1,13) SSWTCHF(3)
   13 WRITE(59,12)
   12 FORMAT(31H TYPE  MONTH, DAY, HOUR, MINUTE)
      READ(58,11)MOIS1,JOUR1,IHR1,IMN1
   11 FORMAT(4I2)
      READ(6,1000)IDENT
      READ(6,1000)IDATES
 1000 FORMAT(72R1)
      IMN1 = IMN1 - 2
      IF(IMN1)4,3,3
    4 IHR1 = IHR1 - 1
      IMN1 = IMN1 + 60
      IF(IHR1)5,3,3
    5 JOUR1 = JOUR1 - 1
      IHR1 = IHR1 + 24
    3 READ(6,1002)MOIS,JOUR,IHR,IMN,R1,R2,D
 1002 FORMAT(4I2,3E18.11)
      IF(MOIS-MOIS1)3,6,1
    6 IF(JOUR-JOUR1)3,7,1
    7 IF(IHR-IHR1)3,8,1
    8 IF(IMN-IMN1)3,1,1
    1 IRUN=1
      RETURN
      END
```

Fig. A-2. Continued.

```
      SUBROUTINE INIT
      COMMON MOIS0,JOUR0,IHR0,FIMN0
      COMMON IRUN,ITITLE(18),IER,ICNT,IFCNT,IBLOCK(2050)
      COMMON ITIME1(100),ITIME2(100)
      TYPE DOUBLE(2) SPECTRA
      COMMON/DATA/ITR(512),ITI(512),SPECTRA(1024)
      COMMON/DATA/ICOSP0(610),ISINP0(610),ICOSD0(610),ISIND0(610)
      DIMENSION IWR(256),IWI(256),ITR2(256)
      DIMENSION REPH(15),RPHD(15),DOP(15)
      GO TO (20,21) SSWTCHF(3)
   20 WRITE(59,223)
  223 FORMAT(37H TYPE IN ROTATION IN CPS, FORMAT F6.3)
      READ(58,222) FCPS
  222 FORMAT(F6.3)
      ARG1=FCPS*2.0*3.1415926536
      ARG2=-ARG1/512.0
      DO 44 J=1,610
      A=ARG1*(J-1)
      ICOSP0(J)=8388607.0*COS(A)
      ISINP0(J)=8388607.0*SIN(A)
      ICOSD0(J)=8388607.0*COS(ARG2)
   44 ISIND0(J)=8388607.0*SIN(ARG2)
      GO TO 22
   21 WRITE(59,112)
  112 FORMAT(55H FORMAT 5I2 , TYPE MONTH, DAY, HOUR, MINUTE, SECOND     )
      READ(58,110) MOIS0,JOUR0,IHR0,MN,ISEC
  110 FORMAT(5I2)
      FIMN0=MN+ISEC/60.0
      TWOPI = 2.*3.1415926536
      INTERM = FIMN0 $ IF((FIMN0-INTERM) - 0.5)2,11,11
    2 IMN0 = INTERM $ GO TO 13
   11 IMN0 = INTERM + 1
   13 IMNI = IMN0 - 2 $ IHRI = IHR0 $ JOURI = JOUR0 $ MOISI = MOIS0
      FIMNI = FIMN0 $ IF(IMNI)30,1,1
   30 IHRI = IHRI - 1 $ IMNI = IMNI + 60 $ IF(IHRI)31,1,1
   31 JOURI = JOURI - 1 $ IHRI = IHRI + 24
    1 READ(6,1002)MOIS,JOUR,IHR,IMN,REPH(1),RPHD(1),DOP(1)
 1002 FORMAT(4I2,3E18.11)
      IF(MOIS-MOISI)1,5,100
    5 IF(JOUR-JOURI)1,8,100
    8 IF(IHR-IHRI)1,9,100
    9 IF(IMN-IMNI)1,10,100
  100 DO 24 I=1,10
   24 BACKSPACE 6
      GO TO 1
   10 DO 7 J=2,15
      READ(6,1002)MOIS,JOUR,IHR,IMN,REPH(J),RPHD(J),DOP(J)
    7 CONTINUE
      J = 1 $ I = 1
   15 LL = J + 2
      AP = REPH(LL)
      BP=(8.*(REPH(LL+1)-REPH(LL-1))-(REPH(LL+2)-REPH(LL-2)))/12.
      CP=(16.*(REPH(LL+1)+REPH(LL-1)-2.*AP)-(REPH(LL+2)+REPH(LL-2)-2.*AP
     1))/24.
      DP=((REPH(LL+2)-REPH(LL-2))-2.*(REPH(LL+1)-REPH(LL-1)))/12.
      EP=((REPH(LL+2)+REPH(LL-2)-2.*AP)-(1./3.)*(REPH(LL+1)+REPH(LL-1)-
     12.*AP))/24.
      AD = RPHD(LL)
      BD=(8.*(RPHD(LL+1)-RPHD(LL-1))-(RPHD(LL+2)-RPHD(LL-2)))/12.
      CD=(16.*(RPHD(LL+1)+RPHD(LL-1)-2.*AD)-(RPHD(LL+2)+RPHD(LL-2)-2.*AD
```

Fig. A-2. Continued.

```
  1))/24.

   DD=((RPHD(LL+2)-RPHD(LL-2))-2.*(RPHD(LL+1)-RPHD(LL-1)))/12.
   ED=((RPHD(LL+2)+RPHD(LL-2)-2.*AD)-(1./3.)*(RPHD(LL+1)+RPHD(LL-1)-
  12.*AD))/24.
   DT = FIMNI - IMN0 $ DELT = (1. - DOP(J+2)/.784E10)/60.
17 PHITI = (((EP*DT + DP)*DT + CP)*DT + BP)*DT + AP
   ARG = PHITI*TWOPI
   ICOSP0(I) = COS(ARG)*8388607. $ ISINP0(I) = SIN(ARG)*8388607.
   DPHTI = (((ED*DT + DD)*DT + CD)*DT + BD)*DT + AD
   ARG=-DPHTI*TWOPI/(60.*512.)
   ICOSD0(I) = COS(ARG)*8388607. $ ISIND0(I) = SIN(ARG)*8388607.
   I = I + 1 $ IF((FIMNI-FIMN0).GE.10.)18,19
19 DT = DT + DELT $ FIMNI = FIMNI + DELT
   IF((FIMNI-IMN0).LT.(0.5))17,12
12 J = J + 1 $ IMN0 = IMN0 + 1 $ GO TO 15
18 CONTINUE
   DO 6 I=1,20
   BACKSPACE 6
 6 CONTINUE
22 NPTS=512
   IBITS=12
   CALL  FORINIT2(ITR,ITI,IWR,IWI,ITR2,NPTS,1,IBITS)
   CALL CINIT
   RETURN
   END
```

Fig. A-2. Continued.

```
      SUBROUTINE ENDRUN
      COMMON MOISO,JOURO,IHRO,FIMNO
      COMMON IRUN,ITITLE(18),IER,ICNT,IFCNT,IBLOCK(2050)
      COMMON ITIME1(100),ITIME2(100)
      TYPE DOUBLE(2) SPECTRA
      COMMON/DATA/ITR(512),ITI(512),SPECTRA(1024)
      COMMON/DATA/ICOSPO(610),ISINPO(610),ICOSDO(610),ISINDO(610)
      DIMENSION HAYSPEC(512),WESPEC(512)
      DIMENSION P(200),X(200)
      EQUIVALENCE (P,IBLOCK),(X,IBLOCK(500))
C      CONVERT TO FLOATING POINT
      DO 2 I=1,256
      HAYSPEC(I)=SPECTRA(I+256)
      WESPEC(I)=SPECTRA(I+768)
      HAYSPEC(I+256)=SPECTRA(I)
    2 WESPEC(I+256)=SPECTRA(I+512)
      WRITE(61,200) (ITITLE(I),I=1,18)
  200 FORMAT(18A4)
      WRITE(61,2000) IRUN
 2000 FORMAT(9X,11H RUN NUMBER,I5)
      WRITE(61,7007) ICNT,IFCNT,IER
 7007 FORMAT(6X,17H NO. OF BUFFERS =,I8,16H NO. OF FAULTS =,I8,23H NO. O
     1F PARITY ERRORS =,I8)
      DO 3 K=1,64
      IFQ=-256+8*(K-1)
      J1=(K-1)*8+1
      J2=J1+7
      WRITE(61,203) (IFQ,(HAYSPEC(J),J=J1,J2),(WESPEC(L),L=J1,J2))
  203 FORMAT(1X,I5,8F16.0,/,6X,8F16.0)
    3 CONTINUE
      WRITE(61,101) (ITIME1(I),ITIME2(I),I=30,40)
  101 FORMAT(1X,2I8)
C     TEMPORARY TIME PRINTOUT
      K=308
      DO 4 I=1,200,2
      P(I)=HAYSPEC(K)
      P(I+1)=WESPEC(K)
      K=K+1
      X(I)=50+I/2
    4 X(I+1)=X(I)+.5
      CALL SKETCH(X,P,200)
      IRUN=IRUN+1
      RETURN
      END
```

Fig. A-2. Continued.

```
HAYFORD EPHEMERIS
▲FORTRAN S,LS
      C  COMPUTATION OF PARAMETERS PERTINENT TO THE 'HAYFORD' INTERFEROMETER
      C  EXPERIMENT
           DIMENSION MH(-1:1),M(-1:1),APAZ(-1:1),APEL(-1:1),ALPHA(-1:1),DELTA
          *(-1:1),REPH(-1:1),IDENT(72),IDATES(72),ST(12)
           NAME LIST FREQ,GCLA1,GCL01,GCDI1,GCLA21,GCL021,GCDI21,SMALLD,
          *SMALAZ,OBJRRA,OBJRDE,OBJSP,OBJRAD,EPSILO,SMALLE,T,P,E,OMEGAI
           T = 283.15 ; P = 1013.25 ; E = 10.
           ST(1)=23989.709;ST(2)=31322.982;ST(3)=37946.527;ST(4)=45279.704
           ST(5)=52376.353;ST(6)=59709.608;ST(7)=66806.344;ST(8)=74139.627
           ST(9)=81472.863;ST(10)= 216.947;ST(11)=9502.646;ST(12)=16599.356
           PI=3.1415926536;DETORA=PI/180.;FREQ=7840.;GCLA1=42.62325*DETORA
           C=.2997925E6 ; GCDI1=6368.4844944;GCLA21=-0.01049*DETORA
           GCL021=-0.00672*DETORA;GCL01=71.48869*DETORA
                                EPSILO=+0.3E-3;OBJRRA=90.3*DETORA;OBJRAD=6089.
           SMALLD = 1.239365568 ; SMALAZ = 201.896389*DETORA
           SMALLE=-1.38138889*DETORA;GCDI21=SMALLD*SIN(SMALLE)
           OBJRDE=-66.7*DETORA;OBJSP=21176640.;OMEGAI=.29670359E-6
         7 LICO = 30
           READ(7,1030)IAN ,MOIS1,JOUR1,IHR1,IMN1,IAN ,MOIS2,JOUR2,IHR2,IMN2
      1030 FORMAT(10I3)
           CALL DAJU67(MOIS1,JOUR1,JULD1)
           CALL DAJU67(MOIS2,JOUR2,JULD2)
           WRITE(5,1032)
      1032 FORMAT($IF STANDARD PARAMETERS, CR.  IF NEW VALUES, TYPE 1, CR AND
          * INPUT NAME LIST$)
         1 READ(5,1020)I
      1020 FORMAT(I)
           IF(I)2,3,2
         2 INPUT(5)
         3 CONTINUE
           WRITE(4,1010)
      1010 FORMAT(21HOEXPERIMENT 'HAYFORD')
           READ(3,1000)IDENT
           READ(3,1000)IDATES
           WRITE(6,1000)IDENT
           WRITE(6,1000)IDATES                                              A
      1000 FORMAT(72R1)
           WRITE(4,1011)IDENT,IDATES
      1011 FORMAT(40HOINTERFEROMETER EPHEMERIS DERIVED FROM :/72R1/72R1)
           WRITE(4,1012)FREQ
      1012 FORMAT(32HOSITE 1 : HAYSTACK,  FREQUENCY =,F8.2,$ MHZ,  SITE 2 : W
          *ESTFORD$)
           WRITE(4,1013)AZ21/DETORA,EL21/DETORA,GCLA21/DETORA,GCL021/DETORA,
```

Fig. A-3. Hayford ephemeris program.

```
HAYFORD EPHEMERIS
      *GCDI21
 1013 FORMAT(32HODIFFERENCES (SITE 2 - SITE 1) :/$  AZIMUTH AXIS DIFF. =
     *$,F8.5,$ DEGREES, ELEVATION AXIS DIFF. =$,F8.5,$  DEGREES$/$  GEOC
     *ENTRIC LATITUDE DIFF. =$,F8.5,$ DEGREES,  GEOCENTRIC LONGITUDE DIF
     *F. =$,F8.5,$ DEGREES,$/$  HEIGHT DIFF. =$,F8.5,$ KM$)
       WRITE(4,1014)JULD1,IHR1,IMN1
 1014 FORMAT(30H0OBJECT : VENUS,  JULIAN DAY =,I8,$,  GMT =$,2(1X,I2))
       WRITE(4,1015)OBJRRA/DETORA,OBJRDE/DETORA,OBJSP,OBJRAD
 1015 FORMAT(38HOCOORDINATES OF VENUS ROTATION AXIS : ,/$  R.A. =$,F5.1,
     *$ DEGREES, DECL. =$,F5.1,$ DEGREES, SIDEREAL PERIOD =$,F8.0,$ SECO
     *NDS, RADIUS =$,F8.2,$ KM$)
       FACTOR = (77.6/T)*(P + 4810.*E/T)
       FREQ=FREQ*1.E6;FC=FREQ/C;SLA1=SIN(GCLA1);CLA1=COS(GCLA1)
       DELTX = -SMALLD*COS(SMALLE)*COS(SMALAZ)
       DELTY = SMALLD*COS(SMALLE)*SIN(SMALAZ)
       DELTZ = SMALLD*SIN(SMALLE)
       IMN1=IMN1-1 ; IF(IMN1)9,19,19
     9 IMN1=IMN1+60 ; IHR1=IHR1-1 ; IF(IHR1)18,19,19
    18 IHR1=IHR1+24 ; JOUR1=JOUR1-1
    19 IMN2=IMN2+1 ; IF(IMN2-60)10,22,22
    22 IMN2=IMN2-60 ; IHR2=IHR2+1 ; IF(IHR2-24)10,23,23
    23 IHR2=IHR2-24 ; JOUR2=JOUR2+1
    10 READ(3,1001)JDAY,JEXP,MH(-1),M(-1),IST,ELD,IELEXP,AZD,IAZEXP,TM1,
     *DOP,DTM,DDOP
       IF(MH(-1).EQ.24)GO TO 14
       GO TO 15
    14 READ(3,1001)JDAY,JEXP,MH(-1),M(-1),IST,ELD,IELEXP,AZD,IAZEXP,THRTM
     *,THRDOP,DTM,DDOP
    15 CONTINUE
 1001 FORMAT(3X,I7,2X,4I3,2(4X,I9,1X,I3),F11.6,F12.3,2F11.4)
       CALL DAJU67(MOIS1,JOUR1,JULD1)
       CALL DAJU67(MOIS2,JOUR2,JULD2)
       IF(JDAY-JULD1)10,24,11
    24 IF(MH(-1)-IHR1)10,25,11
    25 IF(M(-1)-IMN1)10,11,11
    11 APAZ(-1)=AZD*(10.**(IAZEXP-9))*DETORA
       CAZ = COS(APAZ(-1)); SAZ = SIN(APAZ(-1))
       APEL(-1) = ELD*10.**(IELEXP-9)
       ROEL = APEL(-1)*DETORA
       CREL = COS(ROEL) ; SREL = SIN(ROEL)
       TAU = 180.*1.E-6*(COS(APEL(-1)*DETORA)/SIN(APEL(-1)*DETORA) -
      1 42.5/(APEL(-1) + 0.4)**2.64)*FACTOR/PI - 40./(APEL(-1) + 2.7)**4.
       APEL(-1) = (APEL(-1) + TAU)*DETORA
       CEL = COS(APEL(-1)) ; SEL = SIN(APEL(-1))
```

Fig. A-3. Continued.

```
HAYFORD EPHEMERIS
      CALL JUDA67(JDAY,MOIS,JOUR)
      SGMT=ST(MOIS)+(JOUR-1)*236.5
      SGMTU = SGMT + (MH(-1)*3600. + M(-1)*60.)*(1. + 236.5/(24.*3600.))
      STL=SGMTU-GCL01*(12./PI)*3600.
      SINDEL=SEL*SLA1+CEL*CAZ*CLA1;COSDEL=SQRT(1.-SINDEL*SINDEL)
      SNRDEL=SREL*SLA1+CREL*CAZ*CLA1;CSRDEL=SQRT(1.-SNRDEL*SNRDEL)
      SINTHE=-(CEL*SAZ)/COSDEL;COSTHE=(SEL*CLA1-CEL*CAZ*SLA1)/COSDEL
      SNRTHE=-(CREL*SAZ)/CSRDEL;CSRTHE=(SREL*CLA1-CREL*CAZ*SLA1)/CSRDEL
      THETA = ATAN2(SNRTHE,CSRTHE)
      ALPHA(-1) = STL*PI/(3600.*12.) - THETA
      IF(ALPHA(-1).GE.(2.*PI))ALPHA(-1) = ALPHA(-1) - 2.*PI
      DELTA(-1) = ATAN(SNRDEL/CSRDEL)
      DELZ = CEL*(SMALLD*COS(SMALLE)*COS(APAZ(-1)-SMALAZ) + EPSILO) +
     *SIN(SMALLE)*SEL*SMALLD
      DELZ = DELZ*(1. + FACTOR*1.E-6)
      REPH(-1) = DELZ*(FC + DOP/C)
      READ(3,1001)JDAY,JEXP,MH(0),M(0),IST,ELD,IELEXP,AZD,IAZEXP,TMO,
     *DOPO,DTM,DDOP
      IF(MH(0).EQ.24)GO TO 20
      GO TO 21
   20 READ(3,1001)JDAY,JEXP,MH(0),M(0),IST,ELD,IELEXP,AZD,IAZEXP,THRTM,
     *THRDOP,DTM,DDOP
   21 CONTINUE
      APAZ(0) =AZD*(10.**(IAZEXP-9))*DETORA
      CAZ0= COS(APAZ(0)) ; SAZ0= SIN(APAZ(0))
      APEL(0)  = ELD*10.**(IELEXP-9)
      ROEL = APEL(0)*DETORA
      CREL0 = COS(ROEL) ; SREL0 = SIN(ROEL)
      TAU = 180.*1.E-6*(COS(APEL( 0)*DETORA)/SIN(APEL( 0)*DETORA) -
     1 42.5/(APEL( 0) + 0.4)**2.64)*FACTOR/PI - 40./(APEL( 0) + 2.7)**4.
      APEL( 0) = (APEL( 0) + TAU)*DETORA
      CEL0= COS(APEL(0) ) ; SEL0= SIN(APEL(0) )
      CALL JUDA67(JDAY,MOIS,JOUR0)
      SGMT = ST(MOIS) + (JOUR0-1)*236.5
      SGMTU = SGMT + (MH(0) *3600. + M(0) *60.)*(1. + 236.5/(24.*3600.))
      STL=SGMTU-GCL01*(12./PI)*3600.
      SINDE0=SEL0*SLA1+CEL0*CAZ0*CLA1;COSDE0=SQRT(1.-SINDE0*SINDE0)
      SNRDE0=SREL0*SLA1+CREL0*CAZ0*CLA1;CSRDE0=SQRT(1.-SNRDE0*SNRDE0)
      SINTH0=-(CEL0*SAZ0)/COSDE0
      SNRTH0 = -(CREL0*SAZ0)/CSRDE0
      COSTH0=(SEL0*CLA1-CEL0*CAZ0*SLA1)/COSDE0
      CSRTH0 = (SREL0*CLA1-CREL0*CAZ0*SLA1)/CSRDE0
      THETA = ATAN2(SNRTH0,CSRTH0)
      ALPHA(0)  = STL*PI/(3600.*12.) - THETA
```

Fig. A-3. Continued.

```
HAYFORD EPHEMERIS
   132:        IF(ALPHA(0) .GE.(2.*PI))ALPHA(0)  = ALPHA(0)  - 2.*PI
   133:        DELTA(0) = ATAN(SNRDE0/CSRDE0)
   134:        DELZ =CEL0*(SMALLD*COS(SMALLE)*COS(APAZ(0) -SMALAZ) + EPSIL0) +
   135:       *SIN(SMALLE)*SEL0*SMALLD
   136:        DELZ = DELZ*(1. + FACTOR*1.E-6)
   137:        REPH(0) = DELZ*(FC + D0P0/C)
   138:     12 READ(3,1001)JDAY,JEXP,MH(1),M(1),IST,ELD,IELEXP,AZD,IAZEXP,TM,D0P,
   139:       *DTM,DD0P
   140:        IF(MH(1).EQ.24)GO TO 16
   141:        GO TO 17
   142:     16 READ(3,1001)JDAY,JEXP,MH(1),M(1),IST,ELD,IELEXP,AZD,IAZEXP,THRTM,
   143:       *THRD0P,DTM,DD0P
   144:     17 CONTINUE
   145:        APAZ(1) =AZD*(10.**(IAZEXP-9))*DETORA
   146:        CAZ = COS(APAZ(1)) ; SAZ = SIN(APAZ(1))
   147:        APEL(1)  = ELD*10.**(IELEXP-9)
   148:        ROEL = APEL(1)*DETORA
   149:        TAU = 180.*1.E-6*(COS(APEL( 1)*DETORA)/SIN(APEL( 1)*DETORA) -
   150:       1 42.5/(APEL( 1) + 0.4)**2.64)*FACTOR/PI - 40./(APEL( 1) + 2.7)**4.
   151:        APEL( 1) = (APEL( 1) + TAU)*DETORA
   152:        CEL = COS(APEL(1) ) ; SEL = SIN(APEL(1) )
   153:        CREL = COS(ROEL) ; SREL = SIN(ROEL)
   154:        DELZ = CEL*(SMALLD*COS(SMALLE)*COS(APAZ(1) -SMALAZ) + EPSIL0) +
   155:       *SIN(SMALLE)*SEL*SMALLD
   156:        DELZ = DELZ*(1. + FACTOR*1.E-6)
   157:        REPH(1)  = DELZ*(FC + D0P/C)
   158:        REPHD = (REPH(1) - REPH(-1))/2.
   159:        SINDEL=SEL*SLA1+CEL*CAZ*CLA1;COSDEL=SQRT(1.-SINDEL*SINDEL)
   160:        SNRDEL=SREL*SLA1+CREL*CAZ*CLA1;CSRDEL=SQRT(1.-SNRDEL*SNRDEL)
   161:        SINTHE=-(CEL*SAZ)/COSDEL;COSTHE=(SEL*CLA1-CEL*CAZ*SLA1)/COSDEL
   162:        SNRTHE=-(CREL*SAZ)/CSRDEL;CSRTHE=(SREL*CLA1-CREL*CAZ*SLA1)/CSRDEL
   163:        CALL JUDA67(JDAY,MOIS,JOUR)
   164:        SGMT=ST(MOIS)+(JOUR-1)*236.5
   165:        SGMTU = SGMT + (MH(1) *3600. + M(1) *60.)*(1. + 236.5/(24.*3600.))
   166:        STL=SGMTU-GCL01*(12./PI)*3600.
   167:        THETA = ATAN2(SNRTHE,CSRTHE)
   168:        ALPHA(1)  = STL*PI/(3600.*12.) - THETA
   169:        IF(ALPHA(1) .GE.(2.*PI))ALPHA(1)  = ALPHA(1)  - 2.*PI
   170:        DELTA(1) = ATAN(SNRDEL/CSRDEL)
   171:        DXDP=DELTX*(SIND E0*SLA1*COSTHO+CLA1*COSDE0)-DELTY*SINDEC*SINTHO+
   172:       * DELTZ*(CLA1*COSTHO*SINDE0-SLA1*COSDE0)
   173:        DYDP=DELTX*SLA1*SINTHO+DELTY*COSTHO+DELTZ*CLA1*SINTHO
   174:        GAMHW=ATAN(-DYDP/DXDP)
   175:        ALPHAD = (ALPHA(1) - ALPHA(-1))/120.
```

Fig. A-3. Continued.

```
HAYFORD EPHEMERIS
   176:        DELTAD = (DELTA(1) - DELTA(-1))/120.
   177:        OMGXDP=OMEGAI*(COS(OBJRRA-ALPHA(0))*COS(OBJRDE)*SNRDEO-SIN(OBJRDE)
   178:       **CSRDEO)+ALPHAD*CSRDEO
   179:        OMGYDP=OMEGAI*(SIN(OBJRRA-ALPHA(0))*COS(OBJRDE))+DELTAD
   180:        OMORTH=SQRT(OMGYDP*OMGYDP+OMGXDP*OMGXDP)
   181:        CTOLD = 2.**(FC + DOPO/C)*OBJRAD*OMORTH
   182:        GAMAXS=ATAN(-OMGYDP/OMGXDP)
   183:        BL = (FC+DOPO/C)*SQRT(DXDP*DXDP+DYDP*DYDP)*(1. + FACTOR*1.E-6)
   184:        WRITE(6,1002)MOIS,JOURO,MH(0),M(0),REPH(0),REPHD,DOPO
   185:  1002 FORMAT(4I2,3E18.11)
   186:        IF(LICO-30)30,31,30
   187:     31 WRITE(4,1052)JDAY,MOIS,JOURO,IAN
   188:  1052 FORMAT(14H1JULIAN DATE =,I8,$,  GMT DATE =$3I3)
   189:        WRITE(4,1051)
   190:  1051 FORMAT(106HO GMT      APP.EL.    APP.AZ.     REL.PHASE     REPHDOT  BA
   191:       1SELINE   BL DIR.    C.L.DOP  DOP.AX.DIR.  TIME DELAY/$ HR MN     DEG
   192:       2REES   DEGREES   WAVELENGTHS   WL/MIN  WAVELENGTHS DEGREES       HZ
   193:       3      DEGREES       SECONDS$//)
   194:        LICO = 0
   195:     30 CONTINUE
   196:        WRITE(4,1050)MH(0),M(0),APEL(0)/DETORA,APAZ(0)/DETORA,REPH(0),
   197:       *REPHD,BL,GAMHW/DETORA,CTOLD,GAMAXS/DETORA,TMO
   198:  1050 FORMAT(2I3,1X,2F10.3,3X,2F10.2,F10.0,3F10.1,4X,F10.2)
   199:        LICO = LICO + 1
   200:        APAZ(-1) = APAZ(0) ; APAZ(0) = APAZ(1)
   201:        APEL(-1) = APEL(0) ; APEL(0) = APEL(1)
   202:        ALPHA(-1) = ALPHA(0) ; ALPHA(0) = ALPHA(1)
   203:        DELTA(-1) = DELTA(0) ; DELTA(0) = DELTA(1)
   204:        REPH(-1) = REPH(0) ; REPH(0) = REPH(1)
   205:        MH(-1) = MH(0) ; MH(0) = MH(1)
   206:        M(-1) = M(0) ; M(0) = M(1)
   207:        CAZO=CAZ;SAZO=SAZ;CELO=CEL;SELO=SEL;CRELO=CREL;SRELO=SREL
   208:        SINDEO=SINDEL;COSDEO=COSDEL;SINTHO=SINTHE;COSTHO=COSTHE
   209:        SNRDEO=SNRDEL;CSRDEO=CSRDEL;SNRTHO=SNRTHE;CSRTHO=CSRTHE
   210:        DOPO = DOP ; TM1 = TMO ; TMO = TM ; JOURO = JOUR
   211:        IF(JULD2-JDAY)13,26,12
   212:     26 IF(IHR2-MH(1))13,27,12
   213:     27 IF(IMN2-M(1))13,13,12
   214:     13 PAUSE 13
   215:        IF(SENSE SWITCH 1)7,8
   216:      8 STOP
   217:        END
***GLOBAL VARIABLES***
```

Fig. A-3. Continued.

```
      PROGRAM HAYFORD2
      CHARACTER CH
      COMMON    RA(50),DECS(50),NDAY(50),DIST(50),IDATA(7940),WA(64,31),
     1CROTFR(64),W(2,64),CROT(64),SROT(64),C(2,64,31),H(2,64),SROTFR(64)
     2,WFOUR3(64)
      DIMENSION SCRATA(64,31),SCRATB(2,64,31),WA(64,31 ),CH(84)
      EQUIVALENCE(IDATA,SCRATA,SCRATB,CH),(WA,HA)
      PI=3.1415926536
      DO 2 I=1,50
      READ 1, HRS,AMIN,SECS,DEGS,DMINS,DSEC,DIST(I),NDAY(I)
    1 FORMAT (7F10.7,I3)
      RA(I)=HRS*PI/12.0 +AMIN*PI/720.0+SECS*PI/43200.0
    2 DECS(I)=DEGS*PI/180.0+SIGN((DMINS*PI/10800.0+DSEC*PI/648000.0
     1),DEGS)
    3 CONTINUE
      REWIND 30
      INR=0
      IDA=0
      MOIS=0
      ICOUNT=0
      WESN=WESS=AWESS=AWESN=HAYN=HAYS=AHAYS=AHAYN=0.0
      DO 4 I=1,64
      DO 4 K=1,31
    4 WA(I,K)=WA(I,K)=C(1,I,K)=C(2,I,K)=0.0
      BUFFER IN(30,1)(IDATA(1),IDATA(21))
   10 GO TO (10,11),UNITSTF(30)
   11 PRINT 12,(CH(I),I=1,84)
   12 FORMAT(84R1)
      DO 19 I=1,72
      IF(IDA.EQ. 0)111,19
  111 IF(CH(I)    .LE. 9)13,19
   13 IF(CH    (I),GE. 0)14,19
   14 IF(CH    (I+1),LE. 9)15,17
   15 IF(CH    (I+1),GE. 0)16,17
   16 IDAY=CH    (I)*10+CH    (I+1)
      GO TO 18
   17 IDAY=CH    (I)
      GO TO 18
   18 IDA=I
   19 CONTINUE
      DO 130 I=IDA,72
      IF(CH    (I),EQ.1RA)120,125
  120 IF(CH    (I+1),EQ.1RU)121,125
  121 MOIS=8
      GO TO 130
  125 IF(CH    (I),EQ.1RS)  126,130
  126 IF(CH    (I+1),EQ.1RE)127,130
  127 MOIS=9
  130 CONTINUE
      IF(MOIS.EQ. 0)131,134
  131 WRITE(59,132)
  132 FORMAT(7HNO DATE)
      READ(58,133)MOIS,IDAY
  133 FORMAT(2I2)
  134 TIME=(((((CH(80)+0)*64.+CH(81))*64.+CH(82))*64.+CH(83))*64.+CH(84
     1))/36000000.0
      NDAYT=MOIS*100+IDAY
      I8=0
      DO 304 I=1,50
      IF(NDAYT-NDAY(I)) 304,305,304
```

Fig. A-4. Coded-pulse phase calibration and fringe rotation program.

```
305 IB=I
304 CONTINUE
    PRINT 306,NDAYT,NDAY(IB),RA(IB),DECS(IB),TIME
306 FORMAT(2I20,3F20.5)
    IC=IB+1$ID=IB-1
    CRA=RA(IB)+(RA(IC)-RA(ID))*TIME/48.0
    CDEC=DECS(IB)+(DECS(IC)-DECS(ID))*TIME/48.0
    ANG=CRA-179.7*PI/180.0
    NDAYN=(MOIS-8)*31 + IDAY  +212
    STIME=((TIME/24.0)+(NDAYN-212))*2.0*PI*1.002737909
   1 +(15.0/24.0+45.0/1440.0 +45.868/(24.0*3600.0))*2.0*PI
    BN=32450.0$BA=44.0*PI/180.0+19.0*PI/(180.0*60.0)
    BHA=31.0*PI/180.0 + 22.0*PI/(180.0*60.0)
    BLN=BN*(COS(CDEC)*SIN(BA)+COS(BA)*COS(BHA-STIME+CRA)*SIN(CDEC))
    BLW=BN*(COS(BA)*SIN(BHA-STIME+CRA))
    BLA=ATAN(BLW/BLN)
    BLL=SQRT(BLN*BLN+BLW*BLW)
    FLN=94.7*(COS(23.3*PI/180.0)*COS(CDEC)-SIN(CDEC)*SIN(23.3*PI/180.0
   1)*SIN(ANG))+1.068*(RA(IC)-RA(ID))*180.0*30.0/PI-0.72*COS(CRA-ST
   2IME)/DIST(IB)
    FLW=94.7*SIN(23.3*PI/180.0)*COS(ANG)-1.068*(DECS(IC)-DECS(ID))
   1*180.0*30.0/PI
    DOPA=ATAN(FLW/FLN)
    FL=SQRT(FLN*FLN+FLW*FLW)
    ROT=2.0*PI*SIN(DOPA-BLA)*BLL*6.055/(FL*DIST(IB)*149600.0)
    THETA=360.0*COS(DOPA-BLA)*BLL*6.055/(DIST(IB)*149600.0)
    DO 144 I=1,64
    $ROTFR(I)=SIN((I-33)*ROT)
144 CROTFR(I)=COS((I-33)*ROT)
    PRINT 307,NDAYN,CRA,CDEC,ANG,STIME,BLA,BLL,DOPA,FL,ROT,THETA
307 FORMAT(1X,I3,10F12.4)
140 STIME=STIME+15.*2.*PI/(60.*60.*24.)
    PHLR=BN*COS(BA)*COS(CDEC)*SIN(BHA-STIME+CRA)*2.0*PI/86164.0
    PHL=BN*COS(BA)*COS(CDEC)*COS(BHA-STIME+CRA)
    PRINT 141,PHLR,PHL
141 FORMAT(10X,2F20.6)
142 DO 143 I=1,64
    $ROT(I)=SIN(PHLR*2.0*PI*((I-1)/64.0+ICOUNT-1.0)*PHL*2.0*PI)
143 CROT(I)=COS(PHLR*2.0*PI*((I-1)/64.0+ICOUNT-1.0)*PHL*2.0*PI)
    IP=IPP=0
 20 BUFFER IN(30,1)(IDATA(1),IDATA(3970))
 30 GO TO(30,40,50,60),UNITSTF(30)
 60 PRINT 61,IP
 61 FORMAT(1X,12HPARITY ERROR,I10)
    IP=IP+1
 40 BUFFER IN(30,1)(IDATA(3971),IDATA(7940))
 41 GO TO(41,70,50,80),UNITSTF(30)
 80 PRINT 81,IPP
 81 FORMAT(1X,12HPARITY ERROR,I10)
    IP=IP+1
 70 PRINT 82, IDATA(1),IDATA(3971)
 82 FORMAT(1X,6HRECORD,2I20)
    IF(IP-1)84,83,83
 83 DO 85 I=1,7940
 85 IDATA(I)=0
 84 DO 78 IR=1,31
    DO 71 I=1,64
    K=4*IR+(I-1)*124+ISIGN(1,-1+2*(I-32))
```

Fig. A-4. Continued.

```
      H(1,I)=IDATA(K)$H(2,I)=IDATA(K+1)
      W(1,I)=IDATA(K+2)*CROT(I)+IDATA(K+3)*SROT(I)
   71 W(2,I)=-IDATA(K+2)*SROT(I)+IDATA(K+3)*CROT(I)
      CALL FOURIER3(H,WFOUR3,64,-1,0)
      CALL FOURIER3(W,WFOUR3,64,-1,0)
      DO 72 I=1,64
      L=I+ISIGN(32,1+2*(32-I))
      IF(IR-3)73,74,77
   73 WESN=WESN+(W(1,L)*W(1,L)+W(2,L)*W(2,L))/(64.0*      2.0)
      HAYN=HAYN+(H(1,L)*H(1,L)+H(2,L)*H(2,L))/(64.0*      2.0)
      GO TO 77
   74 IF(I-30)77,77,75
   75 IF(I-36)76,77,77
   76 WESS=WESS+(W(1,L)*W(1,L)+W(2,L)*W(2,L))/(5.0      )
      HAYS=HAYS+(H(1,L)*H(1,L)+H(2,L)*H(2,L))/(5.0      )
   77 HA(I,IR)=HA(I,IR)+H(1,L)*H(1,L)+H(2,L)*H(2,L)
      A=W(1,L)*CROTFR(I)-W(2,L)*SROTFR(I)
      B=W(1,L)*SROTFR(I)+W(2,L)*CROTFR(I)
      C(1,I,IR)=C(1,I,IR)+A*H(1,L)+B*H(2,L)
   72 C(2,I,IR)=C(2,I,IR)+B*H(1,L)-A*H(2,L)
   78 CONTINUE
      ICOUNT=ICOUNT+1
      IF(ICOUNT-15)142,200,200
  200 ICOUNT=0
      GO TO (908,909),SSWTCHF(5)
  908 M=4 $ GO TO 910
  909 M=3
  910 CONTINUE
      AA=BB=0.0
      AWESS=AWESS+WESS
      AWESN=AWESN+WESN
      AHAYS=AHAYS+HAYS
      AHAYN=AHAYN+HAYN
      WESN=WESS=HAYS=HAYN=0.0
      DO 201 I=31,35
      AA=AA+C(1,I,M)
  201 BB=BB+C(2,I,M)
      PHASE=(180.0/PI)*(ATAN(BB/AA)+(0.5-SIGN(0.5,AA))*SIGN(PI,BB))
      PRINT 202,PHASE
  202 FORMAT(20X,9H PHASE = ,F7.2)
      PRINT 203,AHAYN,AWESN,AHAYS,AWESS,C(1,33,M),C(2,33,M)
     1,HA(33,3),HA(33,2)
  203 FORMAT(10X,8F15.2)
      AL=SQRT(AA*AA+BB*BB)
      DO 220 IR=1,31
      DO 220 I=1,64
      AC=C(1,I,IR)*AA/AL+C(2,I,IR)*BB/AL
      AD=C(2,I,IR)*AA/AL-C(1,I,IR)*BB/AL
      C(1,I,IR)=AC
  220 C(2,I,IR)=AD
      DO 221 I=29,37
      AA=C(1,I,M)
      BB=C(2,I,M)
      PHASE=(180.0/PI)*(ATAN(BB/AA)+(0.5-SIGN(0.5,AA))*SIGN(PI,BB))
      CC=SQRT(C(1,I,M)*C(1,I,M)+C(2,I,M)*C(2,I,M))/SQRT(ABS((AHAYS-AHAYN
     1)*(AWESS-AWESN)))
      CC=CC*(INR+1)
      PRINT 230,PHASE,CC
```

Fig. A-4. Continued.

```
230 FORMAT(10X,2HPH,F30.2,4HCORR,F30.2)
221 CONTINUE
    CALL YYDISK(0,2,INR*15872+3968,WA,3968)
    CALL YYWAIT(0)
    CALL YYDISK(0,2,INR*15872+7936,C,7936)
    CALL YYWAIT(0)
    INR=INR+1
    DO 222 IR=1,31
    DO 222 I=1,64
222 WA(I,IR)=WA(I,IR)=C(1,I,IR)=C(2,I,IR)=0.0
    GO TO 140
 50 IAB=INR-1
    DO 380 IR=1,31
    DO 380 I=1,64
380 WA(I,IR)=WA(I,IR)=C(1,I,IR)=C(2,I,IR)=0.0
    DO 400 INR=0,IAB
    CALL YYDISK(0,1,INR*15872+3968,SCRATA,3968)
    CALL YYWAIT(0)
    DO 391 IR=1,31
    DO 391 I=1,64
391 WA(I,IR)=WA(I,IR)+SCRATA(I,IR)
    CALL YYDISK(0,1,INR*15872+7936,SCRATB,7936)
    CALL YYWAIT(0)
    DO 392 IR=1,31
    DO 392 I=1,64
    DO 392 J=1,2
392 C(J,I,IR)=C(J,I,IR)+SCRATB(J,I,IR)
400 CONTINUE
    DO 601 K=1,3
    M=(K-1)*10+1
    N=M+10
    PRINT 602, M,N
602 FORMAT(1X,21HPOWER AND CORRELATION,2I30)
    PRINT 603
603 FORMAT(1X,5HPOWER)
    DO 700 I=1,64
700 PRINT 600,(  WA(I,IR),IR=M,N)
    PRINT 604
604 FORMAT(1X,4HREAL)
    DO 701 I=1,64
701 PRINT 600,(  C(1,I,IR),IR=M,N)
    PRINT 605
605 FORMAT(1X,4HIMAG)
    DO 702 I=1,64
702 PRINT 600,(  C(2,I,IR),IR=M,N)
601 CONTINUE
600 FORMAT(1X,   11F12.0)
    GO TO(900,901) SSWTCHF(1)
901 CALL SEFF(20)
    BACKSPACE 20
900 CONTINUE
    WRITE (20) NDAYN,CRA,CDEC,ANG,TIME,BLA,BLL,DOPA,FL,ROT,THETA
    WRITE (20) WA,C,AHAYS,AHAYN,AWESS,AWESN
    END FILE 20
    BACKSPACE 20
    PAUSE
    GO TO 3
    END
```

Fig. A-4. Continued.

```
      PROGRAM HFPLOT2
      CHARACTER MAP,MA
      COMMON              ICR(4,64,28),P(64,31) ,CR(2,64,31),  INFO(200)
      DIMENSION MAP(121,121),MA(101,101),                PP( 64,31)
      EQUIVALENCE (MA,CR),(P,MAP),(ICR,     PP)
      DIMENSION IAA(1)$IAD=77777B+1655B-LOC(IAA(1))$IAA(IAD)=146000108
      PI=3.1415926536
      DO 10 I=1,64
      DO 10 IR=1,28
      DO 10 K=1,4
      ICR(K,I,IR)=0
   10 CONTINUE
   11 NDAYA=ACRA=ACDEC=ADOPA=AFL=ATHETA=0.0
      AAHAYN=0.0
      REWIND 30
      G=0.0
   20 READ(30) NDAYN,CRA,CDEC,ANG,TIME,BLA,BLL,DOPA,FL,RGT,THETA
      GO TO (61,21),EOFCKF(30)
   21 READ (30) P,CR,AHAYS,AHAYN,AWESS,AWESN
      ENCODE(800,60,INFO) NDAYN,TIME,FL,THETA
   60 FORMAT(4HDAY , I7,1X,5HTIME ,F5.2,1X,2HFL,F5.2,1X,6HTHETA ,F7.2)
      CALL LIMITS(0.0,100.0,0.0,120.0)
      CALL POINTS(33.0,AHAYS/(10.0**8.0),1RH,1)
      CALL POINTS(33.0,AWESS/(10.0**8.0),1RW,1)
      CALL POINTS(1.0,AHAYN/(10.0**8.0),1RH,1)
      CALL POINTS(1.0,AWESN/(10.0**8.0),1RW,1)
      DO 500 I=1,64
      A=I
      PHASE=(60.0/PI)*(ATAN(CR(2,I,4)/CR(1,I,4))+(0.5-SIGN(0.5,CR(1,I,4)
     1))*SIGN(PI,CR(2,I,4)))+60.0
      CORR=CR(1,I,4)*CR(1,I,4)+CR(2,I,4)*CR(2,I,4)
      CALL POINTS(A,PHASE,1R*,1)
      CALL POINTS(A,SQRT(CORR)/(10.0**8.0),1RC,1)
  500 CALL POINTS(A,P(I,4)/(10.0**8.),1RP,1)
      CALL LABELS(4HFREQ,1,3HPOW,1)
      CALL GRIDS(0.0,10.0,0.0,20.0)
      CALL GRAPHS(INFO,15,200,1)
      PAUSE
      GO TO (20,504) SSWTCHF(2)
  504 GO TO(41,503),SSWTCHF(6)
   41 DO 42 I=1,64
      DO 42 IR=1,31
   42 PP(I,IR)=PP(I,IR)+P(I,IR)-AHAYN
      AAHAYN=AAHAYN+AHAYN
      GO TO 43
  503 DO 40 IR=4,31
      DO 40 I=1,64
      IK=IR-3
      Y=(I-33)*1.008/FL
      R1=SQRT(1.0-((84.94-IR)/81.0)**2)
      R2=SQRT(1.0-((83.94-IR)/81.0)**2)
      IF(R2*R2-Y*Y) 40,40,30
```

Fig. A-5. Coded-pulse averaging program.

```
 30 Z2=SQRT(R2*R2-Y*Y)
    IF(R1*R1-Y*Y) 31,31,32
 31 Z1=0.0
    GO TO 33
 32 Z1=SQRT(R1*R1-Y*Y)
 33 Z=(2.0*Z1+Z2)/3.0
    R=R1
    SCA=(0.11**3)/((R+.11*SQRT(1.0-R*R))**3)
    PHI=-THETA*Z*PI/180.0
    ICR(1,I,IK)=ICR(1,I,IK)+CR(1,I,IR)*1000.0*COS(PHI)/(SCA*SQRT
   1(ABS((AHAYS-AHAYN)*(AWESS-AWESN))))
    ICR(2,I,IK)=ICR(2,I,IK)+CR(2,I,IR)*1000.0*SIN(PHI)/(SCA*SQRT
   1(ABS((AHAYS-AHAYN)*(AWESS-AWESN))))
    ICR(3,I,IK)=ICR(3,I,IK)+COS(PHI)*COS(PHI)*1000.0
    ICR(4,I,IK)=ICR(4,I,IK)+SIN(PHI)*SIN(PHI)*1000.0
 40 CONTINUE
 43 C=C+1.0
    NDAYA=NDAYA+NDAYN
    ACRA=ACRA+CRA
    ACDEC=ACDEC+CDEC
    ADOPA=ADOPA+DOPA
    AFL=AFL+FL
    ATHETA=ATHETA+THETA
 61 PAUSE
    GO TO (900,20) SSWTCHF(3)
900 GO TO (901,62),SSWTCHF(6)
901 DO 902 L=1,101
    DO 902 N=1,101
902 MA(L,N)=0
    DO 903 I=1,64
    DO 903 IR=1,31
903 PP(I,IR)=PP(I,IR)/(C*1000.0)
    AAHAYN=AAHAYN/(C*1000.0)
    DO 904 I=1,64
904 PRINT 910,(PP(I,IR),IR=1,16)
    PRINT 911, AAHAYN
911 FORMAT (10X,F20.6)
    DO 905 I=1,64
905 PRINT 910,(PP(I,IR),IR=16,31)
910 FORMAT(1X,16F8.)
    FL=AFL/C
    DO 970 L=1,101
    DO 970 N=1,101
    I=(L-51)*FL/60.0+33.5
    R=SQRT(((L-51)*(L-51)+(N-51)*(N-51))/3600.0)
    IF(1.0-R) 970,970,974
974 IR=(1.0-SQRT(1.0-R*R))*81.0+3.94
    IF(ABS(I-33.0)-ABS(64.0-R*1.008/FL)) 973,973,970
973 IF(I-64) 966,966,970
966 IF(I-1) 970,967,967
967 IF(IR-31) 968,968,970
968 IF(IR-4) 970,969,969
```

Fig. A-5. Continued.

```
969 SCA=(0.11**3)/((R+.11*SQRT(1.0-R*R))**3)
    MA(L,N)=PP(I,IR)/(SCA*PP(33,4))
970 CONTINUE
    GO TO 971
 62 DO 63 L=1,101
    DO 63 N=1,101
 63 MA(L,N)=0
    DO 603 K=1,4
    PRINT 601,K
601 FORMAT(10X,I20)
    DO 602 I=1,64
    PRINT 600,(ICR(K,I,IR),IR=1,14)
600 FORMAT(1X,14I8)
602 CONTINUE
    DO 603 I=1,64
    PRINT 600,(ICR(K,I,IR),IR=15,28)

603 CONTINUE


    SNR=AWAYS*2.0/AWAYN
    DO 64 I=1,64
    DO 64 IR=1,28
    A1=ICR(1,I,IR)
    A2=ICR(2,I,IR)
    A3=ICR(3,I,IR)
    A4=ICR(4,I,IR)
    ICR (1,I,IR)=(A1*A4+A2*A3)*1000.0/(SNR*A3*A4)
 64 ICR (2,I,IR)=(A1*A4-A2*A3)*1000.0/(SNR*A3*A4)
    DO 665 K=1,2
    PRINT 601, K
    DO 65 I=1,64
    PRINT 600,(ICR (K,I,IR),IR=1,14)
 65 CONTINUE
    DO 665 I=1,64
    PRINT 600,(ICR (K,I,IR),IR=15,28)
665 CONTINUE
    FL=AFL/C
    DO 70 L=1,101
    DO 70 N=1,101
    I=(L-51)*FL/60.0+33.5
    R=SQRT(((L-51)*(L-51)+(N-51)*(N-51))/3600.0)
    IF(1.0-R)70,70,74
 74 IR=(1.0-SQRT(1.0-R*R))*81.0+0.94
    IF(ABS(I-33.0)-ABS(64.0-R*1.008/FL)) 73,73,70
 73 IF(I-64) 66,66,70
 66 IF(I-1) 70,67,67
 67 IF(IR-28) 68,68,70
 68 IF(IR-1) 70,69,69
 69 IF(N-51) 71,71,72
 72 MA(L,N)=ICR (1,I,IR) /1000
    GO TO 70
```

Fig. A-5. Continued.

```
 71 MA(L,N)=ICR (2,I,IR)/1000
 70 CONTINUE
971 NDAY=NDAYA/C
    DEC=ACDEC*180.0/(PI*C)
    ANG=ACRA*180.0/(PI*C)
    THETA=ATHETA/C
    FL=AFL/C
    DOPA=ADOPA*180.0/(PI*C)
    ENCODE(800,141,INFO)NDAY,THETA,FL,C,SNR
141 FORMAT(4HDAY ,I7,5X,5HTHETA,5X,F7.2,5X,2HFL,F7.2,5X,1HC,5X,F7.2,5X
   1,3HSNR,5X,F7.2)
    CALL LIMITS(1.0,101.0,51.0,111.0)
    DO 140 N=51,101
    DO 140 L=1,101
    A1=N
    A2=L
    MQ=MA(L,N)
140 CALL POINTS(A2,A1,MQ,1)
    CALL GRAPHS (INFO,15,200,1)
    CALL LIMITS (1.0,101.0,-9.0,51.0)
    DO 150 N=1,51
    DO 150 L=1,101
    A1=N
    A2=L
    MQ=MA(L,N)
150 CALL POINTS(A2,A1,MQ,1)
    CALL GRAPHS (0,0,0,1)
155 DO 156 K=1,121
    DO 156 M=1,121
156 MAP(K,M)=0
    ANG=ANG-179.7
    CDEC=COS(DEC*PI/180.0)
    SDEC=SIN(DEC*PI/180.0)
    CANG=COS(ANG*PI/180.0)
    SANG=SIN(ANG*PI/180.0)
    CTH=COS(23.3*PI/180.0)
    STH=SIN(23.3*PI/180.0)
    ALATR=(180.0/PI)*ASINF(-CTH*SDEC-STH*SANG*CDEC)
    ALONR=(180.0/PI)*ATAN((SANG*CDEC*CTH-SDEC*STH)/CANG*CDEC)
    ALONR=ALONR+16.0+(NDAY-241)*360.0/245.0
    PLA=ATAN(CANG*STH/(CTH*CDEC-STH*SDEC*SANG))
    APA=PLA*180.0/PI
    CDOP=COS(DOPA*PI/180.0)
    SDOP=SIN(DOPA*PI/180.0)
    NRUN=NDAY*10000+TIME*100
    PRINT 160,NRUN,NDAY,DEC,ANG,THETA,FL,DOPA,ALATR,ALONR,APA
160 FORMAT(2I10,8F10.2)
    PE=PI/180.0*(16.0+(NDAY-241)*360.0/245.0)
    DO 180 L=1,101
    DO 180 N=1,101
    Y=(L-51)*CDOP/60.0-(N-51)*SDOP/60.0
    Z=(L-51)*SDOP/60.0+(N-51)*CDOP/60.0
    IF(1-Y*Y-Z*Z)180,161,161
```

Fig. A-5. Continued.

```
161 X=SQRT(1-Y*Y-Z*Z)
    XA=X*CANG*CDEC-Y*SANG*Z*SDEC*CANG
    YA=X*(CTH*SANG*CDEC-STH*SDEC)+Y*CANG*CTH+Z*(CTH*SDEC*SANG+STH*CDEC
   1 )
    ZA=X*(-CTH*SDEC-STH*SANG*CDEC)-Y*CANG*STH+Z*(CTH*CDEC-STH*SDEC*SAN
   1G)
    XB=XA*COS(PE)+YA*SIN(PE)
    YB=XA*SIN(PE)+YA*COS(PE)
    K=YB*60.0+61.5
    M=ZA*60.0 +61.5
    IF(XB) 170,175,175
170 MAP(K,M)=1R$
    GO TO 180
175 MAP(K,M)=MAP(K,M)+ MA(L,N)
180 CONTINUE
    DO 190 J=1,19
    AA=(J-10)*PI/18.0
    DO 190 I=1,361
    BB=(I-181)*PI/360.0
    K=COS(AA)*SIN(BB)*60.0+61.5
    M=SIN(AA)*60.0+61.5
    IF(MAP(K,M)) 190,181,190
181 MAP(K,M)=1R*
190 CONTINUE
    DO 200 J=1,19
    AA=(J-10)*PI/18.0
    DO 200 I=1,361
    BB=(I-181)*PI/360.0
    K=COS(BB)*SIN(AA)*60.0+61.5
    M=SIN(BB)*60.0 +61.5
    IF(MAP(K,M)) 200,191,200
191 MAP(K,M)=1R*
200 CONTINUE
    CALL LIMITS(1.0  ,61.0,61.0,121.0)
    DO 210 K=1,61
    DO 210 M=61,121
    MAPK=MAP(K,M)


    AK=K
    AM=M
    IF(MAPK)209,210,209
209 CALL POINTS(AK,AM,MAPK,1)
210 CONTINUE
    CALL GRAPHS (0,0,0,1)
    CALL LIMITS(61.0,121.0,61.0,121.0)
    DO 220 K=61,121
    DO 220 M=61,121
    AK=K
    AM=M
    MAPK=MAP(K,M)
    IF(MAPK)219,220,219
```

Fig. A-5. Continued.

```
219 CALL POINTS(AK,AM,MAPK,1)
220 CONTINUE
    CALL GRAPHS (0,0,0,1)
    CALL LIMITS (1.0  ,61.0,1.0,61.0)
    DO 230 K=1,61
    DO 230 M=1 61
    AK=K
    AM=M
    MAPK=MAP(K,M)
    IF(MAPK)229,230,229
229 CALL POINTS(AK,AM,MAPK,1)
230 CONTINUE
    CALL GRAPHS (0,0,0,1)
    CALL LIMITS(61.0,121.0,1.0,61.0)
    DO 240 K=61,121
    DO 240 M=1,61
    AK=K
    AM=M
    MAPK=MAP(K,M)
    IF(MAPK)239,240,239
239 CALL POINTS(AK,AM,MAPK,1)
240 CONTINUE
    CALL GRAPHS (0,0,0,1)
    PAUSE
    GO TO(242,241) SSWTCHF(1)
241 CALL SEFF(20)
    BACKSPACE 20
    CALL SEFF (10)
    BACKSPACE 10
242 CONTINUE
    DOPAA=DOPA-APA
    GO TO(800,801),SSWTCHF(6)
801 WRITE(20) NDAY,THETA,FL,DOPAA,ALATR,ALONR,DOPA,APA,C,DEC,ANG
    GO TO 802
800 WRITE(20) PP,AAPAYN
    DO 806 I=1,64
    DO 806 IR=1,28
    DO 806 K=1,4
806 ICR(K,I,IR)=0
    GO TO 803
802 WRITE(20)(((ICR(I,J,K),I=1,2),J=1,64),K=1,28)
    WRITE (10) MAP,NDAY
    DO 807 I=1,64
    DO 807 IR=1,31
807 PP(I,IR)=0.0
803 END FILE 20
    BACKSPACE 20
    END FILE 10
    BACKSPACE 10
    GO TO (11 ,250) SSWTCHF(4)
250 END
```

Fig. A-5. Continued.

```
      PROGRAM VENPLOT
C LU 24 IS THE INPUT TAPE.  LU 27 IS THE OUTPUT TAPE.
C SSW4 DOWN TO OMIT PHOTOS.
C SSW5 DOWN TO CANCEL A SPOTTING COMMAND.
C ARRAYS IN COMMON
      COMMON IDISPLAY(100),PWRARAY(64,31),IWTFCN(2,64,28),INP(101,101)
      COMMON SCATLAW(31)
C VARIABLES IN COMMON
      COMMON EL PRIME,BPRIME,FCL,DOPA,NOISEBX,A,RBSHIFT,ISUB,ISCALE,INP
     1 MIN,INPMAX,IPOINT,ISTEER,RADIAN,IDAYNUM,DAYRUNS,IFLAG,PI,SMDYRN,
     2 INPMAX1,INPMIN1,XMAC,AAHAYN,DEC,ANG,DOPPLER A,PLANETA,FBSHIFT
      DIMENSION INP1(101,101)
      EQUIVALENCE (INP1,PWRARAY),(DOPA,GAMMA)
      REWIND 27
      IFLAG=37654321B
      PI=3.141592654    $  RADIAN = PI/180.0  $ C=2.997929E+08
      XMAC=3777777B     $  DT=5.0E-04  $  INPMIN=377777778 $ INPMAX=-1
1     WRITE(59,99)
   99 FORMAT(17H LOAD DATA CARDS. /10H PRESS GO.  )
      GO TO(51,213),SSWTCHF(4)
 213  PAUSE 4444
 51   ISTEER=2    $  GO TO 52
 52   CONTINUE
      DO 53 KRANGE=1,31
      DO 53 NFREQ=1,64
 53   PWRARAY(NFREQ,KRANGE)=0.0
      READ(60,98)ISUB,ISCALE,IPOINT,NOISEBX,RBSHIFT,FCLX,A,ID,FBSHIFT
 98   FORMAT(4I5,3F10.0,I5,F10.0)
      IF(ISUB)215,214,215
 214  ISUB=3
 215   IF(ISCALE)217,216,217
 216  ISCALE=100
 217   IF(IPOINT)219,218,219
 218  IPOINT=2
 219  IF(NOISEBX)221,220,221
 220  NOISEBX=2
      RBSHIFT=0.975
 221  IF(A)223,222,223
 222  A=6.055
 223  A=A*1.0E+06
      WRITE(61,90)ISUB,ISCALE,IPOINT,NOISEBX,RBSHIFT,FCLX,A,ID,FBSHIFT
 90   FORMAT(4I5,3F10.4,I5,F10.4)
 19   READ(24)IDAYNUM,THETA,FCL,DOPA,B PRIME,EL PRIME,DOPPLER A,
     1 PLANET A,DAYRUNS,        DEC,ANG
      GO TO(198,199)EOFCKF(24)
 199  READ(24) ((( IWTFCN(I,J,K),I=1,2),J=1,64),K=1,28)
      READ(24)PWRARAY,AAHAYN
      IF(SSWTCHF(5) .LT. 2)21,22
 22   IF(ID .EQ. 0 .OR. ID .EQ. IDAYNUM)20,19
```

Fig. A-6. Coded-pulse display and coordinate transformation program.

```
20     IF(FCLX)225,224,225
 225   FCL=FCLX
 224   WRITE(61,97)IDAYNUM,THETA,FCL,DOPA,EL PRIME,B PRIME,DAY RUNS,
      1  AAHAYN,DOPPLERA,PLANET A,DEC,ANG
 97    FORMAT(12HODAY NO. IS  I6, 2X 18H FRINGE RADIUS IS E11.3,2X
      1 35H CENTER-TO-LIMB DOPPLER IN HERZ IS F9.4/ 18H DOPPLER ANGLE IS F9.4,
      2 F9.4, 2X 29H SUB RADAR LONG. AND LAT. IS F8.4, 2X 4H AND 2X
      3F8.4/16H NO. OF RUNS IS F6.0/22H DAYS AVERAGE NOISE IS  E11.3/
      451H ANGLE BETWEEN DOPPLER AXIS AND CELESTIAL NORTH IS F9.4/
      554H ANGLE BETWEEN HESPERIAN NORTH AND CELESTIAL NORTH IS F9.4/
      6 41H MEAN DECLINATION AND RIGHT ASCENSION IS F9.4,2X 4H AND F9.4)
       KDEX=NOISEBX+1
       DO 200 KRANGE=KDEX,31
       DO 200 NFREQ=1,64
       PWRARAY(NFREQ,KRANGE)=AMAX1(0.0,PWRARAY(NFREQ,KRANGE))
 200   CONTINUE
C APPLY SCATTERING LAW, ETC, , AND XFORMATION TO GRID OF MAPPING PLANE.
       CALL MAPXFORM
       GO TO(23,24),SSWTCHF(4)
C MAKE TEST PHOTOGRAPHS.
 24    CALL TESTFOTO(1)
 23    CONTINUE
C AT A LATER DATE ENTER EDITING ROUTINES.
       GO TO(208,212),SSWTCHF(4)
 212   WRITE(59,101)
 101   FORMAT(35H TYPE 1, IF DATA IS UNSATISFACTORY.)
       READ(58,102)QUESTION
 102   FORMAT(F10.0)
       IF(QUESTION)208,208,209
 209   DO 109 KK=1,3
       BACKSPACE 27
 109   BACKSPACE 24
       GO TO 1
 208   GO TO(210,211)ISTEER
 210   CALL TAPEADD
       GO TO 1
 211   CALL TAPEPACK
       GO TO 1
 198   WRITE(59,103)
       WRITE(61,103)
 103   FORMAT(18H EOF ON DATA TAPE./
      1 48H LOAD NEW DATA TAPE OR ABORT RUN AND SAVE LU 27.     )
 21    REWIND 24    $ GO TO 1
       END
```

Fig. A-6. Continued.

```
      SUBROUTINE TESTFOTO(K)
C MAKES PHOTOGRAPHS AND PROVIDES SAMPLE PRINTOUTS TO TEST  GOODNESS OF RUN
C IN A ROUGH FASHION
C ARRAYS IN COMMON
      COMMON IDISPLAY(100),PWRARAY(64,31),INTFCN(2,64,28),INP(101,101)
      COMMON SCATLAW(31)
C VARIABLES IN COMMON
      COMMON EL PRIME,BPRIME,FCL,DOPA,NOISEBX,A,RBSHIFT,ISUB,ISCALE,INP
     1 MIN,INPMAX,IPOINT,ISTEER,RADIAN,IDAYNUM,DAYRUNS,IFLAG,PI,SMDYRN,
     2 INPMAX1,INPMIN1,XMAC,AAHAYN,DEC,ANG,DOPPLER A,PLANETA,FBSHIFT
      DIMENSION INP1(101,101)
      EQUIVALENCE (INP1,PWRARAY),(DOPA,GAMMA)
      BP=BPRIME/RADIAN $ ELP=EL PRIME/RADIAN
      GO TO(401,402),K
 401  WRITE(61,100)IDAYNUM,FCL,ELP,BP,DAYRUNS,AAHAYN,DEC,ANG,DOPPLERA
     1 ,PLANETA
 100  FORMAT(13H1DAY NUMBER= I6,2X 24H CENTER-TO-LIMB DOPPLER= F8.3,
     12X 18H SUBRADAR LONG IS F8.3, 2X 12H AND LAT IS F8.3/
     2 27H NO. OF RUNS IN THE DAY IS F6.0, 2X
     3 46H THE AVERAGE NOISE (FIRST TWO RANGE BOXES) IS E10.2/
     4 22H THE MEAN DEC AND RA = F9.4, 1H, 2X F9.4, 1H./
     5 55H DOPPLER AND HESPERIAN NORTH W.R.T. CELESTIAL NORTH IS F9.4,
     6 2X 4H AND F9.4, 2X 1H.)
C     DO 54 MM=1,101
C     M=102-MM
C     WRITE(61,101)(INP(M,L),L=46,55)
C101  FORMAT(2X 10I10)
C54   CONTINUE
C     IMP=37777776B
      IMP=2750000
      GO TO 403
 402  WRITE(61,102)SMDYRN,IDAYNUM
 102  FORMAT(19H1TOTAL NO. OF RUNS=F10.0, 2X
     1 33H THE LAST INCLUDED DAY NUMBER IS  I6)
C     DO 454 MM=1,101
C     M=102-MM
C     WRITE(61,101) (INP1(M,L),L=46,55)
C454  CONTINUE
      IMP=INPMAX/2
 403  WRITE(59,103)
 103  FORMAT(24H READY POLAROID. HIT GO.)
      PAUSE 1717
 73   CALL RESETD(-6,-10)
        UL=VB=0  UR=VT=100.0
      CALL SCALE(UL,UR,VB,VT,0,23,0,23)
      DO 26KK=1,18
 26   CALL GRID(0,-60.0,40.0,-40.0,60.0,10.0,10.0,2,2,-2,-2,5,5,1)
 413  GO TO(407,408),K
 407  CALL INTRPLOT(INP,101,101,0,2,0,2,5,5,0,45,INPMIN,IMP)
      GO TO 409
 408  CALL INTRPLOT(INP1,101,101,0,2,0,2,5,5,0,45,0,IMP)
 409  CALL ADVFILM(0,1)
      WRITE(59,105)IMP
 105  FORMAT(21H THE PRESENT PMAX IS I8/
     1 33H TYPE IN A NEW PMAX IN FORMAT I7.  )
      READ(58,106)IMP
 106  FORMAT(I7)
      IF(IMP)71,71,73
 71   RETURN
      END
```

Fig. A-6. Continued.

```
      SUBROUTINE TAPEADD
C ARRAYS IN COMMON
      COMMON IDISPLAY(100),PWRARAY(64,31),IWTFCN(2,64,28),INP(101,101)
      COMMON SCATLAW(31)
C VARIABLES IN COMMON
      COMMON EL PRIME,BPRIME,FCL,DOPA,NOISEBX,A,RBSHIFT,ISUB,ISCALE,INP
     1 MIN,INPMAX,IPOINT,ISTEER,RADIAN,IDAYNUM,DAYRUNS,IFLAG,PI,SMDYRN,
     2 INPMAX1,INPMIN1,XMAC,AAHAYN,DEC,ANG,DOPPLER A,PLANETA,FBSHIFT
      DIMENSION INP1(101,101)
      EQUIVALENCE (INP1,PWRARAY),(DOPA,GAMMA)
      GO TO 15
      ENTRY TAPEPACK
 15   CONTINUE
      DOPA=DOPA/RADIAN $ EL PRIME=EL PRIME/RADIAN $BPRIME=BPRIME/RADIAN
      WRITE(27)IDAYNUM,DOPA,EL PRIME,B PRIME,FCL,NOISEB X,RBSHIFT,INPMIN,
     1 ,INPMAX,DAYRUNS
      WRITE(27)INP
      WRITE(27)IFLAG
      ISTEER=2
      RETURN
      END


      SUBROUTINE TEST DATA(KRANGE,NFREQ,X1,X1SQ,X2,X2SQ,X1PRSQ,X2PRSQ,
     1 X1PR,AREA1,AREA2,XMULT)
      COMMON IDISPLAY(100),PWRARAY(64,31),IWTFCN(2,64,28),INP(101,101)
      COMMON SCATLAW(31)
C VARIABLES IN COMMON
      COMMON EL PRIME,BPRIME,FCL,DOPA,NOISEBX,A,RBSHIFT,ISUB,ISCALE,INP
     1 MIN,INPMAX,IPOINT,ISTEER,RADIAN,IDAYNUM,DAYRUNS,IFLAG,PI,SMDYRN,
     2 INPMAX1,INPMIN1,XMAC,AAHAYN,DEC,ANG,DOPPLER A,PLANETA,FBSHIFT
      DIMENSION INP1(101,101)
      EQUIVALENCE (INP1,PWRARAY),(DOPA,GAMMA)
      WRITE(61,100)KRANGE,NFREQ,X1,X1SQ,X2,X2SQ,X1PRSQ,X2PRSQ,X1PR,
     1 AREA1,AREA2,XMULT
100   FORMAT(8H0KRANGE=  I3, 3X 7H NFREQ=  I3//
     1 4H X1=E11.4, 3X 6H X1SQ= E11.4, 3X 4H X2= E11.4, 3X/6H X2SQ= E11.4, 3X
     2 4, 3X 8H X1PRSQ= E11.4, 3X 8H X2PRSQ= E11.4,3X/6H X1PR= E11.4, 3X 7H AREA
     3 7H AREA1= E11.4, 7H AREA2= E11.4, 3X 7H XMULT= E11.4//)
      RETURN
      END
```

Fig. A-6. Continued.

```
      FUNCTION AREAFCN(X1,X2,Z1,Z2)
      COMMON IDISPLAY(100),PWRARAY(64,31),IWTFCN(2,64,28),INP(101,101)
      COMMON SCATLAW(31)
C VARIABLES IN COMMON
      COMMON EL PRIME,BPRIME,FCL,DOPA,NOISEBX,A,RBSHIFT,ISUB,ISCALE,INP
     1 MIN,INPMAX,IPOINT,ISTEER,RADIAN,IDAYNUM,DAYRUNS,IFLAG,PI,SMDYRN,
     2 INPMAX1,INPMIN1,XMAC,AAHAYN,DEC,ANG,DOPPLER A,PLANETA,FBSHIFT
      DIMENSION INP1(101,101)
      EQUIVALENCE (INP1,PWRARAY),(DOPA,GAMMA)
      ISTEE =1
      IF(Z1-1.0)1,2,1
2     ISTEE =2
      XI1=0.0
1     D1=1.0/SQRT(1.0-X1*X1)
      D2=1.0/SQRT(1.0-X2*X2)  $ B2=1.0/SQRT(1.0-Z2*Z2)
      GO TO(3,4),ISTEE
3     B1=1.0/SQRT(1.0-Z1*Z1)
4     XI22=X2*ACOSF(Z2*D2)-Z2*ASINF(X2*B2)+ASINF(X2*Z2*B2*D2)
      XI12=X1*ACOSF(Z2*D1)-Z2*ASINF(X1*B2)+ASINF(X1*Z2*D1*B2)
      XI2=XI22-XI12
      GO TO(5,6),ISTEE
5     XI21=X2*ACOSF(Z1*D2)-Z1*ASINF(X2*B1)+ASINF(X2*Z1*D2*B1)
      XI11=X1*ACOSF(Z1*D1)-Z1*ASINF(X1*B1)+ASINF(X1*Z1*B1*D1)
      XI1=XI21-XI11
6     AREAFCN=XI2-XI1
      RETURN
      END
```

Fig. A-6. Continued.

```
      SUBROUTINE MAPXFORM
C ARRAYS IN COMMON
      COMMON IDISPLAY(100),PWRARAY(64,31),IWTFCN(2,64,28),INP(101,101)
      COMMON SCATLAW(31)
C VARIABLES IN COMMON
      COMMON EL PRIME,BPRIME,FCL,DOPA,NOISEBX,A,RBSHIFT,ISUB,ISCALE,INP
     1 MIN,INPMAX,IPOINT,ISTEER,RADIAN,IDAYNUM,DAYRUNS,IFLAG,PI,SMDYRN,
     2 INPMAX1,INPMIN1,XMAC,AAHAYN,DEC,ANG,DOPPLER A,PLANETA,FBSHIFT
      DIMENSION INP1(101,101)
      EQUIVALENCE (INP1,PWRARAY),(DOPA,GAMMA),(RB,SININC)
      REAL KU,KL,KUPLUSKL
      REAL  NOISEBX1,NOISEBX2
      C=2.997929E+08    $ DT=5.0E-04
      TWO A OV C T =(2.0*A)/(DT*C)
      DEL XD =1.0/(0.992*FCL)
      GAMMA=GAMMA*RADIAN
      EL PRIME=EL PRIME*RADIAN
      B PRIME= B PRIME * RADIAN
      COSBPRM=COS(B PRIME)
      SINBPRM=SIN(B PRIME)
      COSGAM=COS(GAMMA)
      SINGAM=SIN(GAMMA)
      COSLPRM=COS(EL PRIME)
      SINLPRM=SIN(EL PRIME)
      DO 91 J=1,101
      DO 91 K=1,101
91    INP(K,J)=0
      KWTMIN=37777777B  $ KWTMAX=-KWTMIN
      DO 270 K=1,28
      DO 270 J=1,64
      DO 270 I=1,2
      IWTFCN(I,J,K)=MAX0(1,IWTFCN(I,J,K))
 270  CONTINUE
CONSTANTS
      CONSTANT=NOISEBX+RBSHIFT+0.5
      XNOISEBX=NOISEBX+1.5 +RBSHIFT
      KDEX=NOISEBX+1
      NOISEBX1=CONSTANT+0.5
      NOISEBX2=CONSTANT-0.5
      DXD=0.5*DEL XD
C *********************************
      DO 509 KRANGE=KDEX,31
C ****************************************
      DEPTH=(KRANGE-CONSTANT)/ TWO A OV C T
      DEPTH1=(KRANGE-NOISEBX1)/ TWO A OV C T
      DEPTH2=(KRANGE-NOISEBX2)/ TWO A OV C T
      Z1=AMIN1(1.0,(1.0-DEPTH1))
      Z2=AMAX1(0.0,(1.0-DEPTH2))
      X1PRSQ=1.0-Z1*Z1
      X2PRSQ=1.0-Z2*Z2
      COSINC=1.0-DEPTH
      SININC=SQRT(AMAX1(0.0,1.0-COSINC*COSINC))
      H=(SININC+0.135*COSINC)/0.135
      SL=H*H*H/COSINC
C     NFREQMIN=1      $      NFREQMAX=64
C     SL=SL*EXP ( 1.0/COSINC)
C     RBSQ=DEPTH*(2.0-DEPTH)
C     RB=SQRT(RBSQ)
C     RB=SININC
      TERM=64.0-(RB/DEL XD)
```

Fig. A-6. Continued.

```
      NFREQMIN=MAX0(1,IFIX(33.0-TERM))


      NFREQMAX=MIN0(64,IFIX(33.0+TERM))
C ***************************
      DO 610 NFREQ=1,64
C ******************************
      IF(PWRARAY(NFREQ,KRANGE))610,610,611
611   IF(NFREQ-NFREQMIN)612,613,613
613   IF(NFREQMAX-NFREQ)612,615,615
612   PWRARAY(NFREQ,KRANGE)=0.0
      GO TO 610
615   XD=(NFREQ-33)*DEL XD
      X1=ABS(XD-DXD)
      X2=ABS(XD+DXD)
      IF(X1-1.0)599,612,612
599   IF(X2-1.0)598,612,612
598   IF(X1-X2)614,616,614
616   XMULT=2.0
      X1=0.0
      GO TO 617
614   XMULT=1.0
      XX1=X1
      XX2=X2
      X2=AMAX1(XX1,XX2)
      X1=AMIN1(XX1,XX2)
617   X1SQ=X1*X1
      IF(X1SQ-X2PRSQ)597,612,612
597   X2SQ=X2*X2
      IF(X2PRSQ-X2SQ)619,618,618
619   X2=SQRT(X2PRSQ)
      GO TO 621
618   IF(X1PRSQ-X2SQ)621,620,620
620   AREA1=0.0
      AREA2=AREAFCN(X1,X2,Z1,Z2)
      GO TO(462,463),SSWTCHF(2)
462   CALL        TEST DATA(KRANGE,NFREQ,X1,X1SQ,X2,X2SQ,X1PRSQ,X2PRSQ,
     1 X1PR,AREA1,AREA2,XMULT)
463   CONTINUE
      GO TO 622
621   IF(X1PRSQ-X1SQ)623,623,624
623   AREA1=0.0
      AREA2=AREAFCN(X1,X2,1.0,Z2)
      GO TO(464,465),SSWTCHF(2)
464   CALL        TEST DATA(KRANGE,NFREQ,X1,X1SQ,X2,X2SQ,X1PRSQ,X2PRSQ,
     1 X1PR,AREA1,AREA2,XMULT)
465   CONTINUE
      GO TO 622
624   X1PR=SQRT(X1PRSQ)
      AREA1=AREAFCN(X1,X1PR,Z1,Z2)
      AREA2=AREAFCN(X1PR,X2,1.0,Z2)
      GO TO(466,467),SSWTCHF(2)
466   CALL        TEST DATA(KRANGE,NFREQ,X1,X1SQ,X2,X2SQ,X1PRSQ,X2PRSQ,
     1 X1PR,AREA1,AREA2,XMULT)
467   CONTINUE
622   AREA=XMULT*(AREA1+AREA2)
      PWRARAY(NFREQ,KRANGE)=PWRARAY(NFREQ,KRANGE)*(SL          /AREA)
610   CONTINUE
509   CONTINUE
      ISUB=1+((MAX0(1,ISUB))/2)*2
      LIMIT=((ISUB-1)/2)+1
      SUBSQ=ISUB*ISUB*ISCALE
```

Fig. A-6. Continued.

```
      ARG=50.0*RADIAN
      ERG=60.0*RADIAN
      XRG=40.0*RADIAN
      DELYV=DELXV=RADIAN
      DDXV=DDYV=DELYV/ISUB
  666 INPMIN=1000000  $  INPMAX=-1
      DO 53 M=1,101
      ENG=-XRG+(M-1)*DELYV
      DO 45 L=1,101
      BANG=-ERG+(L-1)*DELXV
      SUBPOWER=0.0
      SUBLEVEL=0.0
      DO 46 J=1,ISUB
      YVANG=ENG+  (J-LIMIT)*DDYV
      YV=SIN(YVANG)
      COSYVANG=COS(YVANG)
      DO 46 N=1,ISUB
      XVANG=BANG+(N-LIMIT)*DDXV
      XV=COSYVANG*SIN(XVANG)
      ZV=SQRT(1.0-XV*XV-YV*YV)
      Z1=ZV*COSLPRM+XV*SINLPRM
      X1=XV*COSLPRM-ZV*SINLPRM
      Y1=YV
      Z2=Z1*COSBPRM+Y1*SINBPRM
      Y2=Y1*COSBPRM-Z1*SINBPRM
      X2=X1
      XD=X2*COSGAM+Y2*SINGAM
      YD=Y2*COSGAM-X2*SINGAM
      ZD=Z2
      NFREQ=33. +(XD/DEL XD)+FBSHIFT
      GO TO(630,631),SSWTCHF(3)
  630  WRITE(61,632)M,L,J,N,XV,YV,ZV,XD,YD,ZD,NFREQ
  632 FORMAT(   32HOM,L,J,N,XV,YV,ZV,XD,YD,ZD,NFREQ  4I5,6E14.6/I5)
  631 CONTINUE
      IF(NFREQ)48,48,47
   47 IF(NFREQ-64) 300,300,48
  300 KRANGE=(1.0-ZD)*TWO A OV C T +XNOISEBX
      GO TO(629,628),SSWTCHF(3)
  629 WRITE(61,627)KRANGE,PWRARAY(NFREQ,KRANGE)
  627 FORMAT(8H KRANGE=  I5, 9H PWRARAY=  E14.6)
  628 CONTINUE
      IF(KRANGE-31)302,302,48
  302 KU=FLOAT(IWTFCN(1,NFREQ,KRANGE-3))
      KL=FLOAT(IWTFCN(2,NFREQ,KRANGE-3))
      KUPLUSKL=KU+KL
      IF(YD)303,304,304
  304 SUBPOWER=SUBPOWER+PWRARAY(NFREQ,KRANGE)*(KU/KUPLUSKL)
      SUBLEVEL=SUBLEVEL+PWRARAY(NFREQ,KRANGE)
      GO TO 46
  303 SUBPOWER=SUBPOWER+PWRARAY(NFREQ,KRANGE)*(KL/KUPLUSKL)
      SUBLEVEL=SUBLEVEL+PWRARAY(NFREQ,KRANGE)
   46 CONTINUE
      GO TO(305,306),ISTEER
  306 SOVERS=SUBLEVEL/SUBSQ
      GO TO 307
  305 SOVERS=SUBPOWER/SUBSQ
  307 IF(SOVERS-XMAC)49,49,680
   49 CONTINUE
      INP(M,L)=SOVERS+0.5
      INPMAX=MAX0(INPMAX,INP(M, L))
      INPMIN=MIN0(INPMIN,INP(M,L))
      GO TO 45
```

Fig. A-6. Continued.

```
48     INP(M,L)=0


45     CONTINUE
53     CONTINUE
       ZDIFF=INPMAX-INPMIN
       ARRAYMAX=JMAX=37777776B
       DO 682 L=1,101
       DO 682 M=1,101
682    INP(M,L)=((INP(M,L)-INPMIN)/ZDIFF)*ARRAYMAX
       GO TO(681,308),ISTEER
 308   DP=DOPA/RADIAN $ ELP=EL PRIME/RADIAN $ BP=B PRIME/RADIAN
       WRITE(27)IDAYNUM,DP,ELP,BP,FCL,NOISEBX,RBSHIFT,INPMIN,INPMAX,
      1 DAYRUNS
       WRITE(27)INP
       WRITE(27)IFLAG
       ISTEER=1
       GO TO(666,683),SSWTCHF(4)
 683   CALL TESTFOTO(1)
       GO TO 666
 681   RETURN
680    SUBSQ=SUBSQ*10.0
        GO TO 666
       END
```

Fig. A-6. Continued.

```
      PROGRAM HAYFORD
      DIMENSION RA(50),DECS(50),NDAY(50),DIST(50),IDATA(2050),IH(1024)
     1,IW(1024),RE(512),RI(512),HP(512),WP(512),PH(200),INFO(200)
     2,CROT(512),SROT(512),ARE(512),ARI(512),AHP(512),AWP(512)
      EQUIVALENCE (IH,IDATA(3)),(IW,IDATA(1027)),(EMIN,IDATA(4))
      PI=3.1415926536
      DO 2 I=1,50
      READ 1, HRS,AMIN,SECS,DEGS,DMINS,DSEC,DIST(I),NDAY(I)
    1 FORMAT (7F10.7,I3)
      RA(I)=HRS*PI/12.0 +AMIN*PI/720.0+SECS*PI/43200.0
    2 DECS(I)=DEGS*PI/180.0+SIGN((DMINS*PI/10800.0+DSEC*PI/648000.0
     1),DEGS)
    3 CONTINUE
      IP=0
      ICOUNT=ICHECK=0
      DO 4 I=1,512
      AHP(I)=AWP(I)=0.0
      ARE(I)=ARI(I)=0.0
    4 RE(I)=RI(I)=HP(I)=WP(I)=0.0
    5 BUFFER IN (30,1) (IDATA(1),IDATA(2050))
   10 GO TO (10,20,30,40),UNITSTF(30)
   20 LD=LENGTHF(30)
      IP=0
      IF(LD.EQ.2050) 50,60
   30 PRINT 31
   31 FORMAT(12H EOF UNIT 30)
      GO TO 60
   40 PRINT 41,IP
   41 FORMAT(1X,12HPARITY ERROR,I10)
      IP=IP+1
      IF(IP-5)42,5,5
   42 BACKSPACE 30
      GO TO 5
   50 DO 200 I=1,512
      I1=I+I-1 $ I2=I+I
      H1=IH(I1)$H2=IH(I2)$W1=IW(I1)$W2=IW(I2)
      HP(I)=HP(I)+H1*H1 +H2*H2
      WP(I)=WP(I)+W1*W1+W2*W2
      A=IW(I1)*CROT(I)-IW(I2)*SROT(I)
      B=IW(I1)*SROT(I)+IW(I2)*CROT(I)
      RE(I)=RE(I)+IH(I1)*A+IH(I2)*B
  200 RI(I)=RI(I)+IW(I1)*B-IH(I2)*A
      ICOUNT=ICOUNT+1
      IF(ICOUNT-15) 5,210,210
  210 ICOUNT=0
      AA=BB=0.0
      DO 220 I=92,110
      AA=AA+RE(I)
  220 BB=BB+RI(I)
      PHASE=(180.0/PI)*(ATAN(BB/AA)+(0.5-SIGN(0.5,AA))*SIGN(PI,BB))
      PRINT 221, PHASE
  221 FORMAT(20X,9H PHASE = ,F7.2)
      DO 222 I=1,512
      AHP(I)=AHP(I)+HP(I)
      AWP(I)=AWP(I)+WP(I)
      HP(I)=WP(I)=0.0
      AL=SQRT(AA*AA+BB*BB)
      AC=RE(I)*AA/AL+RI(I)*BB/AL
      AO=RI(I)*AA/AL-RE(I)*BB/AL
      RE(I)=RI(I)=0.0
```

Fig. A-7. CW phase calibration program.

```
      ARE(I)=ARE(I)+AC
  222 ARI(I)=ARI(I)+AD
      ICHECK=1
      GO TO 5
  100 IF(LD.EQ.23) 300,110
  110 PRINT 111
  111 FORMAT(28H NO MORE DATA LOAD NEW TAPE )
      PAUSE
      GO TO 3
  300 NDAYT=IDATA(1)*100+IDATA(2)
      TIME=IDATA(3)+FMIN/60.0
      MOIS=IDATA(1)
      IDAY=IDATA(2)
      IB=0
      DO 304 I=1,50
      IF(NDAYT-NDAY(I)) 304,305,304
  305 IB=I
  304 CONTINUE
      PRINT 306,NDAYT,NDAY(IB),RA(IB),DECS(IB)
  306 FORMAT(2I20,2F20.5)
      IC=IB+1$ID=IB-1
      CRA=RA(IB)+(RA(IC)-RA(ID))*TIME/48.0
      CDEC=DECS(IB)+(DECS(IC)-DECS(ID))*TIME/48.0
      ANG=CRA-179.7*PI/180.0
      NDAYN=(MOIS-8)*31 + IDAY  +212
      STIME=((TIME/24.0)+(NDAYN-212))*2.0*PI*1.002737909
     1 +(15.0/24.0+45.0/1440.0 +45.868/(24.0*3600.0))*2.0*PI
      BN=32450.0$BA=44.0*PI/180.0+19.0*PI/(180.0*60.0)
      BHA=31.0*PI/180.0 + 22.0*PI/(180.0*60.0)
      BLN=BN*(COS(CDEC)*SIN(BA)+COS(BA)*COS(BHA-STIME+CRA)*SIN(CDEC))
      BLW=BN*(COS(BA)*SIN(BHA-STIME+CRA))
      BLA=ATAN(BLW/BLN)
      BLL=SQRT(BLN*BLN+BLW*BLW)
      FLN=94.7*(COS(23.3*PI/180.0)*COS(CDEC)-SIN(CDEC)*SIN(23.3*PI/180.0
     1)*SIN(ANG))+1.068*(RA(IC)-RA(ID))*180.0*30.0/PI-0.72*COS(CRA-ST
     2IME)/DIST(IB)
      FLW=94.7*SIN(23.3*PI/180.0)*COS(ANG)-1.068*(DECS(IC)-DECS(ID))
     1*180.0*30.0/PI
      DOPA=ATAN(FLW/FLN)
      FL=SQRT(FLN*FLN+FLW*FLW)
      ROT=2.0*PI*SIN(DOPA-BLA)*BLL*6.055/(FL*DIST(IB)*149600.0)
      THETA=360.0*COS(DOPA-BLA)*BLL*6.055/(DIST(IB)*149600.0)
      PRINT 307,NDAYN,CRA,CDEC,ANG,STIME,BLA,BLL,DOPA,FL,ROT,THETA
  307 FORMAT(1X,I3,10F12.4)
      ENCODE(800,308,INFO) NDAYN,TIME,FL,THETA
  308 FORMAT(4HDAY , I7,1X,5HTIME ,F5.2,1X,2HFL,F5.2,1X,6HTHETA ,F7.2)
      DO 309 I=1,512
      CROT(I)=COS((I-101)*ROT)
      SROT(I)=SIN((I-101)*ROT)
  309 CONTINUE
      GO TO 3
   60 IF(ICHECK) 100,100,90
   90 ICHECK=ICOUNT=0
      HANO=WESN=0.0
      DO 91 I=257,512
      HANO=HANO+AHP(I)
   91 WESN=WESN+AWP(I)
      DO 92 I=1,256
      AHP(I)=AHP(I)*256.0/HANO - 1.0
      AWP(I)=AWP(I)*256.0/WESN - 1.0
      ARE(I)=ARE(I)*256.0/SQRT(HANO*WESN)
```

Fig. A-7. Continued.

```
      ARI(I)=ARI(I)*256.0/SQRT(HANO*WESN)
      ARI(I)=ARI(I)/SQRT(ABS(AHP(I)*AWP(I)))
      ARE(I)=ARE(I)/SQRT(ABS(AHP(I)*AWP(I)))
   92 CONTINUE
      CALL LIMITS(50.0,150.0,-180.0,180.0)
      DO 93 I=51,151
      A=I-1
      PH(I)=ATAN(ARI(I)/ARE(I))
      PH(I)=PH(I)+(0.5-SIGN(0.5,ARE(I)))*SIGN(PI,ARI(I))
      CALL POINTS (A,PH(I)*180.0/PI,1R*,1)
   93 CALL POINTS (A,180.0*SQRT(ARE(I)*ARE(I)+ARI(I)*ARI(I)),1RC,1)
      CALL LABELS(4HFREQ,1,3HPHA,1)
      CALL GRIDS(50.0,10.0,-180.0,60.0)
      CALL GRAPHS(INFO,15,200,1)
      CALL LIMITS(50.0,150.0,0.0,180.0)
      DO 94 I=51,151
      A=I-1
      CALL POINTS(A,AHP(I),1RH,1)
      Y=10.0*AWP(I)
   94 CALL POINTS(A,Y,1RW,1)
      CALL LABELS(4HFREQ,1,3HPOW,1)
      CALL GRIDS(50.0,10.0,0.0,20.0)
      CALL GRAPHS(INFO,15,200,1)
      HANO=HANO/10000.0
      WESN=WESN/10000.0
      WRITE(20,95) NDAYN,CRA,CDEC,ANG,TIME,ELA,EIL,DOPA,FL,RCT,THETA,
     1HANO,WESN
   95 FORMAT(I3,12F10.4)
      WRITE(20,96)(AHP(I),AWP(I),ARE(I),ARI(I),I=1,200)
   96 FORMAT(4E18.11)
      END FILE 20
      BACKSPACE 20
      IF(LD.EQ.23)300,98
   98 CONTINUE
      CALL UNLOAD (30)
      PAUSE
      GO TO (97,3) SSWTCHF(1)
   97 END
```

Fig. A-7. Continued.

```
      PROGRAM HFPLOT
      CHARACTER MAP
      COMMON    ANH(200),ANW(200),RR(200),RI(200),INFO(200)
     1,ACS(200)
     2,ACH(200),ACW(200),AR(200),AI(200),PHC(200)
     3,MA(101,101),MAP(121,121)
     4,P(1001)
      PI=3.1415926536
  251 CONTINUE
      ICC=0
      DO 7 L=1,101
      DO 7 N=1,101
    7 MA(L,N)=0
      DO 8 K=1,121
      DO 8 M=1,121
    8 MAP(K,M)=0
    1 C=0.0
      NDAYA=ACRA=ACDEC=ADOPA=AFL=ATHETA=0.0
      DO 9 I=1,200
      ACH(I)=0.0
      ACW(I)=0.0
      AR(I)=0.0
    9 AI(I)=0.0
   10 READ(30,20) NDAYN,CRA,CDEC,ANG,TIME,BLA,BLL,DOPA,FL,ROT,THETA
   20 FORMAT(I3,10F10.4)
      READ(30,30)(ANH(I),ANW(I),RR(I),RI(I),I=1,200)
   30 FORMAT(4E18.11)
      ENCODE(800,60,INFO) NDAYN,TIME,FL,THETA
   60 FORMAT(4HDAY , I7,1X,5HTIME ,F5.2,1X,2HFL,F5.2,1X,6HTHETA ,F7.2)
      GO TO (62,61) SSWTCHF(2)
   61 CALL LIMITS(50.0,150.0,-180.0,180.0)
      DO 70 I=1,200
      A=I-1
      PH    =ATAN(RI(I)/RR(I))
      PH    =PH    +(0.5-SIGN(0.5,RR(I)))*SIGN(PI,RI(I))
      PH    =PH    *180.0/PI
      CALL POINTS(A,ANH(I)-180.0,1RH,1)
      CALL POINTS(A,ANW(I)*10.0-180.0,1RW,1)
      CALL POINTS (A,PH     ,1R*,1)
   70 CALL POINTS (A,180.0*SQRT(RR(I)**2+RI(I)**2),1RC,1)
      CALL LABELS (4HFREQ,1,3HPHA,1)
      CALL GRIDS (50.0,10.0,-180.0,60.0)
      CALL GRAPHS  (INFO,15,200,1)
   62 CONTINUE
      PAUSE
      GO TO(10,71) SSWTCHF(5)
   71 DO 80 I=2,200
      K=I-1
      ACH(K)=ACH(K)+ANH(I)
      ACW(K)=ACW(K)+ANW(I)
      AR(K)=AR(K)+RR(I)*SQRT(ABS(ANW(I)*ANH(I)))
   80 AI(K)=AI(K)+RI(I)*SQRT(ABS(ANW(I)*ANH(I)))
      C=C+1.0
      NDAYA=NDAYA+NDAYN
      ACRA=ACRA+CRA
      ACDEC=ACDEC+CDEC
      ADOPA=ADDPA+DOPA
      AFL=AFL+FL
      ATHETA=ATHETA+THETA
      GO TO (90,10)  SSWTCHF(3)
```

Fig. A-8. CW averaging and transform program.

```
 90 CALL LIMITS (50.0,150.0,0.0,120.0)

    DO 100 I=50,150
    R=I
    CALL POINTS (R,ACH(I)/C,1RH,1)
100 CALL POINTS(R,10.0*ACW(I)/C,1RW,1)
    CALL LABELS (4HFREQ,1,3HPOW,1)
    CALL GRIDS (50.0,10.0,0.0,20.0)
    THET=ATHETA/C
    ENCODE(800,101,INFO)NDAYN,TIME,C,THET
101 FORMAT(7HAVERAGE,10X,3HDAY,I7,4X,4HTIME,F10.2,4X1HC,F7.1, X,
   15HTHETA,F7.1)
    CALL GRAPHS(INFO,15,200,1)
    CALL LIMITS (50.0,150.0,-180.0,180.0)
    DO 110 I=50,150
    R=I
    AR(I)=AR(I)/(ABS(ACH(I)*SQRT(ABS(ACW(100)/ACH(100)))))
    AI(I)=AI(I)/(ABS(ACH(I)*SQRT(ABS(ACW(100)/ACH(100)))))
    PHC(I) = ATAN(AI(I)/AR(I))
    PHC(I)=PHC(I)+(0.5-SIGN(0.5,AR(I)))*SIGN(PI,AI(I))
    PHC(I)=PHC(I)*180.0/PI
    CALL POINTS(R,PHC(I),1R*,1)
    AD=SQRT(AR(I)*AR(I)+AI(I)*AI(I))
110 CALL POINTS(R,360.0*AD-180.0,1RC,1)
    CALL LABELS(4HFREQ,1,3HPHA,1)
    CALL GRIDS(50.0,10.0,-180.0,60.0)
    PRINT 116
116 FORMAT(1H1,12X,4HHPOW,6X,4HHPCW,6X,4HCORR,5X,5HPHASE,
   14X,4HCHAN,4X,4HHPOW,6X,4HWPCW,6X,4HCORR,5X,5HPHASE,4X,4HC AN,
    DO 112 I=50,148,2
    AB=ACH(I)/C
    AC=ACW(I)/C
    AD=SQRT(AR(I)*AR(I)+AI(I)*AI(I))
    AE=PHC(I)
    J=I+1
    BB=ACH(J)/C
    BC=ACW(J)/C
    BD=SQRT(AR(J)*AR(J)+AI(J)*AI(J))
    BE=PHC(J)
    PRINT 111, AB,AC,AD,AE,I,BB,BC,BD,BE,J
111 FORMAT(10X,4F10.3,I6,4F10.3,I6)
112 CONTINUE
    CALL GRAPHS(INFO,15,200,1)
    NDAY=NDAYA/C
    DEC=ACDEC*180.0/(PI*C)
    ANG=ACRA*180.0/(PI*C)
    THETA=ATHETA/C
    FL=AFL/C
    DOPA=ADOPA*180.0/(PI*C)
    ACD=ACH(100)
    ALPHA=0.11
    DO 520 I=1,1001
    R=(I-1)/1000.0
520 P(I)=EXP(-1.0/SQRT(1.0-R*R))/(R+ALPHA*SQRT(1.0-R*R))**3
    PXX=0.0
    DO 522 K=0,1000
    IR=SQRT(FLOAT(      K*K))+1.5
522 PXX=PXX+P(IR)
    DO 600 I=50,150
    PX=CX=0.0
    IX=ABS(I-99.00)*1000.0/FL+0.5
```

Fig. A-8. Continued.

```
      IY=SQRT(1000000.0-IX*IX)+0.5
      DO 550 K=0,IY
      IR=SQRT(FLOAT(IX*IX+K*K))+1.5
      PX=PX+P(IR)
  550 CX=CX+COS(PI*THETA*K/180000.0)*P(IR)
      ACP=ACH(I)
      ACH(I)=ACH(I)-PX*ACD/PXX
      CR=CX/PX
      PRINT 560, ACH(I),PX,CR
  560 FORMAT(10X,3F30.4)
      ACS(I)=ACH(I)/(ACP+ACD/100.0)
      AR(I)=AR(I)-CR*0.9
      AR(I)=AR(I)*ACP/(ACP+ACD/100.0)
  600 AI(I)=AI(I)*ACP/(ACP+ACD/100.0)
C     SMOOTHING
      DO 601 I=52,148
      I1=I-2$I2=I-1$I3=I+1$I4=I+2
      RR(I)=AR(I1)+2.0*AR(I2)+2.0*AR(I)+2.0*AR(I3)+AR(I4)
      RI(I)=AI(I1)+2.0*AI(I2)+2.0*AI(I)+2.0*AI(I3)+AI(I4)
  601 ANH (I)=ACS(I1)+2.0*ACS(I2)+2.0*ACS(I)+2.0*ACS(I3)+ACS(I4
      DO 602 I=52,148
      AR(I)=RR(I)/4.0
      AI(I)=RI(I)/4.0
  602 ACS(I)=ANH(I)/4.0
      AR(50)=AR(51)=AR(149)=AR(150)=0.0
      AI(50)=AI(51)=AI(149)=AI(150)=0.0
      ACS(50)=ACS(51)=ACS(149)=ACS(150)=0.0
C     BLANK OUT THE SUB RADAR POINT
      ACS(95)=ACS(96)=ACS(97)=ACS(103)=ACS(104)=ACS(105)=0.0
      DO 603 I=98,102
  603 AR(I)=AI(I)=ACS(I)=0.0
      CALL LIMITS (50.0,150.0,-180.0,180.0)
      DO 620 I=50,150
      R=I
      PHC(I) = ATAN(AI(I)/AR(I))
      PHC(I)=PHC(I)+(0.5-SIGN(0.5,AR(I)))*SIGN(PI,AI(I))
      PHC(I)=PHC(I)*180.0/PI
      CALL POINTS(R,PHC(I),1R*,1)
      CALL POINTS(R,ACS(I)*360.0-180.0,1RM,1)
  620 CALL POINTS(R,(360.0  )*SQRT(AR(I)**2+AI(I)**2)-180.0,1RC 1)
      CALL LABELS(4HFREQ,1,3HPHA,1)
      CALL GRIDS(50.0,10.0,-180.0,60.0)
      CALL GRAPHS (0,0,0,1)
C      FILL MA ARRAY
      DO 130 I=50,150
      CR=AR(I)*100000.0
      CI=AI(I)*100000.0
      CA=ACS(I)*10000.0
      DO 130 N=1,101
      L=I-49
      XF=N-51
  130 MA(L,N)=MA(L,N)+CR*COS(THETA*PI*XF/9000.0) +CI*SIN(THETA* I*
     1XF/9000.0)  *CA*(1-ICC)/2.0
      ICC=1
      CALL LIMITS(1.0,101.0,51.0,111.0)
      DO 140 N=51,101
      DO 140 L=1,101
      A1=N
      A2=L
      MQ=MA(L,N)/1000.0 +0.5
  140 CALL POINTS(A2,A1,MQ,1)
      CALL GRAPHS (0,0,0,1)
```

Fig. A-8. Continued.

```
      CALL LIMITS (1.0,101.0,-9.0,51.0)

      DO 150 N=1,51
      DO 150 L=1,101
      A1=N
      A2=L
      MQ=MA(L,N)/1000.0 +0.5
  150 CALL POINTS(A2,A1,MQ,1)
      CALL GRAPHS (0,0,0,1)
      PAUSE
      GO TO (155,1) SSWTCHF(6)
  155 ANG=ANG-179.7
      CDEC=COS(DEC*PI/180.0)
      SDEC=SIN(DEC*PI/180.0)
      CANG=COS(ANG*PI/180.0)
      SANG=SIN(ANG*PI/180.0)
      CTH=COS(23.3*PI/180.0)
      STH=SIN(23.3*PI/180.0)
      ALATR=(180.0/PI)*ASINF(-CTH*SDEC-STH*SANG*CDEC)
      ALONR=(180.0/PI)*ATAN((SANG*CDEC*CTH-SDEC*STH)/CANG*CDEC)
      ALONR=ALONR+16.0+(NDAY-241)*360.0/245.0
      PLA=ATAN(CANG*STH/(CTH*CDEC-STH*SDEC*SANG))
      APA=PLA*180.0/PI
      CDOP=COS(DOPA*PI/180.0)
      SDOP=SIN(DOPA*PI/180.0)
      NRUN=NDAY*10000+TIME*100
      PRINT 160,NRUN,NDAY,DEC,ANG,THETA,FL,DOPA,ALATR,ALONR,APA
  160 FORMAT(2I10,8F10.2)
      PE=PI/180.0*(16.0+(NDAY-241)*360.0/245.0)
      DO 180 L=1,101
      DO 180 N=1,101
      Y=(L-51)*CDOP/FL+(N-51)*SDOP/50.0
      Z=(L-51)*SDOP/FL - (N-51)*CDOP/50.0
      IF(1-Y*Y-Z*Z)180,161,161
  161 X=SQRT(1-Y*Y-Z*Z)
      XA=X*CANG*CDEC-Y*SANG+Z*SDEC*CANG
      YA=X*(CTH*SANG*CDEC-STH*SDEC)+Y*CANG*CTH+Z*(CTH*SDEC*SANG STH*CDEC
     1 )
      ZA=X*(-CTH*SDEC-STH*SANG*CDEC)-Y*CANG*STH+Z*(CTH*CDEC-STH SDEC*SAN
     1G)
      XB=XA*COS(PE)-YA*SIN(PE)
      YB=XA*SIN(PE)+YA*COS(PE)
      K=YB*60.0+61.5
      M=ZA*60.0 +61.5
      IF(XB) 170,175,175
  170 MAP(K,M)=1R$
      GO TO 180
  175 MAP(K,M)=MAP(K,M)+(MA(L,N)*XB/1000.0)
  180 CONTINUE
      DO 190 J=1,19
      AA=(J-10)*PI/18.0
      DO 190 I=1,361
      BB=(I-181)*PI/360.0
      K=COS(AA)*SIN(BB)*60.0+61.5
      M=SIN(AA)*60.0+61.5
      IF(MAP(K,M)) 190,181,190
  181 MAP(K,M)=1R*
  190 CONTINUE
      DO 200 J=1,19
      AA=(J-10)*PI/18.0
      DO 200 I=1,361
      BB=(I-181)*PI/360.0
```

Fig. A-8. Continued.

```
      K=COS(BB)*SIN(AA)*60.0+61.5
      M=SIN(BB)*60.0 +61.5
      IF(MAP(K,M)) 200,191,200
  191 MAP(K,M)=1R*
  200 CONTINUE
      CALL LIMITS(1.0  ,61.0,61.0,121.0)
      DO 210 K=1,61
      DO 210 M=61,121
      MAPK=MAP(K,M)
      AK=K
      AM=M
      IF(MAPK)209,210,209
  209 CALL POINTS(AK,AM,MAPK,1)
  210 CONTINUE
      CALL GRAPHS (0,0,0,1)
      CALL LIMITS(61.0,121.0,61.0,121.0)
      DO 220 K=61,121
      DO 220 M=61,121
      AK=K
      AM=M
      MAPK=MAP(K,M)
      IF(MAPK)219,220,219
  219 CALL POINTS(AK,AM,MAPK,1)
  220 CONTINUE
      CALL GRAPHS (0,0,0,1)
      CALL LIMITS (1.0  ,61.0,1.0,61.0)
      DO 230 K=1,61
      DO 230 M=1,61
      AK=K
      AM=M
      MAPK=MAP(K,M)
      IF(MAPK)229,230,229
  229 CALL POINTS(AK,AM,MAPK,1)
  230 CONTINUE
      CALL GRAPHS (0,0,0,1)
      CALL LIMITS(61.0,121.0,1.0,61.0)
      DO 240 K=61,121
      DO 240 M=1,61
      AK=K
      AM=M
      MAPK=MAP(K,M)
      IF(MAPK)239,240,239
  239 CALL POINTS(AK,AM,MAPK,1)
  240 CONTINUE
      CALL GRAPHS (0,0,0,1)
      PAUSE
      GO TO(242,241) SSWTCHF(1)
  241 CALL SEFF(20)
      BACKSPACE 20
  242 CONTINUE
      WRITE (20) MAP,ADAY
      END FILE 20
      BACKSPACE 20
      GO TO (251,250) SSWTCHF(4)
  250 END
```

Fig. A-8. Continued.

```
      PROGRAM HFMAP
      CHARACTER MP
      DIMENSION MAP(121,121),MP(121,121)
      PI=3.141592653
      IQ=0
      IC=0
      DO 1 K=1,121
      DO 1 M=1,121
    1 MAP(K,M)=0
    2 READ(30) MP,NDAY
      GO TO(30,3),EOFCKF(30)
    3 GO TO (2,14),SSWTCHF(2)
   14 PAUSE
      DO 10 K=1,121
      DO 10 M=1,121
      IF(MP(K,M).EQ.1R*)4,5
    4 MP(K,M)=0
    5 IF(MP(K,M).EQ.1R$)6,7
    6 MP(K,M)=0
    7 IA=MP(K,M)
      IF(IA-31)9,9,8
    8 IA=IA-64
    9 MAP(K,M)=MAP(K,M)+IA
   10 CONTINUE
      PRINT 20,NDAY
   20 FORMAT(10X,3HDAY,4X,I3)
      IC=IC+1
      GO TO (30,2),SSWTCHF(3)
   30 DO 40 K=1,121
      DO 40 M=1,121
      MD=MAP(K,M)
   40 MAP(K,M)=MD
   41 DO 190 J=1,19
      AA=(J-10)*PI/18.0
      DO 190 I=1,361
      BB=(I-181)*PI/360.0
      K=COS(AA)*SIN(BB)*60.0+61.5
      M=SIN(AA)*60.0+61.5
      IF(MAP(K,M)) 190,181,190
  181 MAP(K,M)=1R*
  190 CONTINUE
      DO 200 J=1,19
      AA=(J-10)*PI/18.0
      DO 200 I=1,361
      BB=(I-181)*PI/360.0
      K=COS(BB)*SIN(AA)*60.0+61.5
      M=SIN(BB)*60.0 +61.5
      IF(MAP(K,M)) 200,191,200
  191 MAP(K,M)=1R*
  200 CONTINUE
      CALL LIMITS(1.0  ,61.0,61.0,121.0)
      DO 210 K=1,61
      DO 210 M=61,121
      MAPK=MAP(K,M)
      AK=K
      AM=M
      IF(MAPK)209,210,209
  209 CALL POINTS(AK,AM,MAPK,1)
```

Fig. A-9. CW display programs.

```
210 CONTINUE
    CALL GRAPHS (0,0,0,1)
    CALL LIMITS(61.0,121.0,61.0,121.0)
    DO 220 K=61,121
    DO 220 M=61,121
    AK=K
    AM=M
    MAPK=MAP(K,M)
    IF(MAPK)219,220,219
219 CALL POINTS(AK,AM,MAPK,1)
220 CONTINUE
    CALL GRAPHS (0,0,0,1)
    CALL LIMITS (1.0  ,61,0,1,0,61.0)
    DO 230 K=1,61
    DO 230 M=1,61
    AK=K
    AM=M
    MAPK=MAP(K,M)
    IF(MAPK)229,230,229
229 CALL POINTS(AK,AM,MAPK,1)
230 CONTINUE
    CALL GRAPHS (0,0,0,1)
    CALL LIMITS(61.0,121.0,1.0,61.0)
    DO 240 K=61,121
    DO 240 M=1,61
    AK=K
    AM=M
    MAPK=MAP(K,M)
    IF(MAPK)239,240,239
239 CALL POINTS(AK,AM,MAPK,1)
240 CONTINUE
    CALL GRAPHS (0,0,0,1)
    WRITE(20)MAP,NDAY
    END FILE 20
    DO 245 K=1,121
    DO 245 M=1,121
245 MAP(K,M)=0
    IQ=IQ+1
    REWIND 30
250 READ(30) MP,NDAY
    GO TO(41,300),EOFCKF(30)
300 DO 310 K=1,121
    DO 310 M=1,121
    IF(MP(K,M).EQ.1R*)304,305
304 MP(K,M)=0
305 IF(MP(K,M).EQ.1R$)306,307
306 MP(K,M)=0
307 IF(MP(K,M)-IQ)310,308,308
308 IF(MP(K,M)-30)309,309,310
309 MAP(K,M)=MAP(K,M)+1
310 CONTINUE
    GO TO 250
    END
```

Fig. A-9. Continued.

```
      PROGRAM HFDISP
      DIMENSION MAP(121,121),X(361),Y(361)
      REWIND 30
      READ(30) ((MAP(K,M),M=1,121),K=1,121 ),NDAY
      PI=3.14159265
    1 CALL RESETD(-6,-10)
      CALL SCALE(-1.,1.,-1.,1.,32,32,0,64)
      DO 10 J=1,19
      AA=(J-10)*PI/18.0
      DO 2 I=1,361
      BB=(I-181)*PI/360.0
      X(I)=COS(AA)*SIN(BB)
    2 Y(I)=SIN(AA)
      DO 3 K=1,5
    3 CALL PLOT(2,360,X,Y,1,1,0)
   10 CONTINUE
      DO 20 J=1,19
      AA=(J-10)*PI/18.0
      DO 12 I=1,361
      BB=(I-181)*PI/360.0
      X(I)=COS(BB)*SIN(AA)
   12 Y(I)=SIN(BB)
      DO 13 K=1,20
   13 CALL PLOT(2,360,X,Y,1,1,0)
   20 CONTINUE
      DO 24 K=1,121
      DO 24 M=1,121
      IF(MAP(K,M)-1R*) 24,22,24
   22 MAP(K,M)=0
   24 CONTINUE
      IMAX=-1.E10
      IMIN=-IMAX
      DO 50 I=1,14641
      IMIN=MIN0(IMIN,MAP(I,1))
50     IMAX=MAX0(IMAX,MAP(I,1))      $  WRITE(59,60)IMIN,IMAX
60     FORMAT(10HIMIN,IMAX=2I5)
      WRITE(59,40)
   40 FORMAT(21HWRITE IMIN,IMAX,NGRAY)
      CALL GETDATA(58,A,B,C)
      IMIN=A$IMAX=B$NGRAY=C
      CALL INTRPLOT(MAP,121,121,32,2,0,2,4,4,0,NGRAY,IMIN,IMAX)
      CALL ADVFILM(0,1)
      PAUSE
      GO TO 1
      END
```

Fig. A-9. Continued.

DOCUMENT CONTROL DATA – R&D

(Security classification of title, body of abstract and indexing annotation must be entered when the overall report is classified)

1. ORIGINATING ACTIVITY *(Corporate author)*
Lincoln Laboratory, M.I.T.

2a. REPORT SECURITY CLASSIFICATION
Unclassified

2b. GROUP
None

3. REPORT TITLE
A Radar Interferometer Study of Venus at 3.8 cm

4. DESCRIPTIVE NOTES *(Type of report and inclusive dates)*
Technical Report

5. AUTHOR(S) *(Last name, first name, initial)*
Rogers, Alan E. E.
Hagfors, Tor
Brockelman, Richard A.
Ingalls, Richard P.
Levine, James I.
Pettengill, Gordon H.
Weinstein, Franklin S.

6. REPORT DATE	7a. TOTAL NO. OF PAGES	7b. NO. OF REFS
14 February 1968	110	10

8a. CONTRACT OR GRANT NO.
AF 19(628)-5167

b. PROJECT NO.
649L

c.

d.

9a. ORIGINATOR'S REPORT NUMBER(S)
Technical Report 444

9b. OTHER REPORT NO(S) *(Any other numbers that may be assigned this report)*
ESD-TR-68-18

10. AVAILABILITY/LIMITATION NOTICES
This document has been approved for public release and sale; its distribution is unlimited.

11. SUPPLEMENTARY NOTES
None

12. SPONSORING MILITARY ACTIVITY
Air Force Systems Command, USAF

13. ABSTRACT

The 120-foot antenna of the Haystack Microwave Facility and the 60-foot antenna of the Westford Communications Terminal, both operated by M.I.T. Lincoln Laboratory, were coupled to form a planetary radar interferometer operating at X-band and were used to observe Venus at a wavelength of 3.8 cm during the 1967 inferior conjunction. The antennas are separated by approximately 4000 feet along a line 22° east of north. At maximum projection in the direction of the planet, this baseline gives a fringe spacing of 5 seconds of arc, or a maximum of about 10 fringes across the planetary disk at inferior conjunction.

By transmitting a CW signal from the 120-foot antenna and frequency analyzing the received echo, it was possible to resolve the planetary surface scattering into strips parallel to the apparent axis of rotation. Crosscorrelation of the complex frequency components obtained at the two sites yielded corresponding spatial Fourier components which resolved the scattering along the strips. With 1-Hz frequency resolution and a maximum of 10 fringes along the rotation axis, the planetary hemisphere visible to the radar during inferior conjunction was mapped with approximately 100 resolution intervals along a direction perpendicular to the apparent rotation axis, with 10 resolution intervals in the orthogonal direction.

For a limited region on the planet, surrounding the center of the visible disk, higher resolution was obtained by transmitting pulses of 500-μsec effective length. The pulse resolution enabled the planet to be resolved in echo delay, leaving only a twofold hemispheric ambiguity to be resolved by the interferometer. In addition, in the range-gated observations the effects of significant interferometer sidelobes (arising from the limited range of projected baselines available) were avoided.

Maps obtained from the observations show Venus to be smoother on the average than the moon at 3.8 cm, although some regions of the planet exhibit strong local radar-scattering enhancement. The positions of these regions agree well with those previously reported if the rotation period of Venus is assumed to be earth-synchronous at 243.16 days retrograde.

14. KEY WORDS

interferometers
interferometry
Haystack
Millstone
Venus radar mapping
signal-to-noise ratio
Doppler radar
correlation techniques
CW transmissions
coded transmissions
Fourier transform
scattering